

Old Dominion University Research Foundation

LANGLEY  
GRANT  
IN-39-CR  
151329  
P-125

DEPARTMENT OF CIVIL ENGINEERING  
COLLEGE OF ENGINEERING AND TECHNOLOGY  
OLD DOMINION UNIVERSITY  
NORFOLK, VIRGINIA 23529

**EXPERIMENTAL AND THEORETICAL INVESTIGATION OF  
PASSIVE DAMPING CONCEPTS FOR  
MEMBER FORCED AND FREE VIBRATION**

By

Zia Razzaq, Principal Investigator

David W. Mykins, Graduate Research Assistant

Progress Report

For the period ended December 31, 1987

Prepared for the  
National Aeronautics and Space Administration  
Langley Research Center  
Hampton, Virginia 23665

Under

**Research Grant NAG-1-336**

Harold G. Bush, Technical Monitor  
SDD-Structural Concepts Branch

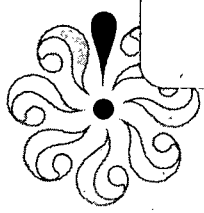
(NASA-CR-183082) EXPERIMENTAL AND  
THEORETICAL INVESTIGATION OF PASSIVE DAMPING  
CONCEPTS FOR MEMBER FORCED AND FREE  
VIBRATION Progress Report, period ending 31  
Dec. 1987 (Old Dominion Univ.) 125 p

N88-26693

Unclas

G3/39 0151329

December 1987



DEPARTMENT OF CIVIL ENGINEERING  
COLLEGE OF ENGINEERING AND TECHNOLOGY  
OLD DOMINION UNIVERSITY  
NORFOLK, VIRGINIA 23529

**EXPERIMENTAL AND THEORETICAL INVESTIGATION OF  
PASSIVE DAMPING CONCEPTS FOR  
MEMBER FORCED AND FREE VIBRATION**

By

Zia Razzaq, Principal Investigator

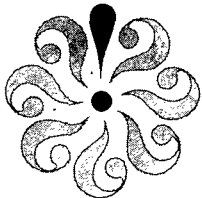
David W. Mykins, Graduate Research Assistant

Progress Report  
For the period ended December 31, 1987

Prepared for the  
National Aeronautics and Space Administration  
Langley Research Center  
Hampton, Virginia 23665

Under  
**Research Grant NAG-1-336**  
Harold G. Bush, Technical Monitor  
SDD-Structural Concepts Branch

Submitted by the  
Old Dominion University Research Foundation  
P.O. Box 6369  
Norfolk, Virginia 23508-0369



December 1987

### ACKNOWLEDGEMENTS

The thought-provoking discussions of Mr. Harold G. Bush and Dr. Martin M. Mikulas, Jr. of SDD-Structural Concepts Branch, NASA Langley Research Center are sincerely appreciated. Thanks are also due to Mr. Robert Miserentino and his technical staff for providing help in calibration of the vibration apparatus.

EXPERIMENTAL AND THEORETICAL INVESTIGATION OF PASSIVE  
DAMPING CONCEPTS FOR MEMBER FORCED AND FREE VIBRATIONS

By

Zia Razzaq<sup>1</sup> and David W. Mykins<sup>2</sup>

ABSTRACT

The results presented in this research report are the outcome of an ongoing study directed toward the identification of potential passive damping concepts for use in space structures. The effectiveness of copper brush, wool swab, and "silly putty" in chamber dampers is investigated through natural vibration tests on a tubular aluminum member. The member ends have zero translation and possess partial rotational restraints. The silly putty in chamber dampers provide the maximum passive damping efficiency. Forced vibration tests are then conducted with one, two, and three silly putty in chamber dampers. Owing to the limitation of the vibrator used, the performance of these dampers could not be evaluated experimentally until the forcing function was disengaged. Nevertheless, their performance is evaluated through a forced dynamic finite element analysis conducted as a part of this investigation. The theoretical results are based on experimentally obtained damping ratios indicate that the passive dampers are considerably more effective under member natural vibration than during forced vibration. Also, the maximum damping under forced vibration occurs at or near resonance.

---

<sup>1</sup> Professor, Department of Civil Engineering, Old Dominion University, Norfolk, Virginia 23529.

<sup>2</sup> Graduate Research Assistant, Department of Civil Engineering, Old Dominion University, Norfolk, Virginia 23529.

## NOMENCLATURE

$[C]$  = damping matrix for member

$[D]$  = displacement vector

$[\dot{D}]$  = velocity vector

$[\ddot{D}]$  = acceleration vector

$[D_j]$  = displacement vector at node  $j$

$E$  = Young's Modulus

$I$  = moment of inertia

$[K]$  = global stiffness matrix for member

$[R]$  = forcing function vector

$\gamma\beta$  = arbitrary constants for Newmark's method

$\Delta_d^*$  = dynamic deflection amplitude

$\Delta_F$  = static midspan deflection

$\Delta_S$  = static midspan deflection

$\Delta t$  = time increment

$\Phi$  = modal vector

$\eta$  = damping efficiency index

$\Omega$  = frequency of applied forcing function

$\omega$  = natural frequency

$\omega_{fe}$  = natural frequency from finite element analysis

$\rho$  = mass density

$\zeta$  = damping ratio

## TABLE OF CONTENTS

	<u>Page</u>
ACKNOWLEDGEMENTS.....	iii
ABSTRACT.....	iv
NOMENCLATURE.....	v
LIST OF TABLES.....	viii
LIST OF FIGURES.....	ix
1. Introduction.....	1
1.1 Background and Previous Work.....	1
1.2 Problem Definitions.....	2
1.3 Objective and Scope.....	3
1.4 Assumptions and Conditions.....	4
2. Theoretical Formulation.....	5
2.1 Finite Element Formulation.....	5
2.2 Newmark's Method.....	8
2.3 Central Difference Formulation.....	10
3. Experimental Study.....	12
3.1 Specimen and Connection Details.....	12
3.1.1 Specimen.....	12
3.1.2 Connection Details.....	12
3.2 Passive Damping Concepts.....	13
3.2.1 Copper Brush Dampers.....	13
3.2.2 Wool Swab Dampers.....	15
3.2.3 Silly Putty in Chamber Dampers.....	15
3.3 Test Setup and Procedures.....	16
3.4 Test Results and Discussion.....	17
3.4.1 Natural Vibration.....	17
3.4.1.1 Copper Brush Dampers.....	19
3.4.1.2 Wool Swab Dampers.....	20
3.4.1.3 Silly Putty in Chambers Dampers.....	20
3.4.2 Forced Then Free Vibration.....	21
3.4.2.1 Silly Putty in Chamber Dampers.....	22
3.5 Comparison of Damping Efficiencies.....	23

TABLE OF CONTENTS - Continued

	<u>Page</u>
4. Numerical Study.....	25
4.1 Natural Vibration.....	25
4.1.1 Finite Element Versus Experimental.....	25
4.1.2 Finite Element versus Finite-Difference.....	25
4.2 Forced Then Free Vibration.....	26
4.3 Finite Element Analysis for Forced Vibration.....	27
5. Conclusions and Future Research.....	29
5.1 Conclusions.....	29
5.2 Future Research.....	30
References.....	31
APPENDIX A      STIFFNESS MATRIX FORMULATION.....	85
APPENDIX B      COMPUTER PROGRAMS.....	90
VITA AUCTORIS.....	114

LIST OF TABLES

<u>Table</u>		<u>Page</u>
1	Member natural vibration test results for copper brush, wood swab, and silly putty in chamber dampers.....	33
2(a)	Dampng ratios from natural vibration tests with copper brushes and no cord tension.....	34
2(b)	Damping ratios from natural vibration tests with copper brushes and nominal cord tension.....	34
3(a)	Damping ratios for natural vibration tests with wool brushes and concentric cord support.....	35
3(b)	Damping ratios for natural vibration tests with wool brushes and eccentric cord support.....	35
4(a)	Damping ratios for natural vibration tests with silly putty and no cord tension.....	36
4(b)	Damping ratios for natural vibration tests with silly putty and nominal cord tension.....	36
5	Member forced then free vibration test results for silly putty in chamber dampers.....	37



## LIST OF FIGURES

<u>Figure</u>	<u>Page</u>
1. Schematic of tubular member.....	39
2. Example of finite element model for the beam.....	40
3. Some end connection details.....	41
4. Member end connection.....	42
5. Copper brush damper.....	43
6. Schematic of attachments for passive damper inside tubular member.....	44
7. Schematic for spacing of passive dampers.....	45
8. Helical spring attachment at end e.....	46
9. Stretched helical spring at end e.....	47
10. Wool swab damper.....	48
11. Silly putty in chamber damper.....	49
12. Schematic of member natural vibration setup.....	50
13. Proximity probe.....	51
14. Member forced vibration setup.....	52
15. Schematic of member forced vibration setup.....	53
16. Vibrator connector details.....	54
17. Vibrator connector in engaged and disengaged positions.....	55
18. Average $\Delta$ -t plot for member with no dampers.....	56
19. Average $\Delta$ -t plot for member with 3 copper brush dampers.....	57
20. Effect of 3 copper brush dampers on $\Delta$ -t envelope.....	58
21. Average $\Delta$ -t plot for member with 3 wool swab.....	59
22. Average $\Delta$ -t plots for members with 1 wool swab damper.....	60
23. Effect of 3 wool swab dampers on $\Delta$ -t envelope.....	61
24. Effect of 1 wool swab damper on $\Delta$ -t envelope.....	62

LIST OF FIGURES - (Continued)

	<u>Page</u>
25. Average $\Delta$ -t plot for member with 3 silly putty in chamber dampers.....	63
26. Average $\Delta$ -t plot for member with 2 silly putty in chamber dampers.....	64
27. Effect of 3 silly putty in chamber dampers on $\Delta$ -t.....	65
28. Effect of 2 silly putty in chamber dampers on $\Delta$ -t envelope..	66
29. Experimental $\Delta$ -t plots for member "constrained" forced then free vibration with no dampers and frequencies of 2, 5, 7 and 9 Hz.....	67
30. Experimental $\Delta$ -t plot for member "constrained" forced then free vibration with 2 silly putty in chamber damper and forcing function frequencies of 2, 5, 7, and 9 Hz.....	68
31. Experimental $\Delta$ -t plot for member "constrained" forced then free vibration with 1 silly putty in chamber damper and forcing function frequencies of 2, 5, 7, and 9 Hz.....	69
32. Experimental $\Delta$ -t plots for member "constrained" forced free vibration with 3 silly putty in chamber dampers and forcing function frequencies of 2, 5, 7, and 9 Hz.....	70
33. Damping efficiency index versus weight curves for natural vibration tests.....	71
34. Damping efficiency index versus number of dampers for natural vibration tests.....	72
35. Finite element versus average experimental $\Delta$ -t plots for member with no dampers.....	73
36. Finite element versus average experimental $\Delta$ -t plots for member with 3 copper brush dampers.....	74
37. Finite element versus finite difference $\Delta$ -t plots for member with no dampers.....	75
38. Finite element versus finite difference $\Delta$ -t plots for member with 3 copper brush dampers.....	76
39. Finite element versus finite difference $\Delta$ -t plots for simply supported beam with no dampers.....	77
40. Finite element $\Delta$ -t plot for member with no dampers and subjected to a 4.0 lb. force at 2 hz for 1 second.....	78
41. Finite element forced then free $\Delta$ -t plot for member with	

LIST OF FIGURES - (Concluded)

	<u>Page</u>
no dampers and subjected to a 4.0 lb. force at 6 Hz for 1 second.....	79
42. Theoretical and experimental forced then free $\Delta$ -t plots for a 4.0 lb. force at 2 Hz for 1 second on member with one silly putty in chamber damper.....	80
43. Theoretical and experimental forced then free $\Delta$ -t plots for a 4.0 lb. force at 2 Hz for 1 second member with no dampers.	81
44. Theoretical dynamic magnification factor versus frequency ratio for damping ratios of 0.0094, 0.0131 and 0.5.....	82
45. Theoretical $\Delta$ -t plots for member with no dampers and with 3 copper brush dampers with a forcing function of 6.35 Hz for one second.....	83

## 1. INTRODUCTION

### 1.1 Background and Previous Work

The space station designs currently under consideration by NASA are three-dimensional space structures composed of long tubular members. Modules providing the required living and working space for astronauts will be attached to this framework. Such a structure, suspended in a weightless environment, would be subjected to many types of dynamic loading. These include differential heating or cooling of the structure, variations in acceleration or gravitational pull, and impact with a solid object. The ability to expeditiously damp these vibrations before they cause permanent damage is a practical problem worth studying.

The necessarily large slenderness ratio of the average space truss member, combined with the flexible, semi-rigid end restraints cause the dynamic response of these members to be characterized by low frequency, small amplitude vibrations. Active damping techniques utilize electronic sensors and movable masses to reduce vibration of structures. This system, although effective, requires regular maintenance and an external power source. An alternative for mechanically damping a system is the concept of "passive" damping. This method uses a device or material permanently attached to the structure or its components and designed to absorb the energy of vibration thereby providing some damping of the system. Unlike "active" damping, this would require minimal maintenance and no external power.

The challenge to developing a passive damping concept, particularly for a space structure is two-fold. First is the necessity to minimize the mass, for without this constraint one obvious solution would be to provide large

mass concentrations at the critical nodal points for the vibration modes. Such an approach would be expensive since the cost of transporting the system into space is directly related to the mass. The second challenge is to identify a concept which will provide passive damping without altering the strength or stiffness of the structure. For example, mild compression of the members provides some damping, however, the safe service loads for the structure are altered.

Recently, investigations into passive damping concepts for slender tubular members have been conducted with various end conditions (References 1-5). The most effective concepts found were the mass-string-whiskers assembly, and brushes for electrostatic and frictional damping. In these experiments, only natural flexural vibration was examined.

The previous work was conducted on hollow tubular steel members with an outer diameter of 0.5 inches. The passive damping concepts which were found to be effective for these members may not be as effective if the dimensions are changed. Factors altered by dimensional changes may include the damper mass required, the extent of the frictional interaction, and the member dynamic characteristics. Clearly research is needed to identify a viable passive damping concepts for members of different sizes and dynamic properties. In the present study, hollow tubular aluminum members with an outside diameter of 2.0 inches are used. These members more closely resemble the actual size and material which may be used in the future space stations.

## 1.2 Problem Definition

Figure 1 shows schematically a slender beam of length  $L$  with a hollow circular cross section. The outer diameter is  $D_0$  the inner diameter is  $D_1$ ,

and the material is aluminum with a Young's modulus of 10,000 ksi. An aluminum member is used because the graphite composite tubes which may possibly be used in space structures are not yet available. The member ends are provided with a prototype connection developed by NASA for the space frames. These connections possess partial rotational restraint characteristics in the plane of motion and a more rigid end condition in the orthogonal plane. No axial or lateral movement of the member ends is permitted.

The problem is to identify potential passive damping concepts to absorb the energy of both natural flexural vibration, and harmonic forced flexural vibration, and to study the effectiveness of each concept. The natural vibration is caused by the sudden release of a constant static load. The harmonic forcing function is applied through a mechanical connection to a harmonic vibrator.

### 1.3 Objective and Scope

The following are the main objectives of this study:

1. Identification of potential passive damping concepts for slender tubular structural members. Specifically, the following damping concepts are investigated:
  - a. wool swabs,
  - b. copper brushes,
  - c. silly putty in chambers.
2. Evaluation of the damping efficiencies of the various damping concepts.
3. Evaluation of the suitability of a theoretical finite element analysis by comparison to experimental results for natural and

forced vibration, and a previous finite-difference solution for natural vibration.

Only flexural member vibration is considered. The natural vibration study is conducted on each of the three passive damping concepts and for one specific initial deflection. Only the most efficient damping concept is considered for further study under forced vibration. Also, the vibration is induced by load application at the member midspan.

#### 1.4 Assumptions and Conditions

The following assumptions and conditions have been adopted in this study:

1. The deflections are small.
2. The material of the member is linearly elastic.
3. Only planar vibration is considered.
4. Damping force is opposite but proportional to the velocity at any location along the member.
5. The damping force is uniform along the length of the member.
6. The member is tested at 1-g and room temperature.
7. The effect of secondary induced forces such as varying axial tension and compression developed in the member during vibration is considered to be negligible.

## 2. THEORETICAL FORMULATION

### 2.1 Finite Element Formulation

The beam shown in Figure 1 may be divided into N finite elements along the length. For the discretized system, the governing equation of motion can be expressed in the following matrix form (Reference 6):

$$[K](D) + [M](\dot{D}) + [C](\ddot{D}) = (R) \quad (1)$$

where:

$(D)$  = displacement vector,

$(\dot{D})$  = velocity vector,

$(\ddot{D})$  = acceleration vector,

$[K]$  = global stiffness matrix for the "structure",

$[M]$  = global modified lumped mass matrix,

$[C]$  = damping matrix,

$(R)$  = forcing function vector.

The boundary and initial conditions for the problem shown in Figure 1 are given in Reference 2 and are summarized here:

$$D(0,t) = 0 \quad (2)$$

$$D(L,t) = 0 \quad (3)$$

$$EI D''(0,t) = k_1 D'(0,t) \quad (4)$$

$$EI D''(L,t) = -k_2 D'(L,t) \quad (5)$$

$$\dot{D}(x,0) = 0 \quad (6)$$

$$D(x,0) = 0(x; K, EI, L) \quad (7)$$



where primes represent differentiation relative to  $x$ , and dots represent time differentiation. The displacement vector at any node  $j$  along the member can be written as:

$$(D_j) = \begin{Bmatrix} d_j \\ d'_j \end{Bmatrix} \quad (8)$$

where  $d_j$  and  $d'_j$  represent, respectively, the deflection and slope of  $j$ .

Equations 2 to 5 represent the boundary conditions whereas Equations 6 and 7 are the initial conditions. Equation 7 simply states that at time zero, the member deflected shape is dependent on  $x$ ,  $K$ ,  $EI$  and  $L$ .

The first task toward the solution of the matrix equation is the assembly of the three coefficient matrices. The  $[K]$  matrix is assembled from the individual element matrices combined in such a way so as to enforce the given boundary and inter-element compatibility conditions. To illustrate the procedure, an example of a beam with four elements as shown in Figure 2 is given in Appendix A.

The global mass matrix is a diagonal form of a lumped mass matrix which was developed (Reference 6) for use with elements where translational degrees of freedom are mutually parallel, such as beam or plate elements.



Once all three coefficient matrices have been assembled, the solution of Equation 1 may proceed using any one of several solution algorithms available.

## 2.2 Newmark's Method

Newmark's method for solving the dynamic equilibrium equation is sometimes called the trapezoidal method because it is based on a linear interpolation to find succeeding points. This is done by assuming:

$$(D)_{t+\Delta t} = (D)_t + \Delta t (\dot{D})_t + \Delta t^2 \left( \left( \frac{1}{2} - \beta \right) (\ddot{D})_t + \beta (\ddot{D})_{t+\Delta t} \right) \quad (11)$$

and

$$(\dot{D})_{t+\Delta t} = (\dot{D})_t + \Delta t \left( (1-\gamma) (\ddot{D})_t + \gamma (\ddot{D})_{t+\Delta t} \right) \quad (12)$$

where  $\Delta t$  is a time increment, and  $\beta$  and  $\gamma$  are arbitrary constants. By substituting Equations 11 and 12 into Equation 1 written at time  $t = t + \Delta t$ , one gets (Reference 6):

$$\begin{aligned} & \left( [K] + \frac{\gamma}{\beta \Delta t} [C] + \frac{1}{\beta \Delta t^2} [M] \right) (D)_{t+\Delta t} = (R)_{t+\Delta t} + \\ & [C] \left( \frac{\gamma}{\beta \Delta t} (D)_t + \frac{\gamma}{\beta} - 1 (\dot{D})_t + (\Delta t) \frac{\gamma}{2\beta} - 1 (\ddot{D})_t \right) + \\ & [M] \left( \frac{1}{\beta \Delta t^2} (D)_t + \frac{1}{\beta \Delta t} (\dot{D})_t + \left( \frac{1}{2\beta} - 1 \right) (\ddot{D})_t \right) \end{aligned} \quad (13)$$

For a known loading function we may solve Equation 13 for the deflection at time  $t = t + \Delta t$  using the deflection, velocity and acceleration at time  $t$ .

The algorithm for Newmark's solution is as follows:

1. Compute the coefficient matrices from geometric and material properties.
2. At  $t = 0$ , set initial conditions by prescribing  $(D)_{t=0}$  and  $(\dot{D})_{t=0}$ .
3. Use Equation 1 to solve for  $(\ddot{D})_{t=0}$ .
4. Solve Equation 13 for  $(D)_{t+\Delta t}$ .
5. Solve Equation 11 for  $(\ddot{D})_{t+\Delta t}$ .
6. Solve Equation 12 for  $(\dot{D})_{t+\Delta t}$ .
7. Set  $(D)_t = (D)_{t+\Delta t}$ ;  $(\dot{D})_t = (\dot{D})_{t+\Delta t}$ ;  $(\ddot{D})_t = (\ddot{D})_{t+\Delta t}$ .
8. If  $t < \underline{\text{total time desired}}$ , go to Step 4.
9. Stop.

This method of solution is unconditionally stable if  $\underline{\gamma} > 0.5$  and  $\underline{\beta} > (2\underline{\gamma} + 1)^2/16$ . With  $\underline{\gamma} = 0.5$  and  $\underline{\beta} = 0.25$ , there are no amplitude errors in any sine wave motion regardless of its frequency, although the periods are overestimated. The mode shapes of the member in this study, however, are not known exactly. Nevertheless,  $\underline{\gamma}$  and  $\underline{\beta}$  values of 0.5 and 0.25 respectively, were tentatively chosen. The suitability of these values is evaluated later in Section 4.

The initial static deflection vector required in Step 2 of the algorithm may be determined using any one of the several classical structural analysis techniques. An approximate shape function for the member due to a specified midpoint displacement  $\Delta_0$  at time  $t = 0$  is taken in the following form (Reference 2):

$$d_j = A_1 \left[ \sin \frac{\pi x_j}{L} + \frac{kL}{4\pi EI} \left( 1 - \cos \frac{2\pi x_j}{L} \right) \right] \quad (14)$$

where:

$$A_1 = \frac{\Delta_0}{1 + \frac{kL}{2\pi EI}} \quad (15)$$

The initial slope of the member at any point is found by differentiating Equation 14 resulting in:

$$d'_j = A_1 \left[ \frac{\pi}{L} \cos \frac{\pi x_j}{L} + \frac{k}{2EI} \sin \frac{2\pi x_j}{L} \right] \quad (16)$$

where  $x_j$  is the position of node  $j$  along the member length.

### 2.3 Central Difference Formulation

The governing equations and formulation of the coefficient matrices to be used in the central difference method of solution are precisely the same as those previously given for Newmark's method. Once these geometric and physical properties are determined, one proceeds by writing the central difference expressions for both velocity and acceleration at an arbitrary time  $t$ :

$$\{\dot{D}\}_t = \frac{1}{2(\Delta t)} \left[ \{D\}_{t+\Delta t} - \{D\}_{t-\Delta t} \right] \quad (17)$$

$$\{\ddot{D}\}_t = \frac{1}{(\Delta t)^2} \left[ \{D\}_{t+\Delta t} - 2\{D\}_t + \{D\}_{t-\Delta t} \right] \quad (18)$$

Equations 17 and 18 may then be substituted into Equation 1 to yield, after some rearrangement:

$$\left( \frac{[M]}{(\Delta t)^2} + \frac{[C]}{2(\Delta t)} \right) \{D\}_{t+\Delta t} = \{R\}_t - \left( [K] - \frac{2[M]}{(\Delta t)^2} \right) \{D\}_t + \left( \frac{[M]}{(\Delta t)^2} - \frac{[C]}{2(\Delta t)} \right) \{D\}_{t-\Delta t} \quad (19)$$

The initial conditions  $\{D\}_0$  and  $\{\dot{D}\}_0$  are prescribed and  $\{\ddot{D}\}_0$  is found by solving Equation 1. Once these are known Equations 17 and 18 may be solved simultaneously to yield the displacements  $\{D\}_{-\Delta t}$  required to start the computations.

$$\{D\}_{-\Delta t} = \{D\}_0 - \Delta t \{\dot{D}\}_0 + \frac{(\Delta t)^2}{2} \{\ddot{D}\}_0 \quad (20)$$

The solution algorithm for central difference is as follows:

1. Compute the coefficient matrices from geometric and material properties.
2. Set  $\Delta t$  = time step increment.
3. Set initial conditions by prescribing  $\{D\}_{t=0}$  and  $\{\dot{D}\}_{t=0}$ .
4. Solve Equation 1 for  $\{\ddot{D}\}_{t=0}$ .
5. Solve Equation 20 for  $\{D\}_{-\Delta t}$ .
6. Solve Equation 19 for  $\{D\}_{t+\Delta t}$ .
7. Set  $\{D\}_{t-\Delta t} = \{D\}_t$ , and  $\{D\}_t = \{D\}_{t+\Delta t}$ .
8. If  $t < \underline{\text{total time desired}}$ , go to 6.
9. Stop.

The central difference method is a conditionally stable, explicit method of solution. Conditionally stable implies that if  $\Delta t$  is not chosen small enough, the predicted response of the system will grow unbounded. A preliminary numerical study showed that  $\Delta t$  must be in the range from 0.001 to 0.005, therefore, a  $\Delta t = 0.001$  sec. is used in this study.

### 3. EXPERIMENTAL STUDY

#### 3.1 Specimen and Connection Details

##### 3.1.1 Specimen

The experimental study consisted of conducting natural and forced vibration tests on a tubular aluminum member. The tests were performed both with and without passive damping devices present inside the member. The tubular member used was 14'-9" long with an outside diameter of 2" and a wall thickness of 0.125", yielding an inside diameter of 1.75". A schematic of the member tested is shown in Figure 1. Note that the member was horizontal for all testing, with gravitational forces acting in the plane of motion.

##### 3.1.2 Connection Details

The prototype end connection used in this study is shown in Figure 3. It is constructed of an aluminum alloy, weights 0.595 lbs. excluding fastener bolts, and has a volume of 3.988 in<sup>3</sup>. The connection has a total of nine clevis blades, six of which are in the horizontal plane. One of the blades is in the vertical plane (at C) and two are at 45 degrees to the horizontal plane. These two are located at 45 degrees relative to the vertical clevis and in the planes containing the two lower clevis blades shown in Figure 3(a).

The fastener locations for the clevis blades in the horizontal plane are numbered 1 through 12. The member was fastened at locations 3 and 4 shown in Figure 3(a). Fasteners at locations 5 through 11 are used to mount the connection to a fixed base plate. No fastener was installed at location 12 due to an interference problem with the support underneath the base plate. This did not make any difference since the other fasteners provided

sufficient fixity. Each fastener has a diameter of 0.25 in. and a length of 0.94 in. Washers were used at locations 1 and 2 only.

The ends of the tubular member were threaded to allow one-half of the "snap-lock" connection to be screwed onto it. Small holes were drilled through this threaded connection and pins inserted to prevent rotation and loosening of the connection during testing. The other end of the snap-lock connection had its blade end fit snugly into one of the clevis blades of the prototype end connection and fastened by two bolts. The spring stiffness,  $k$ , shown in Figure 1 was determined by a statical analysis using an experimentally determined midspan deflection for a known concentrated load. This value was 53.1 k-in/rad. The assembled connection is shown in Figure 4.

### 3.2 Passive Damping Concepts

Three different types of passive dampers referred to in Section 1.4 are described in this section.

#### 3.2.1 Copper Brush Dampers

Figure 5 shows a copper brush damper 0.8125 inches in diameter, of total length 3.125 inches and a weight of 13.0 grams. The brush is manufactured by Omack Industries, Onalaska, Wisconsin 54650 with a US Patent 41986 and an inventory control number 07668341989. It has a threaded aluminum piece 1.0 inch long at one end with a twisted wire 2.125 inches in length attached to it. The copper bristles are attached to the entire length of the twisted wire. This type of brush is commonly used in cleaning the bore of a 12 gauge shotgun.

Figures 6 and 7 show schematically the attachments for the passive dampers and their spacing inside the tubular member. As shown in Figure 6,



the assembly consists of several parts. First, a helical spring with a stiffness of 0.44 lb/in. is attached to the inside of the connection through a hook on the snap-lock connector as shown in Figure 8. A nylon line is tied to the other end of the spring and also connected to the first copper brush damper. The nylon line (sportfisher monofilament line manufactured by K-Mart Corporation, Troy, Michigan 48084, 8013.9, No. EPM-40, inventory control number 04528201391) used in this investigation has a 40 lb. capacity. A series of nylon line and dampers are attached along the member length until the other end of the tubular member is reached. The end of the nylon line is passed through a hole in the snap-lock connector and stretched by an amount of 2.0 inches in the longitudinal direction to induce nominal tension in helical spring. It is then secured to the vertical clevis at the support. The stretched helical spring is shown in Figure 9. The resulting passive damping assembly is aligned with the longitudinal axis of the tubular member due to the small amount of axial tension. No axial compression of the member is induced by the passive damping assembly on the tubular member since both ends of the nylon line are connected to the rigid supports. Since the nylon line is flexible, a significant portion of the stretching is due to elongation of the line itself with the remainder of the stretching taking place in the spring. The dampers are installed equidistantly between the ends of the member.

As a part of the present study, the effect of both number of brushes and presence or absence of tension on the nylon line, on member damping was examined.

In addition to baseline experiments on the specimen with no damping devices, a total of ten different conditions were examined. Tests with 1,

2, 3, 5, and 7 brushes were conducted both with and without tension in the line.

### 3.2.2 Wool Swab Dampers

Figure 10 shows a wool swab damper with a 1.0 inch diameter, a total length of 3 inches and a weight of 7.1 grams. The wool swab is manufactured by Omark Industries, Onalaska, Wisconsin 54650 with a US patent 415838 and an inventory control number 076683422187. It has a threaded piece at one end with a twisted wire attached to it to which the wool swab is attached. The aluminum piece is 0.75 inches long while the wool swab has a length of 2.125 inches. This type of brush is commonly used for cleaning 12 gauge shotguns. The dampers are mounted inside the tubular member as shown in Figures 6 and 7. Tests were carried out using 1, 2, 3, 5, and 7 equidistantly spaced wool swab dampers.

### 3.2.3 Silly Putty in Chamber Dampers

The final device examined was the "silly putty" in chamber damper shown in Figure 11. It consists of a sphere approximately 0.75 inches in diameter made from silly putty placed inside a hollow cylindrical chamber. Silly putty is a trade name for an elasto-plastic material commonly used as a children's toy. It is manufactured by Binney and Smith, Inc., Easton, PA 18042, with an inventory control number of 07166208006. The chamber is made from a 1.0 in. long piece of a "Bristole Pipe" (PVC-1120, Schedule 40, ASTM-D-1785, nominal 1 inch pipe) having an original outer diameter of 1.058 in. and a wall thickness of 0.15 in. Since the damping effect was assumed to be provided by the silly putty, two steps were taken to reduce the mass of the damper thereby improving its efficiency. First, the inside diameter is increased by machining it to 0.914 in. resulting in a wall thickness of 0.07

in. Its weight is further reduced by drilling a total of seven 0.25 in. diameter holes around its periphery half-way from its ends. The silly putty is held inside the chamber by means of a plastic wrap ("Saran Wrap") stretched over the ends of the chamber and held in place with tape. The silly putty is then free to bounce around inside the chamber. The total weight of the damper including the silly putty, PCV chamber, and plastic wrap is 7.4 gms. The dampers are mounted inside the tubular member as shown in Figures 6 and 7. Tests were conducted with a nominal tension in the spring and with no tension in the spring using 1, 2, 3, 5 and 7 equidistant silly putty in chamber dampers. An additional test was performed with 11 equidistant dampers and a nominal tension in the spring.

### 3.3 Test Setup and Procedures

The instrumentation used in the tests consisted of a proximity probe, harmonic vibration devices and a deflection-time plotter. This section summarizes the test setup and procedures followed for all the experiments included in this report.

Figure 12 shows a schematic of the member natural vibration test setup. A weight,  $W = 7.9$  lb. was suspended at the member midspan by means of a cord, causing a total midspan deflection of  $5/32$  in. To induce natural vibration, the cord was cut with a pair of scissors, thereby releasing the member. The time dependent deflection at member midspan is recorded by means of a proximity probe shown in Figure 13, and connected to a deflection-time plotter.

Figure 14 shows the member forced vibration setup, a schematic of which is shown in Figure 15. Forced vibration of the specimen was obtained using a vibrator (Model 203-25-DC) with an oscillator (Model TPO-25). The

vibrator applies a forcing function of the type:

$$F(t) = F_0 \cos (\Omega t) \quad (21).$$

in which  $F_0 = 4$  lb.,  $t =$  time, and  $\Omega =$  frequency of the forcing function.

The applied frequency may be controlled using the oscillator.

The forcing function  $F(t)$  is transmitted from the vibrator to the tubular member through a fabricated vibrator connector as indicated in Figure 14. The details of this mechanical connector are shown in Figure 16. It consists of three main segments PQ, QR and RU interconnected at Q and R by means of pins. End P is connected to the vibrator. The end U is connected to the lower part of a metal hose clamp provided around the tubular member at midspan as indicated in Figure 14. The parts QR and RU can be disengaged at R by pulling out the pin RS instantaneously in the RS direction as indicated by the arrow at S. A string attached at S is used to pull out the pin. Once the pin is pulled, the arm QR drops freely and the beam is free to vibrate without constraints. Both joints Q and R are well lubricated to reduce friction. The vibrator connector in the engaged and the disengaged positions is shown in Figures 17(a) and 17(b), respectively. A record is made of the deflection-time response of the member once the forcing function,  $F(t)$ , is removed.

### 3.4 Test Results and Discussion

In this section, the results from the member natural and forced vibration tests are presented and discussed.

#### 3.4.1 Natural Vibration

All passive damping concepts were tested with natural flexural member vibration caused by releasing a weight at midspan as explained in Section 3.3. The initial midspan deflection,  $\Delta_0$ , due to the suspended weight is

0.1563 in. A summary of the test results for the tubular member with no dampers as well as with wool swab, copper brush, and silly putty in chamber dampers is given in Table 1. The number of dampers, the total weight of the damping assembly, the damping ratio and the damping efficiency index are listed for each passive damping assembly. The logarithmic decrement method, as described in Reference 8, was used with the experimentally obtained deflection versus time plots to obtain the damping ratio.

The calculation of the damping ratio for the natural vibration tests was obtained using the first sixteen cycles and reading the amplitudes directly from the experimental deflection versus time plots. Each  $\zeta$  value in Table 1 was then obtained by taking the average results of three tests for each combination of damping devices.

The efficiency index is defined (Reference 1 and 2):

$$\eta = \frac{\zeta - \zeta_0}{M_d} \quad (22)$$

in which  $\zeta$  is the damping ratio with the damping devices,  $\zeta_0$  is the damping ratio in the absence of any passive damping device, and  $M_d$  is the total mass of the damping assembly.

The natural frequency from all of the experiments was found to be 8.4 Hz. The deflection versus time plots referenced in this section are obtained using the average  $\zeta$  value and natural frequency from the experiments, and the following  $\Delta$ -t relationship (Reference 1).

$$\Delta = \Delta_0 e^{-\zeta \omega t} \left( \frac{\omega \zeta}{\omega_d} \sin \omega_d t + \cos \omega_d t \right) \quad (23)$$

The damped circular frequency,  $\omega_d$ , is given by:

$$\omega_d = \omega \sqrt{1 - \zeta^2} \quad (24)$$

The details including the listing of a computer program utilizing Equation

23 to produce a deflection versus time plot are given in Reference 1. A baseline plot of deflection versus time for the member with no dampers is shown in Figure 18.

#### 3.4.1.1 Copper Brush Dampers

For the copper brush dampers the maximum  $\zeta = 0.0131$  is obtained with an assembly of three damping devices. This assembly produces the maximum  $\eta = 16.72$  in/lb-sec<sup>2</sup>. Figure 19 shows the corresponding average  $\Delta$ -t plot for a 10 second duration. Figure 20 shows the effect of the three copper brushes on the deflection time envelopes. The vertical ordinate in this figure is designated by  $\Delta_e$  to indicate that the figure represents the envelopes rather than the complete  $\Delta$ -t relationship. The damping ratios from the experiments are given in Table 2(a). In addition to the test conducted as described in Section 3.3, a series of tests were made with no tension in the damping assembly. These tests, conducted with 1, 2, 3, 5 and 7 devices in the specimen showed no significant increase in member damping regardless of the number of devices used. The results are summarized in Table 2(b). One plausible explanation for this is as follows. The outer diameter of the copper brush is less than the inside diameter of the member. When there is no tension in the damping assembly, the devices are free to bounce inside the specimen. Because the vibrations are relatively small and the natural frequency low, the assembly with no tension has a tendency to move with the specimen, bouncing slightly inside the member. Due to the relatively negligible mass of the damper as compared to the member this nearly coincident movement produces minimal damping of the vibration. With a slight tension in the assembly, it can have its own natural frequency, different from the specimen. As a result, when vibration of the specimen is

induced, the impact of the damping assembly with the side of the tube sets the assembly in motion. Two types of motion then contribute to the damping. First, because of the difference in natural frequency of vibration impact of the dampers against the inside of the tubular member acts to damp the vibration. Secondly, the frictional interaction between the dampers and the member inside surface takes place while the dampers vibrate both in plane but out of phase, and axially. When the number of dampers is increased beyond three with nominal tension, the damping ratio decreases.

#### 3.4.1.2 Wool Swab Dampers

For the wool swab dampers the maximum  $\zeta = 0.0105$  was obtained with an assembly of three dampers resulting in an efficiency of  $9.05 \text{ in/lb-sec}^2$ . The maximum  $\eta = 12.34$  was obtained with a single damper assembly yielding a damping ratio of  $0.0099$ . Figures 21 and 22 represent the  $\Delta$ -t plots for the member with three, and one wool swab damper assemblies, respectively for a 10 second duration. Figures 23 and 24 show the effects of these damping assemblies on the deflection-time envelopes. The damping ratio increased as the number of dampers was increased from one to three. Increasing the number of devices beyond three resulted in a decrease in both damping ratio and efficiency. The small negative efficiency noted for seven devices can be taken as practically zero. It was found that a variation in the method of attachment of the assembly to test specimen from concentric to an eccentric connection had no significant effect on the resulting damping ratio. The results are given in Tables 3(a) and 3(b).

#### 3.4.1.3 Silly Putty in Chambers Dampers

For silly putty in chambers dampers, the maximum  $\zeta = 0.0115$  was obtained with an assembly of three dampers resulting in a  $\eta = 15.73 \text{ in/lb-}$

sec<sup>2</sup>, whereas the maximum  $\eta = 21.35$  in/lb-sec<sup>2</sup> was obtained with an assembly of two dampers corresponding to  $\zeta = 0.0113$ . Figures 25 and 26 represent the  $\Delta$ -t plots for the member with three and two silly putty in chamber damper assemblies, respectively, for 10 second duration. Figures 27 and 28 show the effects of these damping assemblies on the deflection-time envelopes. The damping ratio was found to increase as the number of dampers was increased from one to three. Increasing the number of dampers beyond three resulted in a decrease of both damping ratio and efficiency. The tests conducted with no tension in the assembly showed a slight increase in damping ratio up to the three damper assembly. An increase in the number of dampers beyond three with no tension on the assembly showed no increase in damping ratio above the baseline damping ratio for the empty member. The results are given in Tables 4(a) and 4(b). Of all the passive damping devices tested in this study, the assembly of three silly putty in chamber dampers was found to be the most efficient. Therefore, these dampers were chosen for further study under forced harmonic vibration.

### 3.5 Forced Then Free Vibration

It was discovered during testing that the vibration employed for the forced vibration tests allowed only a limited amount of travel. This meant that the deflection of the member at the location where the vibrator was attached was limited to what the vibrator would allow. Nevertheless, forced vibration tests were conducted on the individual member since it was not known initially whether or not the dynamic deflection would exceed the vibrator capacity. The results presented later in this section indicated that the vibrator constrained the member deflection for a certain range of forcing function frequencies including that which would otherwise have



constituted a resonance condition. This limitation must be taken into account when evaluating the performance of the dampers on an individual member.

### 3.5.1.1 Silly Putty in Chamber Dampers

The results of the experimental study of the member under forced then free vibration are summarized in Table 5. Tests were conducted with no dampers, and 1, 2, and 3 dampers inside the member. Each of these assemblies was subjected to a force of 4 lb. at the member midspan, at frequencies of 2, 5, 7, and 9 Hz, corresponding to  $\Omega/\omega_n$  ratios of 0.238, 0.596, 0.834, and 1.073, respectively. An additional test was conducted on the empty member and the 3 damper assembly using a frequency of 12 Hz ( $\Omega/\omega_n = 1.430$ ). The experimental results are shown in Figures 29 through 32. The free vibration part of the deflection-time graph is obtained by disengaging the forcing function from the member midspan as described in Section 3.3. The constrained dynamic deflection amplitude,  $\Delta^*_D$ , and its dimensionless value,  $\Delta^*_D/\Delta_S$ , where  $\Delta_S$  is the calculated static midspan deflection due to a 4 lb. load, are listed in Table 5. The constrained dynamic deflection amplitude is the measured amplitude of the initial constrained force part of the deflection-time plots. Also listed in Table 5 are the maximum initial free vibration amplitudes,  $\Delta_F$ , for each assembly and frequency considered. Two dimensionless quantities are derived from this value as  $\Delta_F/\Delta_S$  and  $\Delta_F/\Delta^*_D$ . The data in Table 5 shows that the  $\Delta^*_D/\Delta_S$  values range from 0.59 to 0.95. For all the cases, the maximum value was observed for an applied force frequency of 5 Hz. It was also found that the  $\Delta_F/\Delta_S$  and  $\Delta_F/\Delta^*_D$  ratios were gradually increasing for increasing forcing function frequencies. One important consequence of the deflection constraint imposed

by the vibrator is that no resonance phenomenon could be produced in the vicinity of 8.4 Hz. The average damping ratios were obtained from the free vibration part of the deflection-time curves and are listed in Table 5. As seen from this data, the single silly putty in chamber damper configuration provides the maximum decrease in free vibration amplitude. Another important observation to be made is that the  $\zeta$  values in Table 5 are significantly less than the corresponding values for the same damping assemblies given in Table 1. This is attributable to the dependence of the damping ratio on the initial velocity which is considerably greater for the results reported in Table 5 than for those in Table 1.

### 3.5 Comparison of Damping Efficiencies

In Section 3.4, the efficiency index based on Equation 22 was computed for each damping device. The average values of  $\eta$  and the associated damping assembly weight for natural vibration were presented in Table 1. Figure 33 shows the curves between  $\eta$  and the weight of dampers used in the natural vibration tests for various damping concepts. The silly putty in chamber dampers provided the most efficient damping of the member. It is worth noting that all of the curves have ascending and descending portions which define the maximum attainable damping efficiency. In general, an increase in damping assembly weight beyond 50 grams results in a decline in efficiency.

Figure 34 shows the relationships between the damping efficiency and the number of damping devices for natural vibration using all three concepts. These curves also show that, in general, an assembly of more than three damping devices results in a decline in efficiency. This may indicate that the first and second mode shapes are dominating the dynamic response.

By applying the dampers to locations in the vicinity of maximum deflection for these mode shapes, the maximum efficiency was realized. Any increase in the number of dampers beyond three adds mass to the system, and is associated with a decrease in damping.

The average damping efficiency indices for the forced then free vibration tests for 1, 2, and 3 silly putty in chamber dampers are given in Table 5. The maximum efficiency was obtained using one silly putty in chamber damper and a forcing function frequency of 5 Hz. No correlation between the maximum efficiency and the initial vibration amplitude was observed. However, the maximum average damping ratio for each device was found to occur near the theoretical resonance of the member (between 7 and 9 Hz) in spite of the inability of the apparatus to allow the resonance to occur.

## 4. NUMERICAL STUDY

### 4.1 Natural Vibration

#### 4.1.1 Finite Element versus Experiment

The formulation and solution algorithm using Newmark's method for computing the dynamic response of a beam was given in Section 2. In this section, a comparison is made of the deflection versus time relations from this finite element analysis to those obtained experimentally.

A preliminary study showed that for  $\Delta t = 0.0001$  sec., the central difference formulation described in Section 2.3 gave precisely the same results as Newmark's method. Since Newmark's method provides accurate results even with larger time steps, it was used to produce Figure 35 through 43. Figure 35 shows a comparison of the finite element and experimental  $\Delta$ -t plots for the member with no dampers. The solid line is the finite element solution and the dashed line is the experimental curve using a frequency of 8.4 Hz and the average damping ratios from Table 1. Figure 36 shows a comparison of the finite element and experimental  $\Delta$ -t plots for the member with 3 copper brush dampers. In both of these curves, it can be seen that the period of the vibration obtained using finite elements is exaggerated by approximately 32%. However, the amplitudes of the vibration are accurate to within 5%.

#### 4.1.2 Finite Element versus Finite-Difference

The  $\Delta$ -t curves representing the finite-difference solution are obtained using the computer program developed in Reference 2. Figures 37 and 38 show the comparison of the finite element and the finite-difference solutions for the member with no dampers and three copper brush dampers, respectively. The data for these plots is obtained from Table 1. As indicated in these

figures, the difference in the period calculated by these two methods is approximately 26%. However, the amplitudes of the vibration from the two analyses are within 3% of each other. Figure 39 is a comparison of the finite-element and finite difference solutions for a simply supported beam ( $k_1 = k_2 = 0$ ). Similar correlation is also observed for a fixed end beam ( $k_1 = k_2 = \infty$ ). In the presence of end connections of intermediate fixity, the two analyses provide somewhat differing results.

#### 4.2 Forced then Free Vibration

In this section, curves obtained from the finite element solution for various forcing function frequencies are given. Also, a comparison of the theoretical solution to experimental results is made for both the member with no dampers and the member with one silly putty in chamber damper at a forcing function frequency of 2 Hz.

Figure 40 shows the response using Newmark's method for a beam with no dampers and subjected to a 4 lb. force at a frequency of 2 Hz. After 1 second, the forcing function is removed and the beam is allowed to vibrate freely. Figure 41 shows the response of the same system with a forcing function frequency of 6 Hz. This frequency corresponds to a frequency ratio  $\Omega/\omega_{fe}$  of 0.95, where  $\omega_{fe} = 6.3$  Hz is the natural frequency of the beam from the finite element solution. Clearly, this represents a nearly resonant condition as expected. After 1 second, the forcing function is removed and the member is allowed to vibrate freely.

Figures 42 shows the finite element and experimental curves for the member with no dampers and subjected to a 4.0 lb. force at a frequency of 2 Hz. Although the forced vibration portions of the two curves at  $\Omega = 2$  Hz are quite similar, the free vibration amplitudes differ significantly. The

reasons for this difference may be as follows. In the experiment, the forcing function was terminated by pulling the pin RS from the vibrator connector shown in Figure 16. During the tiny time interval in which the pin was being pulled out, the contact and frictional forces involved in disengaging the segment QR from RU were unintentionally transferred to the members thereby retarding its initial amplitude in the free vibration range. Consequently, the ensuing envelope of the experimental free vibration  $\Delta$ -t curve is considerably narrower than the theoretical one. Similar effects are observed in Figure 43 which shows the finite element and experimental results when one silly putty in chamber damper is used.

At larger  $\Omega$  values such as those of the order of 6 Hz, the  $\Delta$ -t relations from the finite element analysis do not match the experimental ones even in the forced vibration range. This is primarily due to the constraints imposed by the vibrator on the maximum member deflecting as explained earlier in Section 3.5.

#### 4.3 Finite Element Analysis for Forced Vibration

As mentioned earlier, the vibrator used in the experimental study constrained the motion of the member in the presence of a forcing function. As a result, the actual effect of passive damping could not be observed for this condition. Therefore, a numerical study was conducted to examine the effect of passive damping in the presence of the forcing function. In this section, the theoretical results showing both the extent of damping which would occur during the forced vibration and the effect of the dampers on the deflection-time envelopes are presented and discussed. Figure 44 shows the theoretical dynamic magnification factor (DMF),  $\Delta_D/\Delta_S$ , versus the frequency ratio  $\Omega/\omega_n$  for damping ratios of 0.0094, 0.0131 and 0.50. The first two

values of the damping ratios were obtained from the member tests with no dampers, and 3 copper brush dampers, respectively. As can be seen in this figure, the copper brush dampers do not change the DMF appreciably for non-resonance frequency ratios. However, the dampers reduce the DMF by approximately 7% at resonance.

Figure 45 shows the deflection versus time relationship for the member with no dampers and with three copper brush dampers, with a forcing function frequency of 6.35 Hz ( $\Omega/\omega_n = 1.0$ ) for one second, and allowed to vibrate freely thereafter. These curves show that the passive damping results in a member amplitude reduction in the forced vibration range, however, its most beneficial effect occurs during the free vibration. After 3 seconds of free vibration, the amplitudes of the member with dampers are approximately 40% less than those corresponding to the empty member.

## 5. CONCLUSIONS AND FUTURE RESEARCH

### 5.1 Conclusions

The following conclusions are drawn from the research conducted herein:

1. The silly putty in chamber concept provides the maximum passive damping efficiency under member natural vibration, as compared to the copper brush or the wool swab concepts.
2. The copper brush concept provides the largest damping ratio of the system under natural vibration.
3. Due to the limitation of the vibrator used, the effectiveness of the passive damping concepts could not be evaluated until the forcing function was disengaged.
4. Frictional and contact forces acting on the member during disengagement from the vibration apparatus caused a reduction of the ensuing free vibration member amplitude.
5. The theoretical results indicate that in the presence of a forcing function, the passive damping devices provide the most effective damping in the vicinity of the resonant frequency.
6. The theoretical results show that passive dampers are considerably more effective under member natural vibration than during forced vibration.
7. Under natural vibration, the finite element solution results in periods which are nearly 30 percent greater than the experimental ones. However, amplitudes are reasonably accurate. The accuracy of the results is improved when the member ends are pinned or fixed.



## 5.2 Future Research

The most successful passive damping concepts identified herein should be examined using forced vibration equipment which would allow investigation of their effectiveness at or near resonance. Attempts should be made to identify a means of disengaging an applied force without adversely affecting the dynamic response of the member. These tests should be conducted on both individual members and structure sub-assemblies.

## REFERENCES

1. Razzaq, Z., El-Aridi, N.F., Passive Damping Concepts for Low Frequency Tubular Members. Progress Report submitted to NASA Langley Research Center Under Research Grant NAG-1-336, NASA Technical Monitor: Harold G. Bush, August 1986.
2. Razzaq, Z., Ekhelikar, R.K., Passive Damping Concepts for Slender Columns in Space Structures. Progress Report Submitted to NASA Langley Research Center Under Research Grant NAG-1-336, May 1985.
3. Razzaq, Z., Passive Damping concepts for Slender Columns in Space Structures. Progress Report submitted to NASA Langley Research Center Under Research Grant NAG-1-336, February 1985.
4. Razzaq, Z., Passive Damping concepts for Slender Columns in Space Structures. Progress report submitted to NASA Langley Research Center Under Research Grant NAG-1-336, August 1984.
5. Razzaq, Z., Voland, R.T., Bush, H.G., and Mikalas, M.M., Jr., Stability, Vibration and Passive Damping of Partially Restrained Imperfect Columns. NASA Technical Memorandum 85697, October 1983.
6. Cook, R.D., Concepts and Applications of Finite Element Analysis, 2nd Ed., John Wiley and Sons, Inc., New York, 1974.
7. Paz, M., Structural Dynamics: Theory and Computations, 2nd Ed., Van Norstrand Reinhold, New York, 1985.
8. Clough, R.W., Pension, Jr., Dynamics of Structures, McGraw-Hill Book Co., New York, 1975.

## TABLES

Table 1. Member natural vibration test results for copper brush, wood swab, and silly putty in chamber dampers.

PASSIVE DAMPING CONCEPT	NUMBER OF DAMPERS	WEIGHT OF DAMPING ASSEMBLY (GM)	AVERAGE DAMPING RATIO $\zeta$	DAMPING EFFICIENCY INDEX (IN/LB. - SEC <sup>2</sup> )
No Dampers		0.00	0.0094	0.00
Copper	1	13.0	0.0098	5.39
Brush	2	26.0	0.0107	8.76
Dampers	3	39.0	0.0131	16.72
	5	65.0	0.0129	9.44
	7	91.0	0.0097	0.48
Wool	1	7.10	0.0099	12.34
Swab	2	14.20	0.0102	9.87
Dampers	3	21.30	0.0105	9.05
	5	35.50	0.0101	3.46
	7	49.70	0.0091	-0.99
Silly	1	7.8	0.0100	13.48
Putty	2	15.6	0.0113	21.35
in	3	23.4	0.0115	15.73
Chamber	5	39.0	0.0109	6.74
Dampers	7	54.6	0.0097	0.96
	11	85.8	0.0094	0.00

Table 2(a): Damping ratios from natural vibration tests with copper brushes and no cord tension.

Number of Devices	$\zeta_1$	$\zeta_2$	$\zeta_3$	$\zeta_{AVG}$
1	0.0097	0.0095	0.0095	0.0096
2	0.0097	0.0097	0.0097	0.0097
3	0.0098	0.0096	0.0096	0.0097
5	0.0094	0.0096	0.0094	0.0095
7	0.0095	0.0095	0.0096	0.0095

Table 2(b). Damping ratios from natural vibration tests with copper brushes and nominal cord tension.

Number of Devices	$\zeta_1$	$\zeta_2$	$\zeta_3$	$\zeta_{AVG}$
1	0.0097	0.0102	0.0096	0.0098
2	0.0105	0.0109	0.0108	0.0107
3	0.0133	0.0128	0.0131	0.0131
5	0.0129	0.0131	0.0128	0.0129
7	0.0096	0.0098	0.0095	0.0096

Table 3(a). Damping ratios for natural vibration tests with wool brushes and concentric cord support.

Number of Devices	$\zeta_1$	$\zeta_2$	$\zeta_3$	$\zeta_{AVG}$
1	0.0098	0.0097	0.0098	0.0098
2	0.0100	0.0098	0.0101	0.0100
3	0.0107	0.0108	0.0101	0.0105
5	0.0096	0.0100	0.0097	0.0098
7	0.0094	0.0094	0.0094	0.0094

Table 3(b). Damping ratios for natural vibration tests with wool brushes and eccentric cord support.

Number of Devices	$\zeta_1$	$\zeta_2$	$\zeta_3$	$\zeta_{AVG}$
1	0.0099	0.0099	0.0098	0.0099
2	0.0103	0.0101	0.0101	0.0102
3	0.0105	0.0105	0.0105	0.0105
5	0.0099	0.0102	0.0102	0.0101
7	0.0093	0.0090	0.0090	0.0091

Table 4(a). Damping ratios for natural vibration tests with silly putty and no cord tension.

Number of Devices	$\zeta_1$	$\zeta_2$	$\zeta_3$	$\zeta_{AVG}$
1	0.0096	0.0097	0.0096	0.0096
2	0.0099	0.0099	0.0102	0.0100
3	0.0101	0.0101	0.0101	0.0101
5	0.0095	0.0095	0.0093	0.0094
7	0.0094	0.0092	0.0096	0.0094

Table 4(b). Damping ratios for natural vibration tests with silly putty and nominal cord tension.

Number of Devices	$\zeta_1$	$\zeta_2$	$\zeta_3$	$\zeta_{AVG}$
1	0.0104	0.0096	0.0100	0.0100
2	0.0112	0.0115	0.0113	0.0113
3	0.0112	0.0115	0.0117	0.0115
5	0.0109	0.0109	0.0109	0.0109
7	0.0096	0.0099	0.0096	0.0097
11	0.0094	0.0094	0.0094	0.0094

Table 5. Member forced then free vibration test results for silly putty in chamber dampers.

Passive Damping Concept	Forcing Function Frequency (Hz)	Constrained Dynamic Amplitudes $\Delta_D^*$ in.	$\Delta_D^* / \Delta_S$	Initial Free Vibration Amplitude $\Delta_F$ max in	$\Delta_F / \Delta_S$	$\Delta_F / \Delta_D^*$	Average Damping Ratio $\zeta$ Avg.	$\eta$
No Dampers	2	0.067	0.84	0.030	0.38	0.45	0.0043	
	5	0.073	0.92	0.067	0.84	0.91	0.0072	
	7	0.070	0.88	0.077	0.97	1.10	0.0073	
	9	0.067	0.84	0.082	1.03	1.23	0.0069	
	12	0.047	0.59	0.082	1.03	1.75	0.0025	
1 Silly Putty in Chamber Damper	2	0.062	0.78	0.030	0.38	0.48	0.0058	33.7
	5	0.073	0.92	0.063	0.80	0.86	0.0089	38.2
	7	0.067	0.84	0.070	0.88	1.05	0.0089	36.0
	9	0.067	0.84	0.073	0.92	1.10	0.0080	24.17
2 Silly Putty in Chamber Damper	2	0.065	0.82	0.030	0.39	0.48	0.0049	6.7
	5	0.075	0.95	0.060	0.76	0.80	0.0069	(-3.4)
	7	0.067	0.84	0.053	0.67	0.80	0.0076	3.4
	9	0.065	0.82	0.083	1.05	1.28	0.0080	12.4
3 Silly Putty in Chamber Damper	2	0.063	0.80	0.030	0.38	0.47	0.0057	10.5
	5	0.075	0.95	0.057	0.71	0.76	0.0055	(-12.7)
	7	0.068	0.86	0.077	0.97	1.12	0.0064	(-6.7)
	9	0.068	0.86	0.090	1.14	1.32	0.0082	9.7
	12	0.047	0.59	0.082	1.03	1.75	0.0036	8.2



**FIGURES**

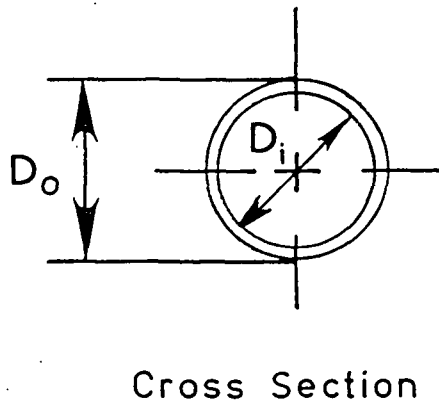
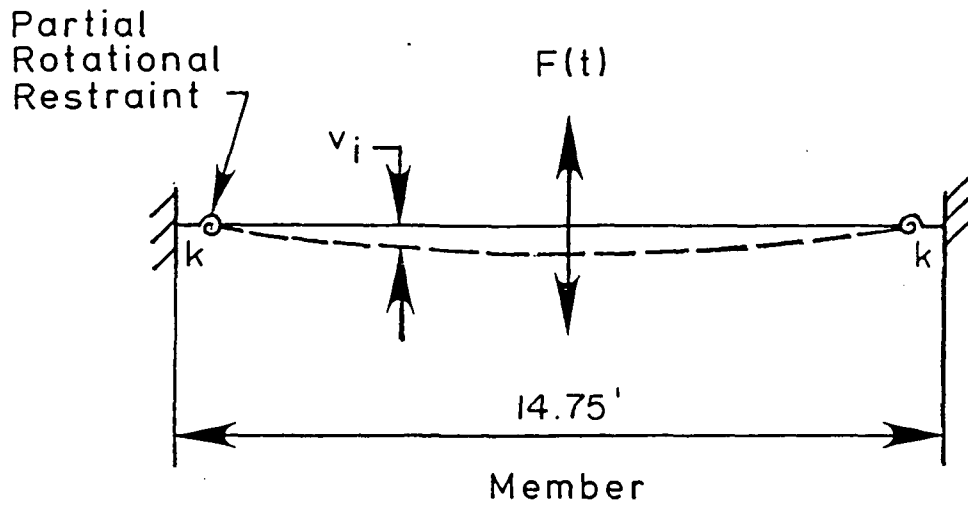


Figure 1. Schematic of tubular member

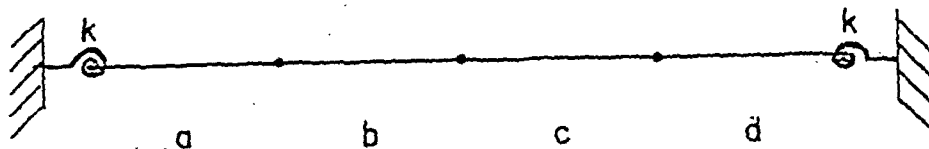


Figure 2. Example of finite element model for the beam.

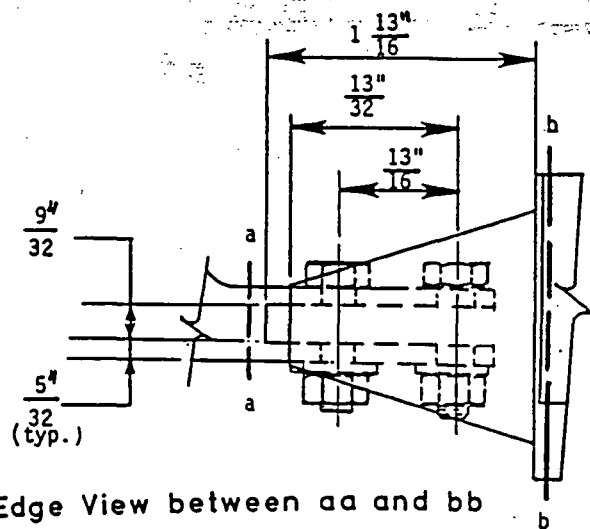
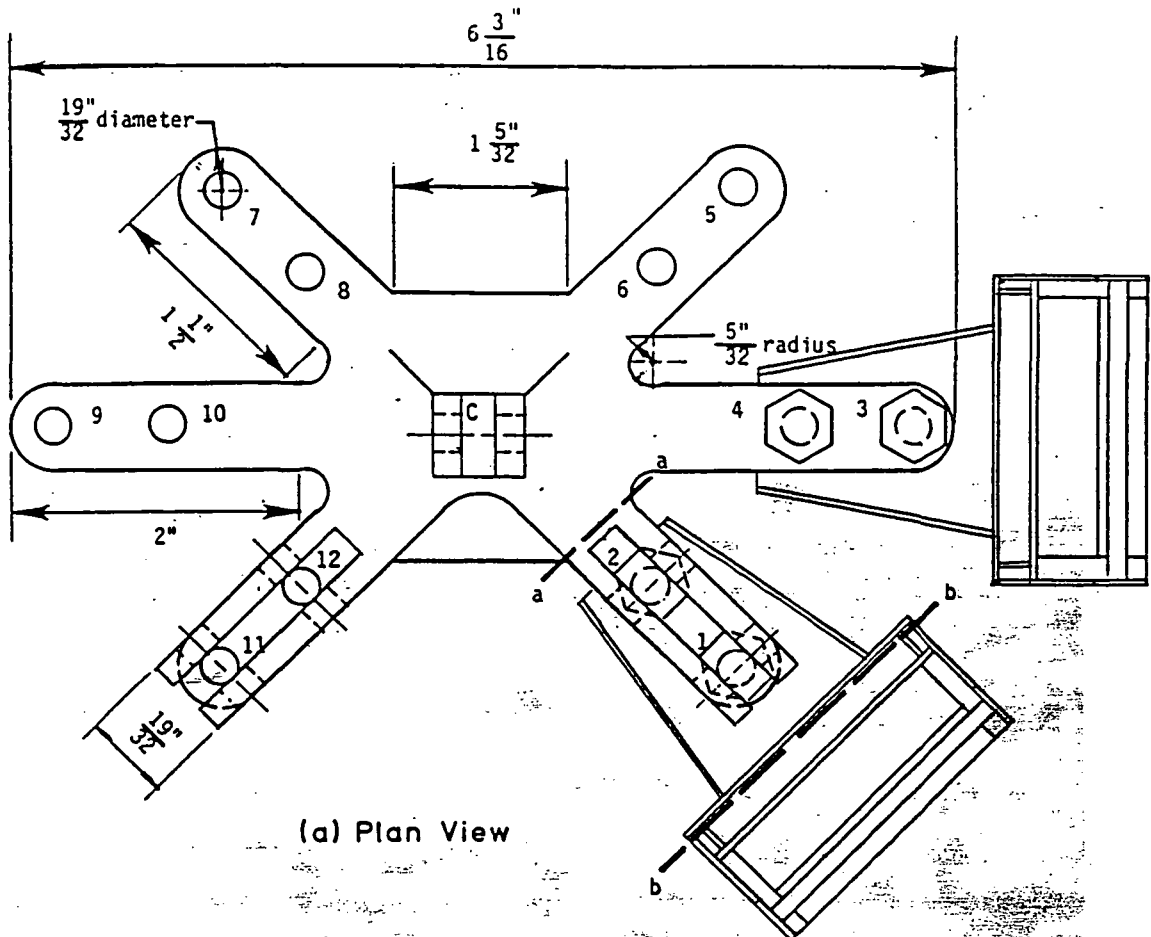


Figure 3. Some end connection details

ORIGINAL PAGE IS  
OF POOR QUALITY

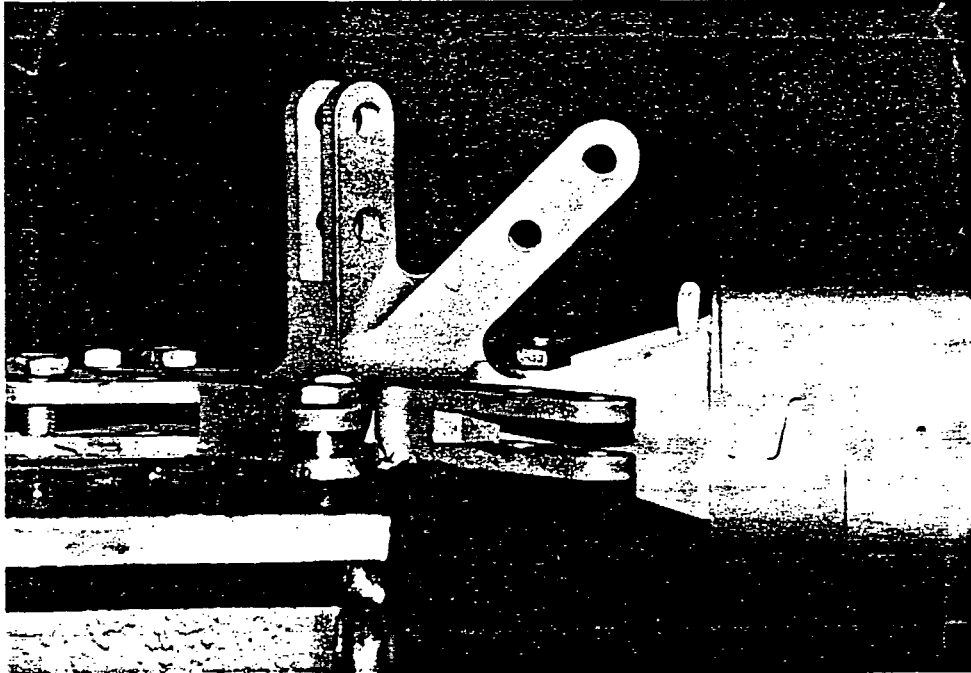


Figure 4. Member end connection

ORIGINAL PAGE IS  
OF POOR QUALITY

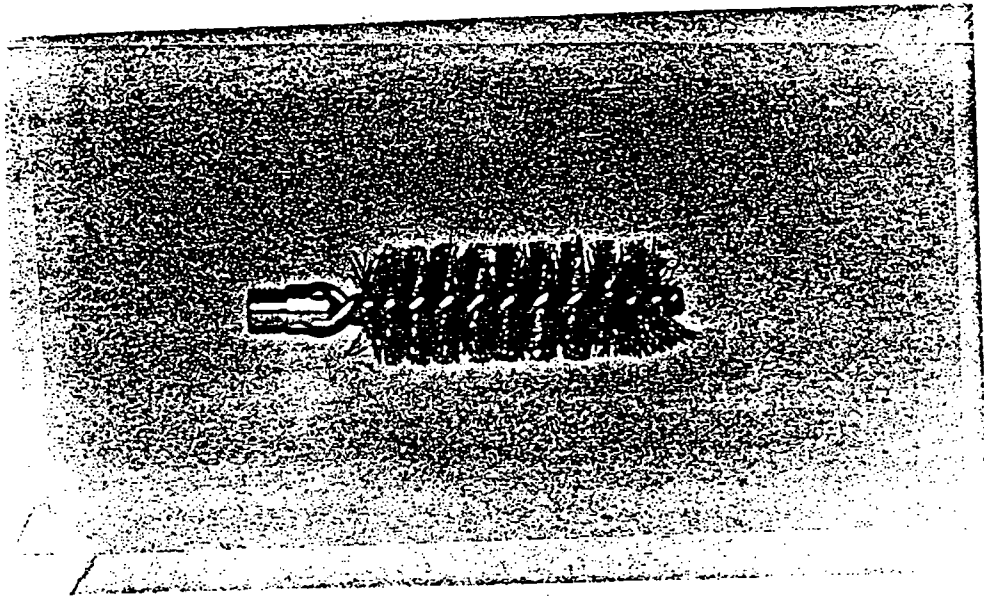


Figure 5. Copper brush damper

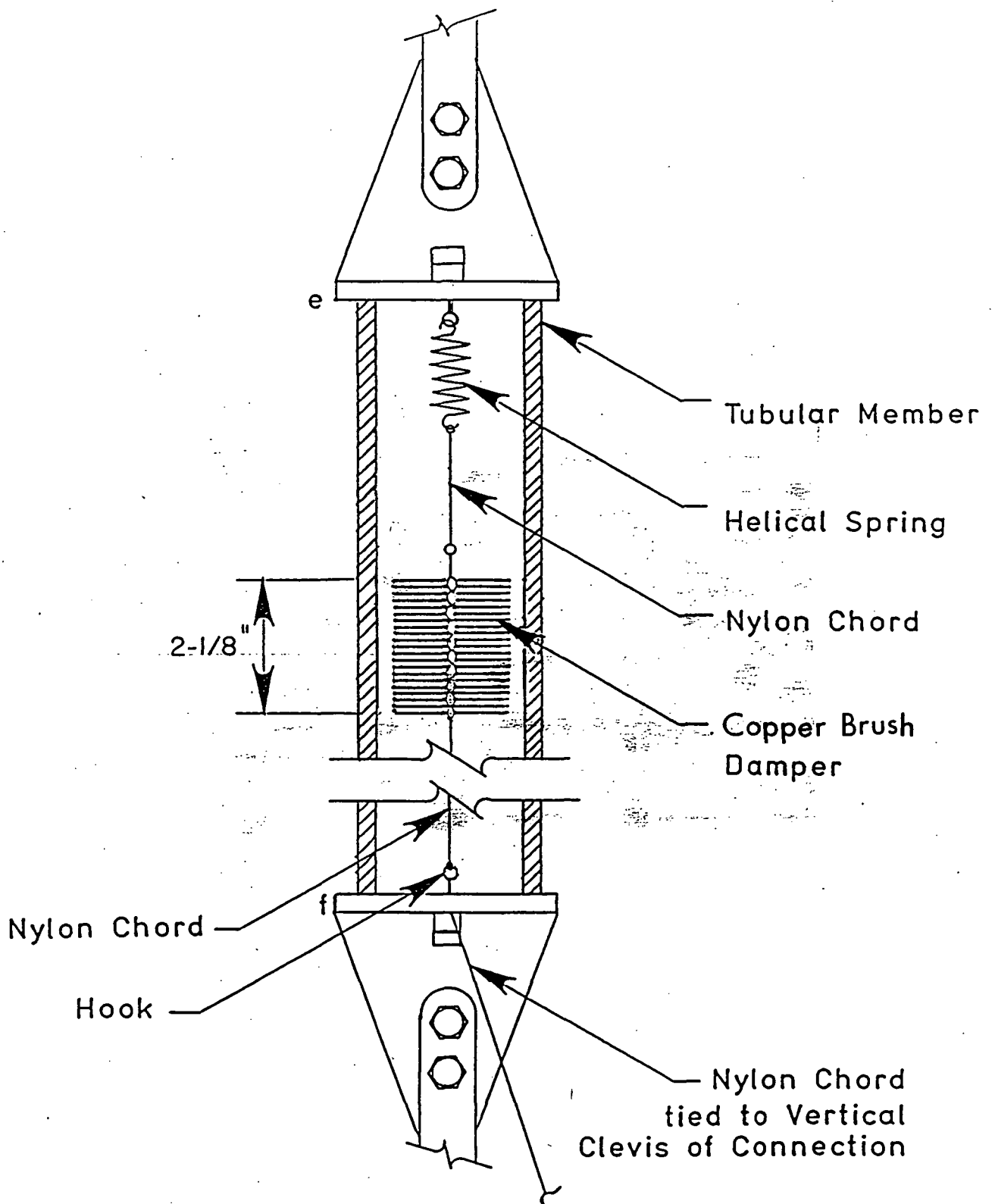


Figure 6. Schematic of attachments for passive damper inside tubular member

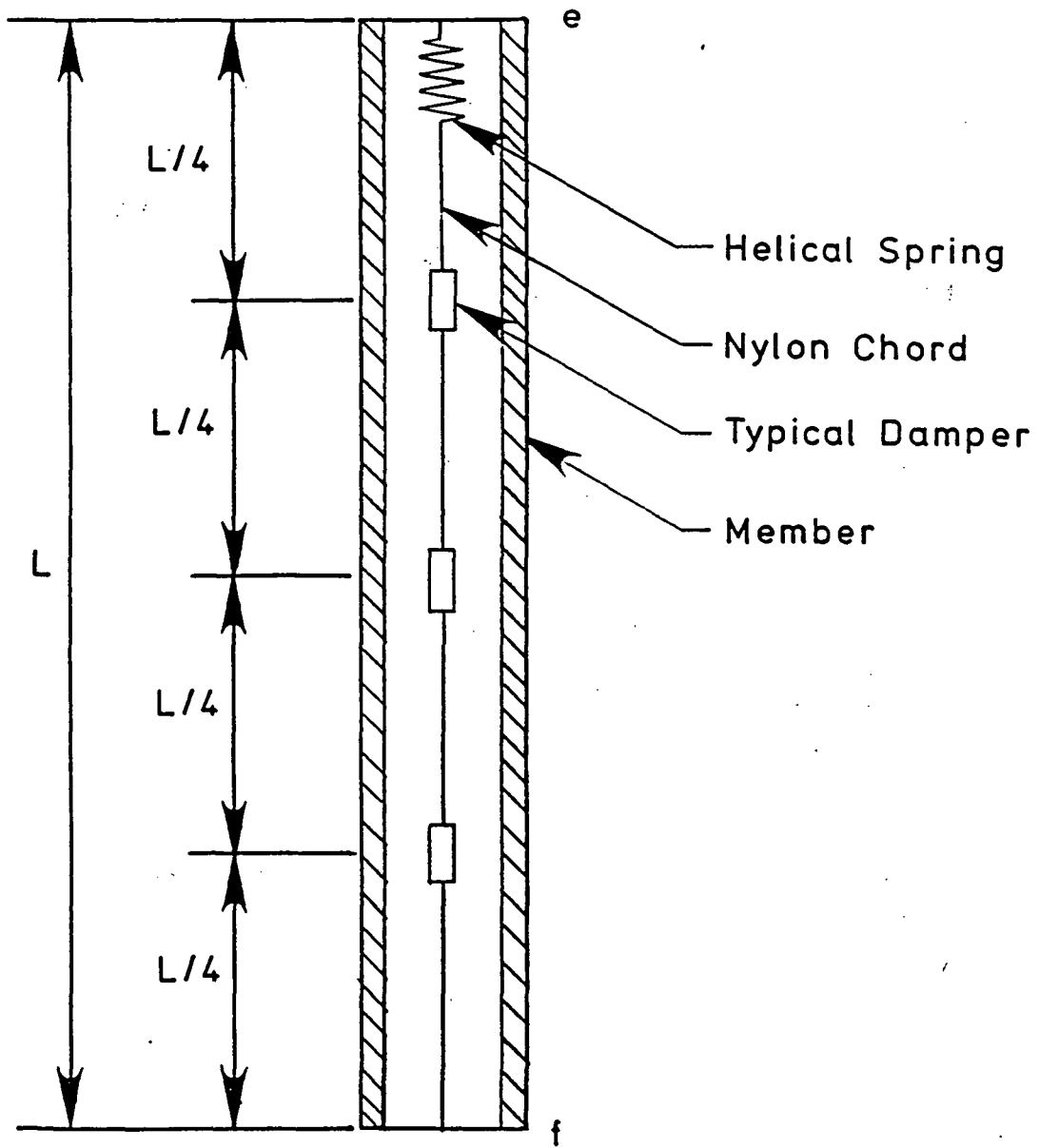


Figure 7. Schematic for spacing of passive dampers



ORIGINAL PAGE IS  
OF POOR QUALITY

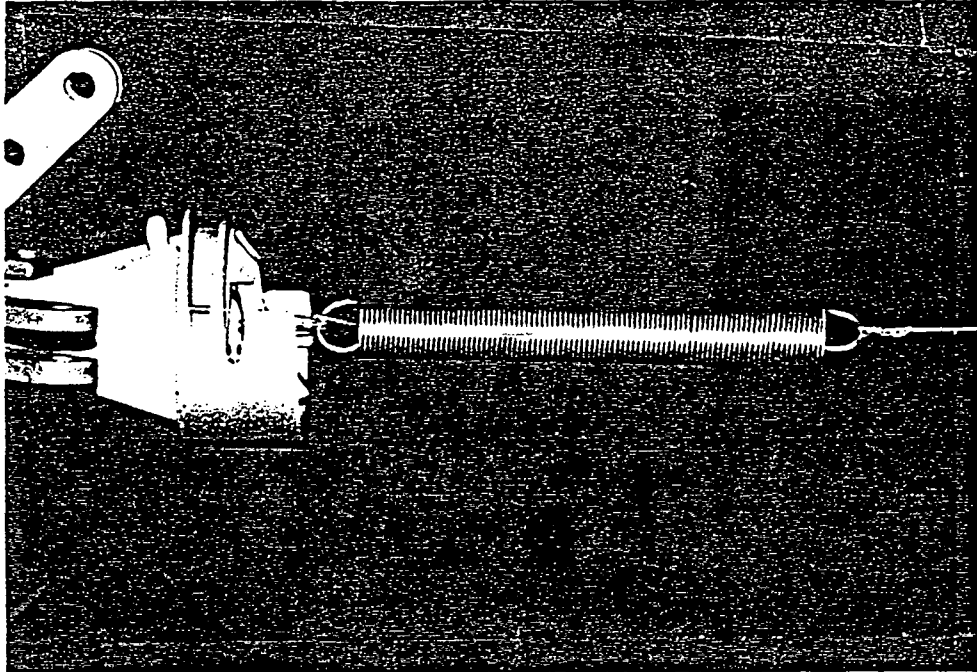


Figure 8. Helical spring attachment at end e

ORIGINAL PAGE IS  
OF POOR QUALITY

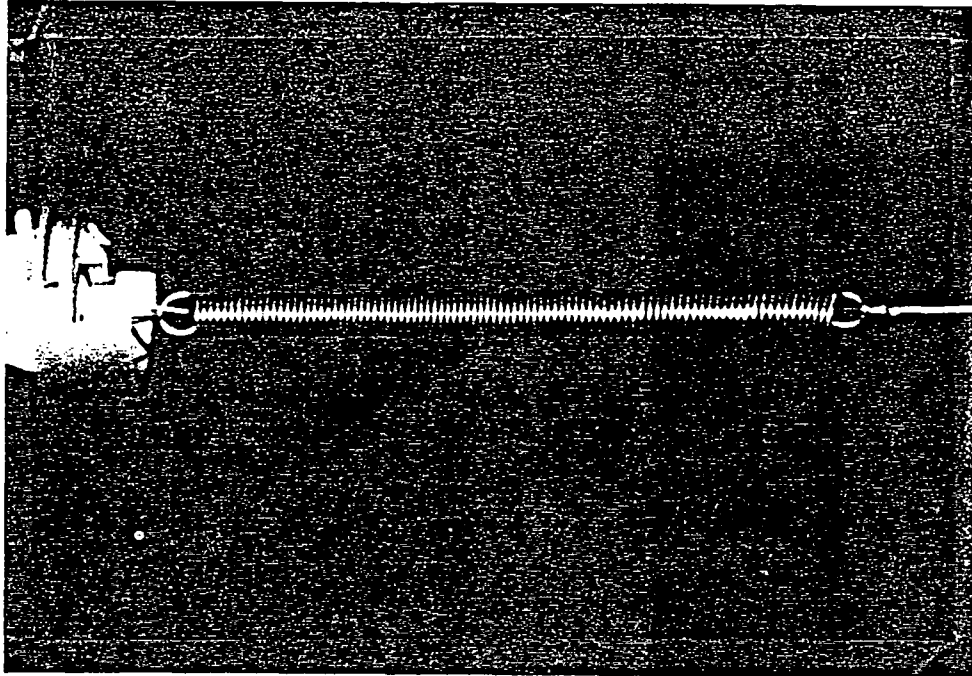


Figure 9. Stretched helical spring at end e

ORIGINAL PAGE IS  
OF POOR QUALITY

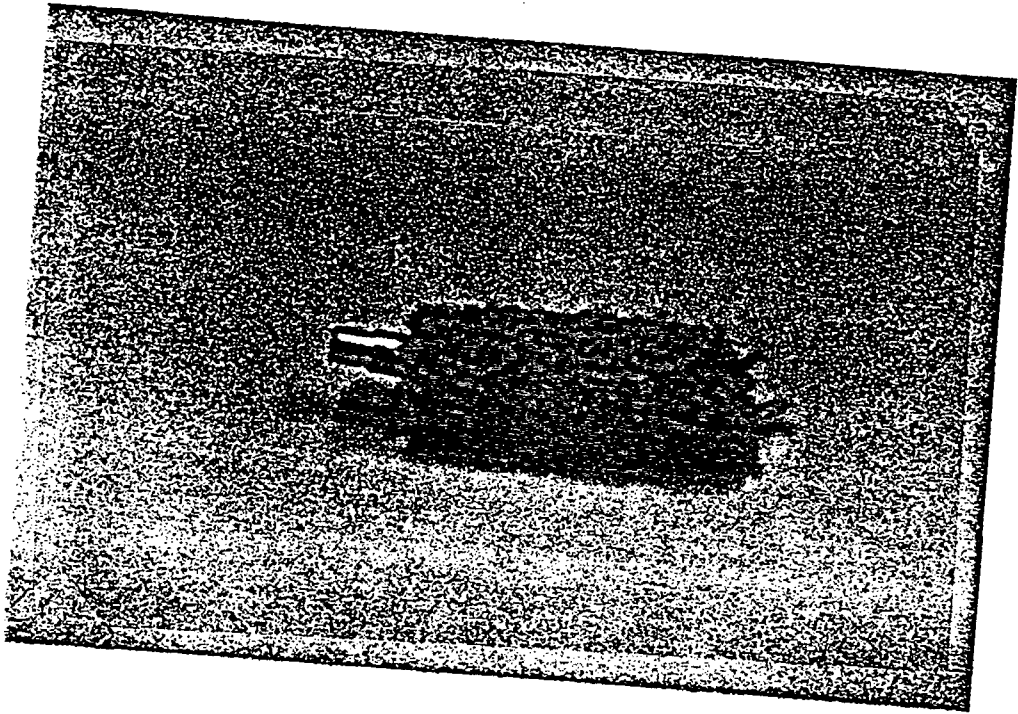


Figure 10. Wool swab damper

ORIGINAL PAGE IS  
OF POOR QUALITY

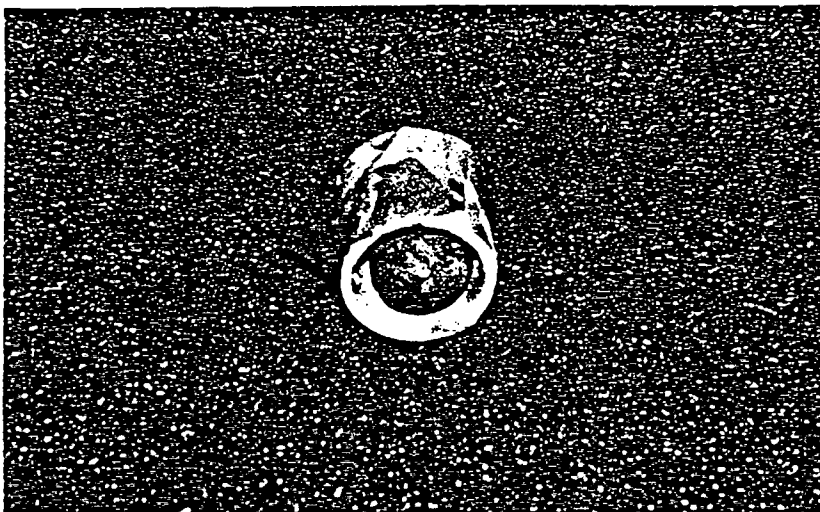


Figure 11. Silly putty in chamber damper

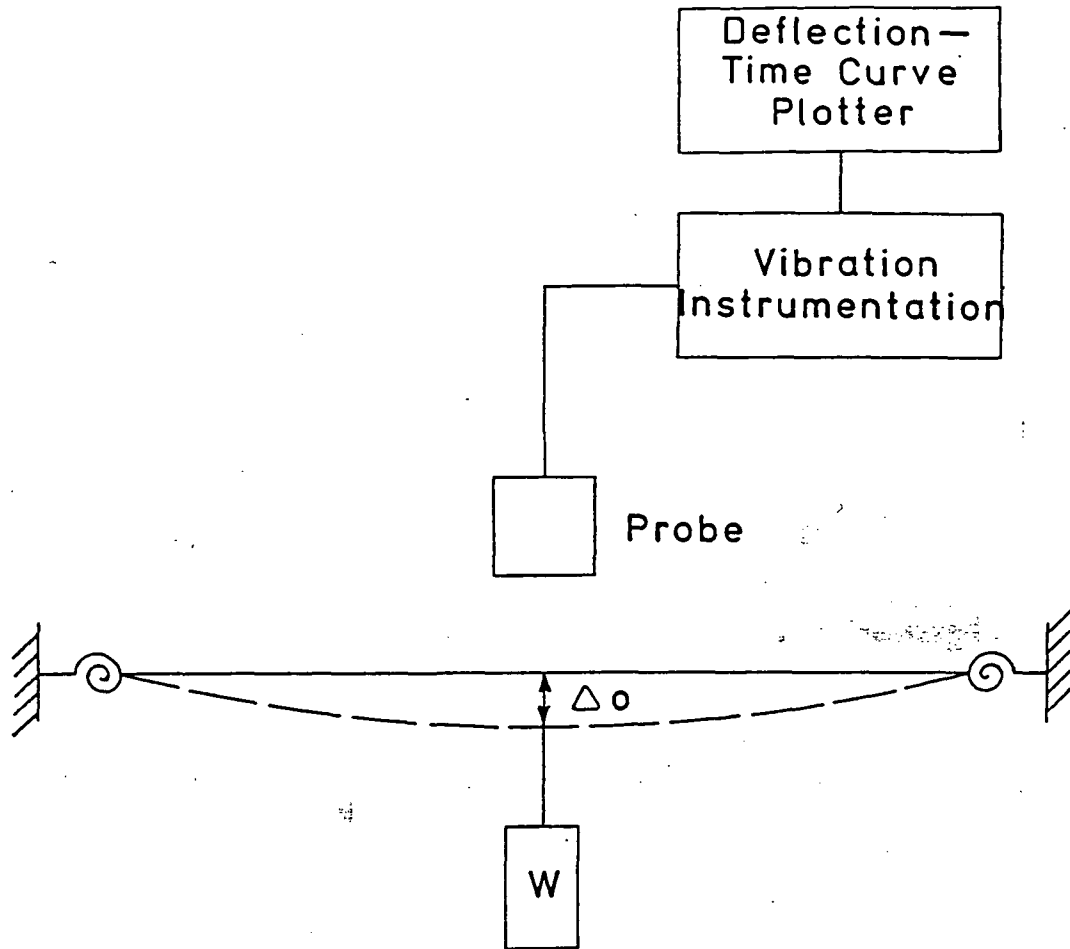


Figure 12. Schematic of member natural vibration setup

ORIGINAL PAGE IS  
OF POOR QUALITY

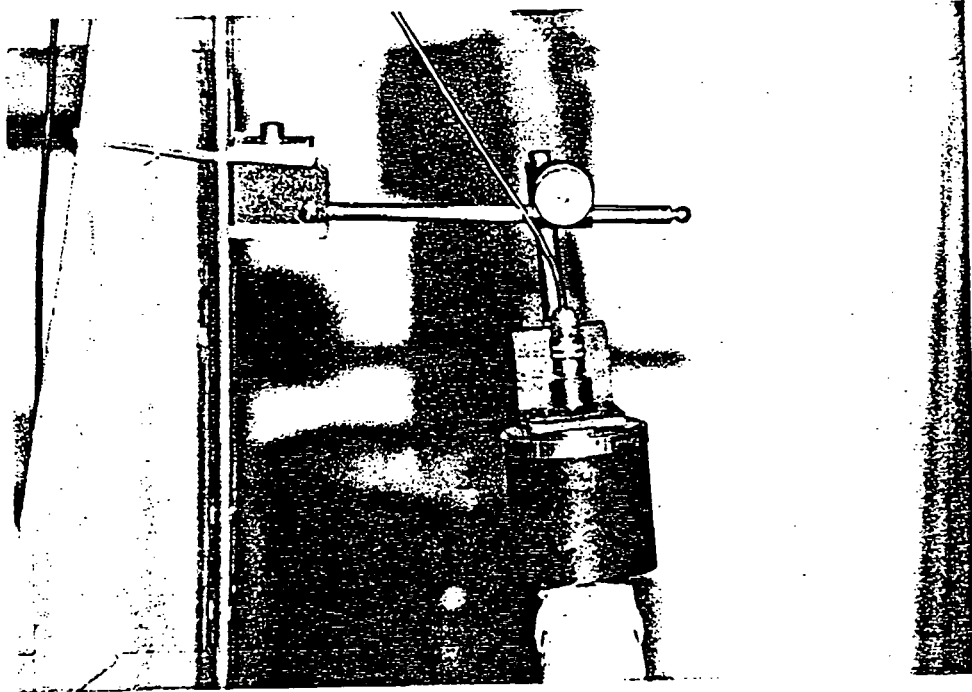


Figure 13. Proximity probe

ORIGINAL PAGE IS  
OF POOR QUALITY

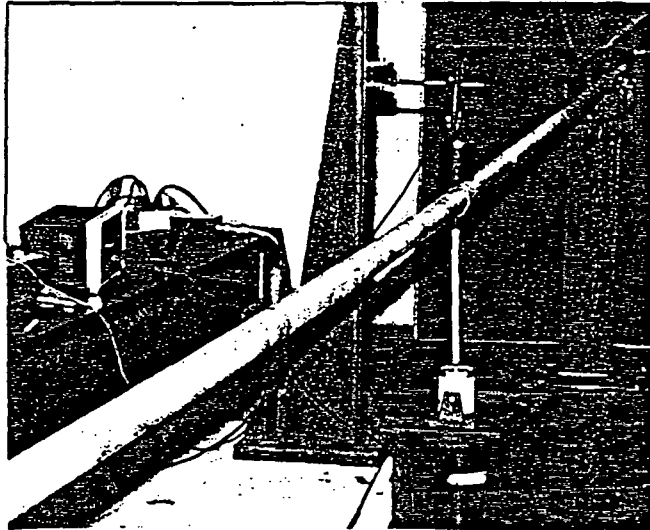


Figure 14. Member forced vibration setup

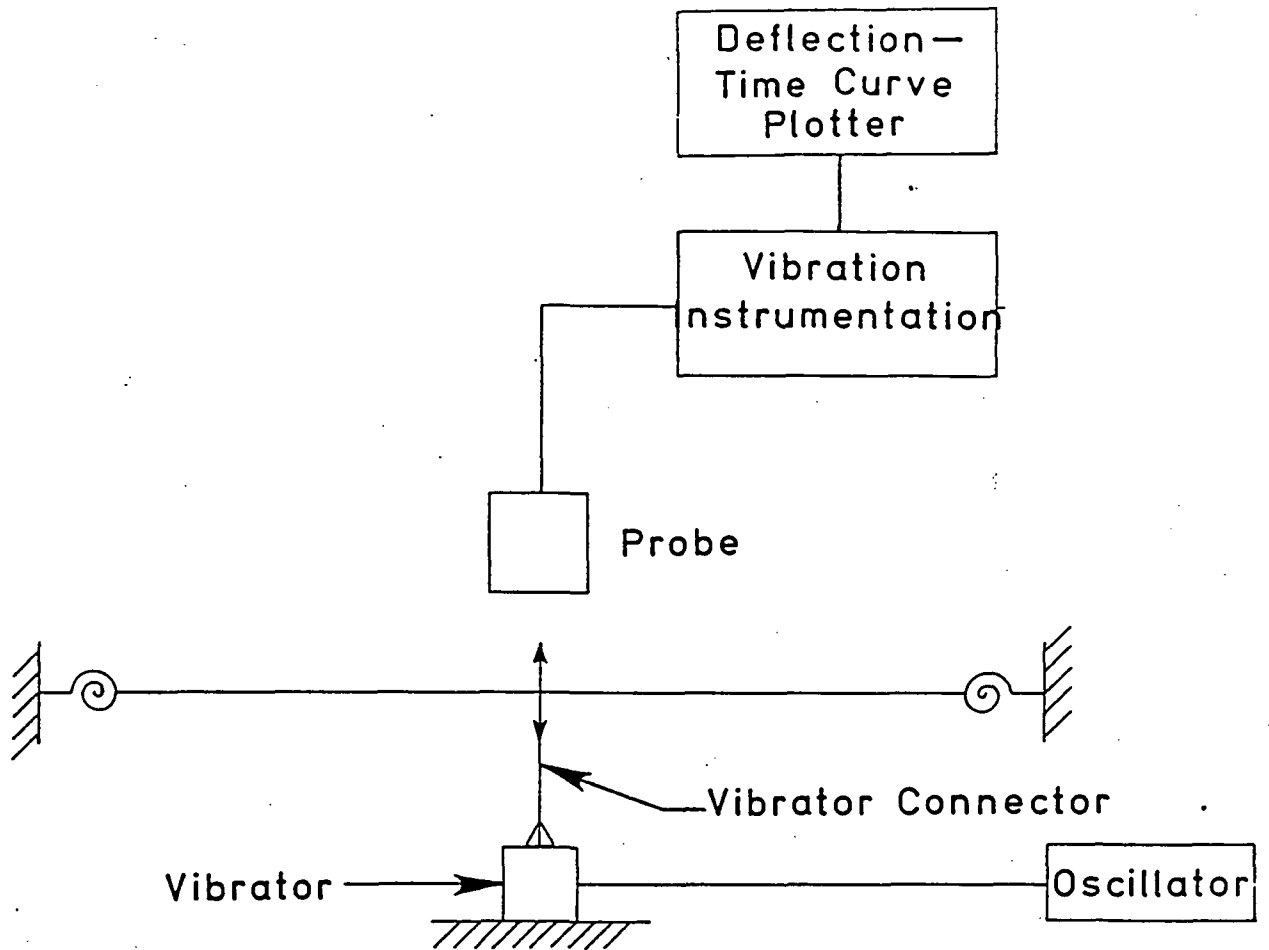


Figure 15. Schematic of member forced vibration setup



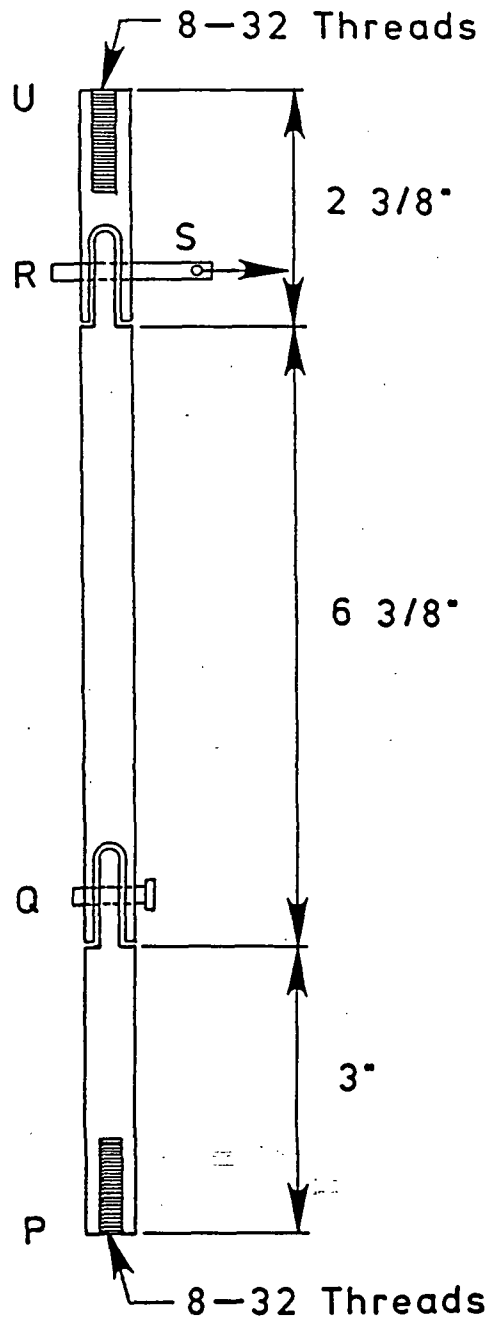
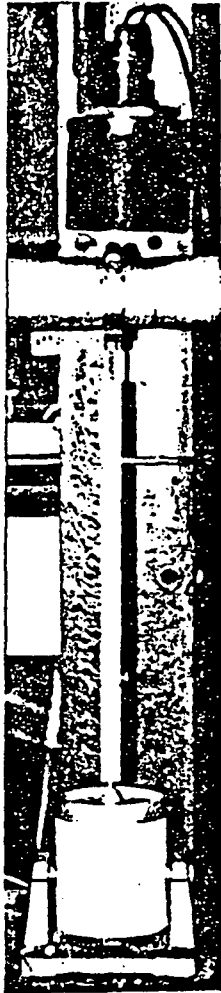


Figure 16. Vibrator connector details

ORIGINAL PAGE IS  
OF POOR QUALITY



(a) Vibrator connector  
in engaged position



(b) Disengaged vibrator  
connector

Figure 17. Vibrator connector in engaged and  
disengaged positions

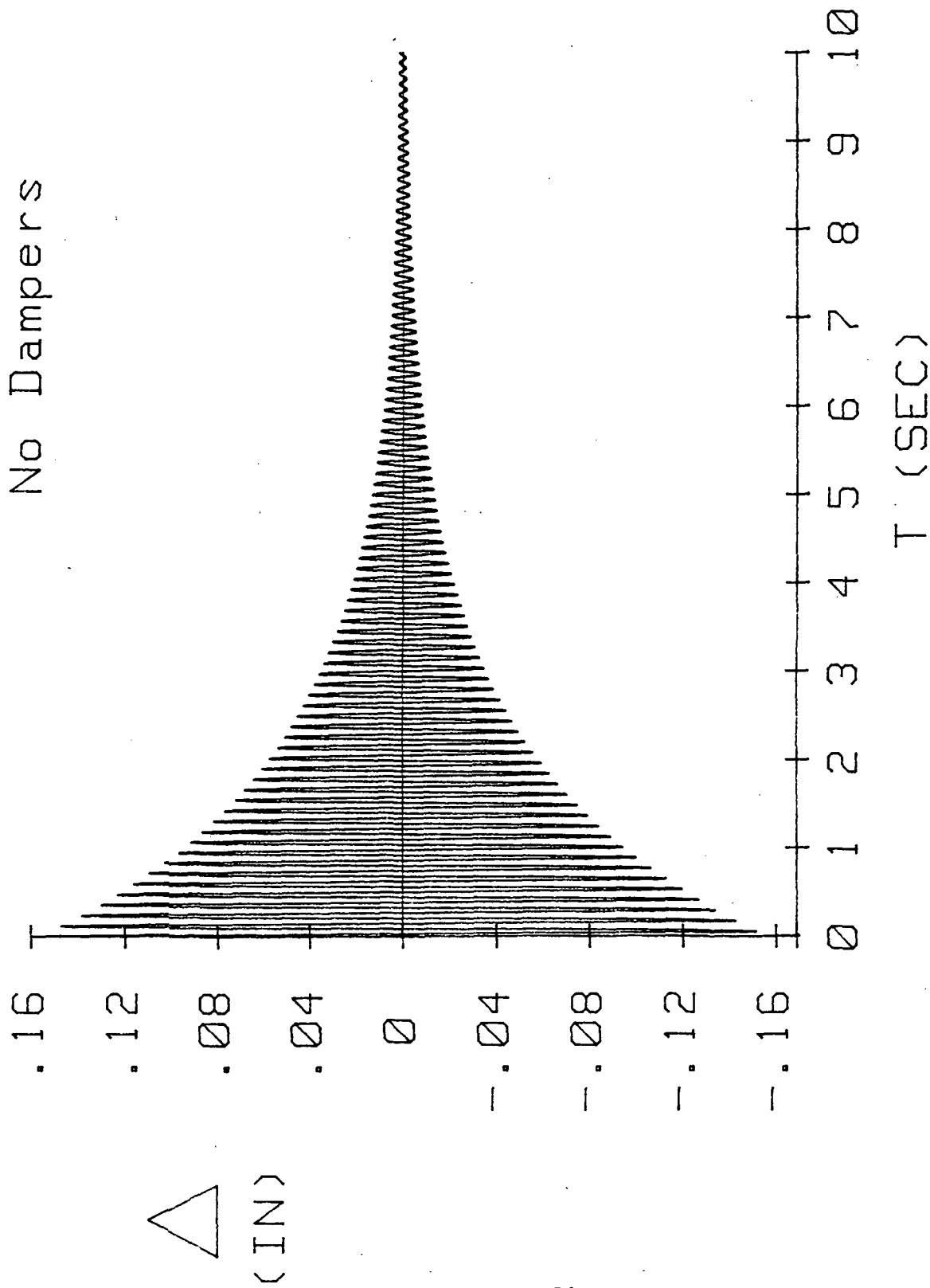


Figure 18. Average  $\Delta$ -t plot for member with no dampers.

# 3 Copper Brush Dampers

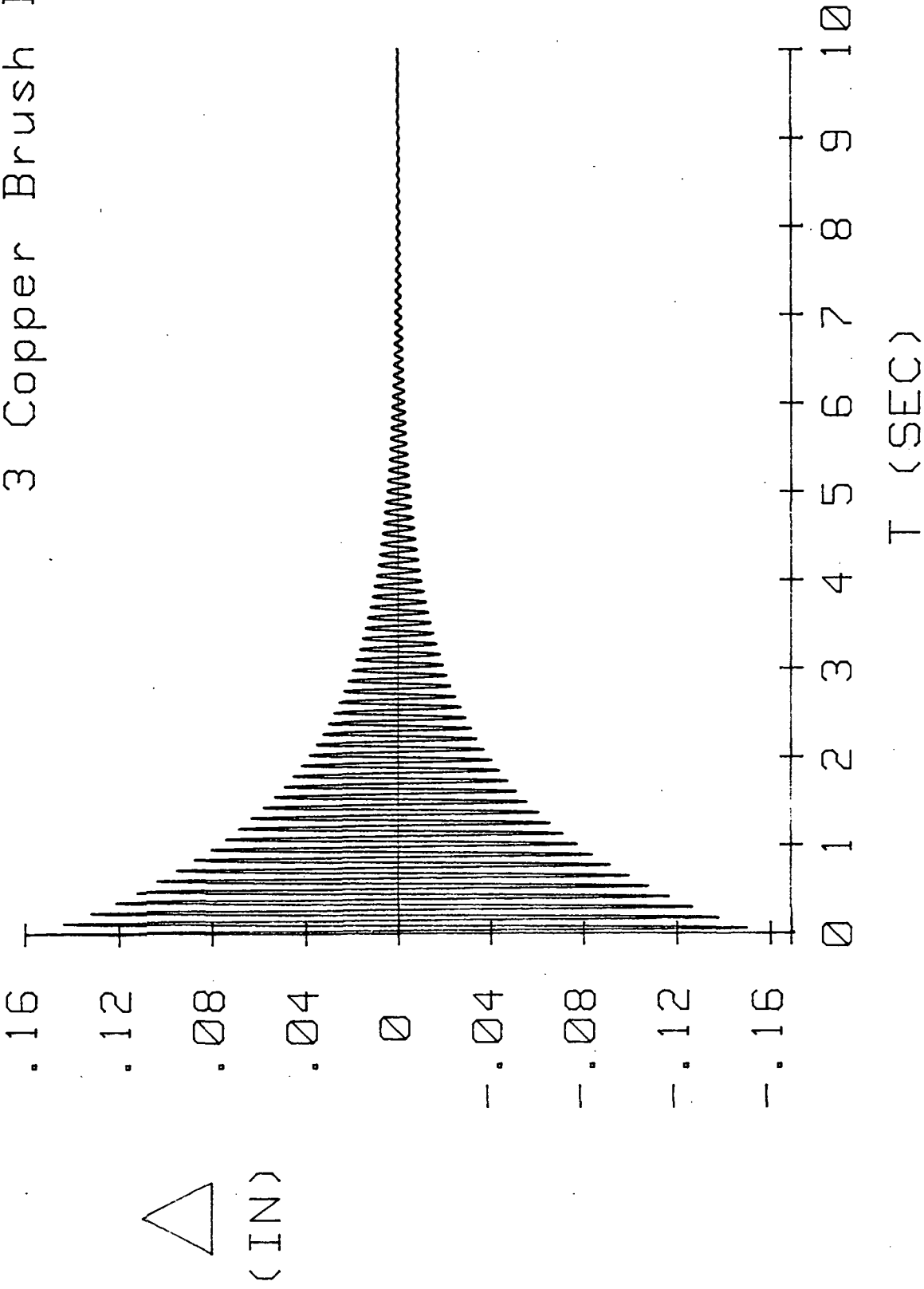


Figure 19. Average  $\Delta$ -t plot for member with 3 copper brush dampers.

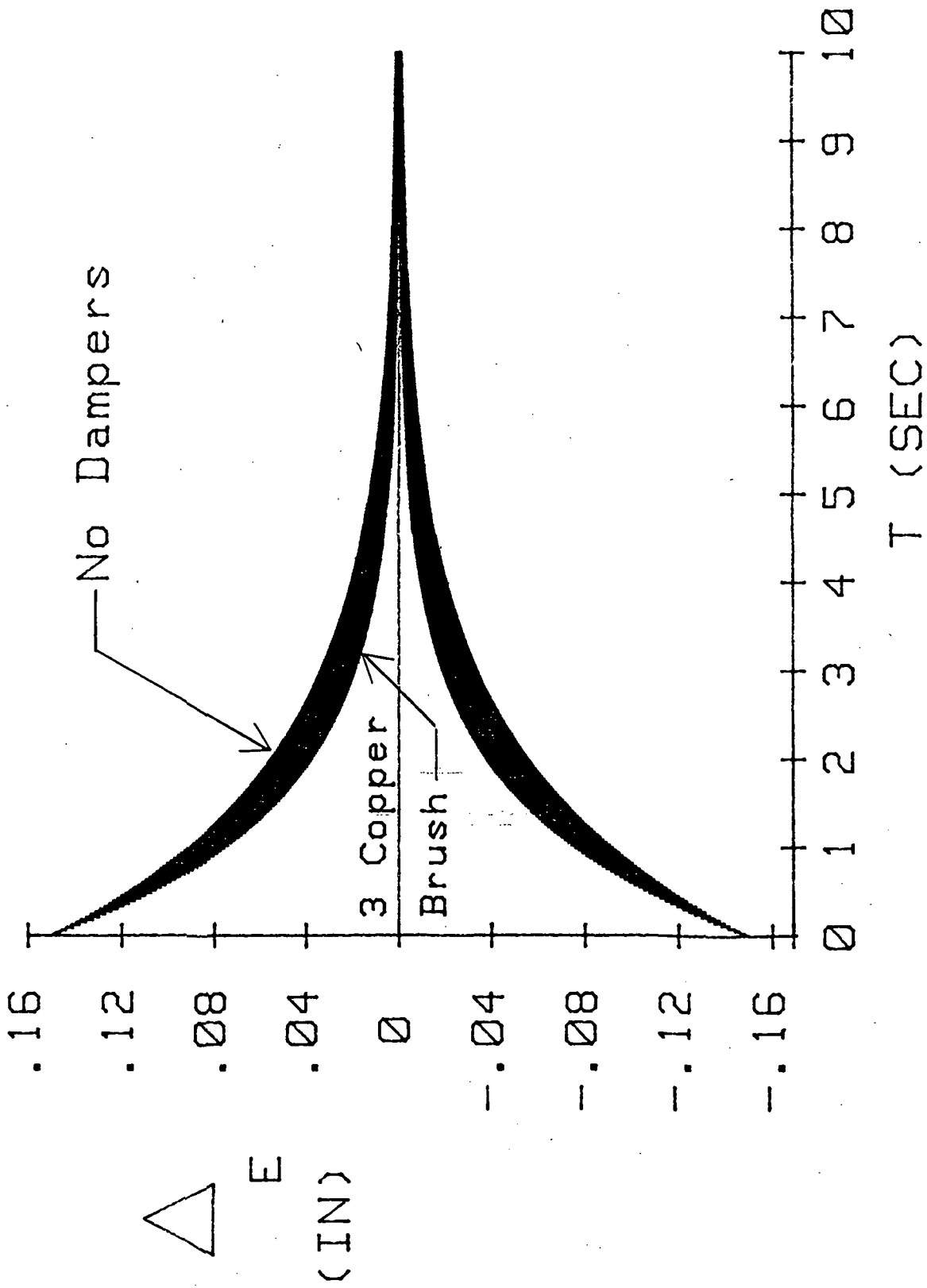


Figure 20. Effect of 3 copper brush dampers on  $\Delta$ -t envelope.

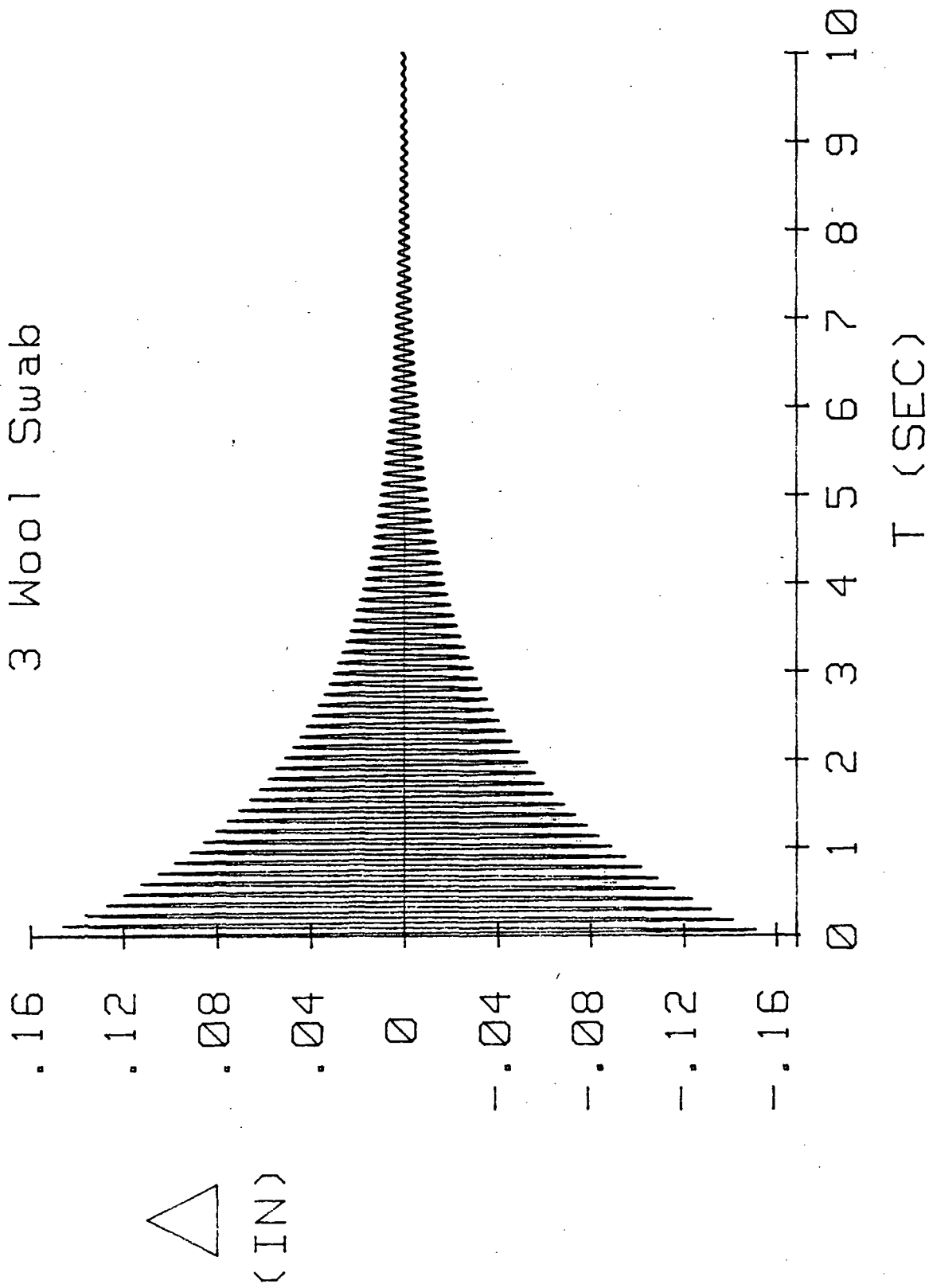


Figure 21. Average  $\Delta$ -t plot for member with 3 wool swab.

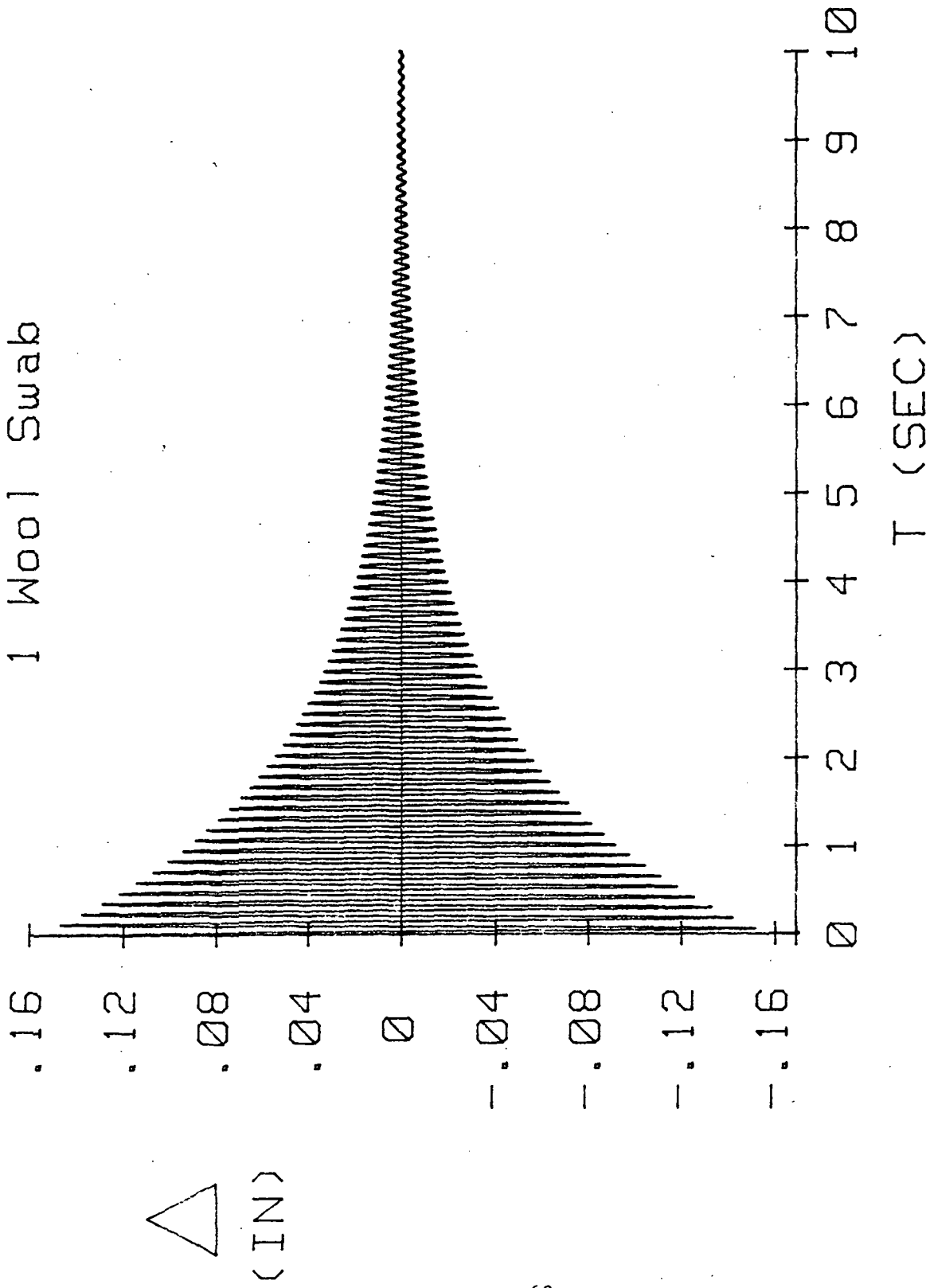


Figure 22. Average  $\Delta$ -t plots for members with 1 wool swab damper.

1107-ess

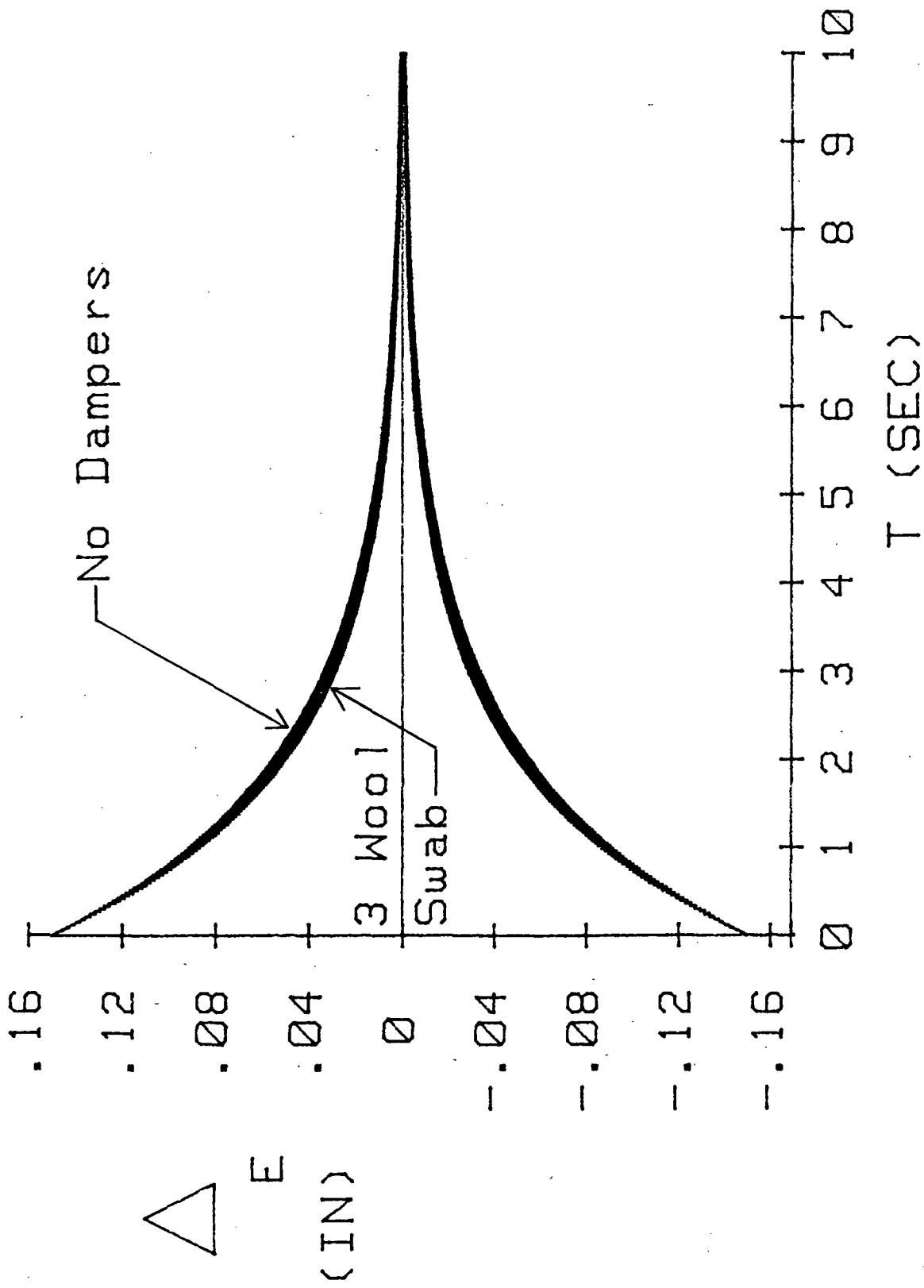


Figure 23. Effect of 3 wool swab dampers on  $\Delta$ -t envelope.



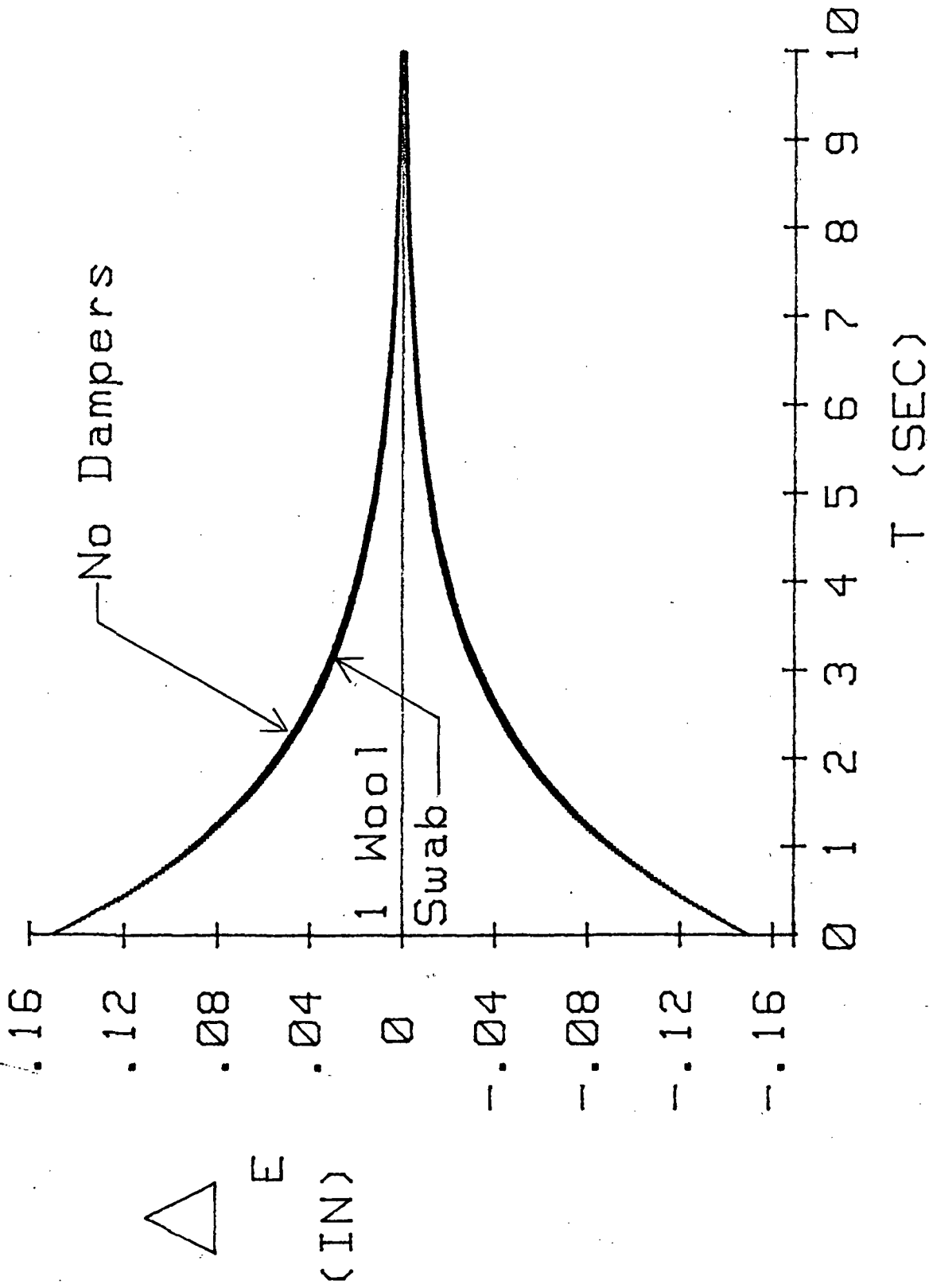


Figure 24. Effect of 1 wool swab damper on  $\Delta$ -t envelope.

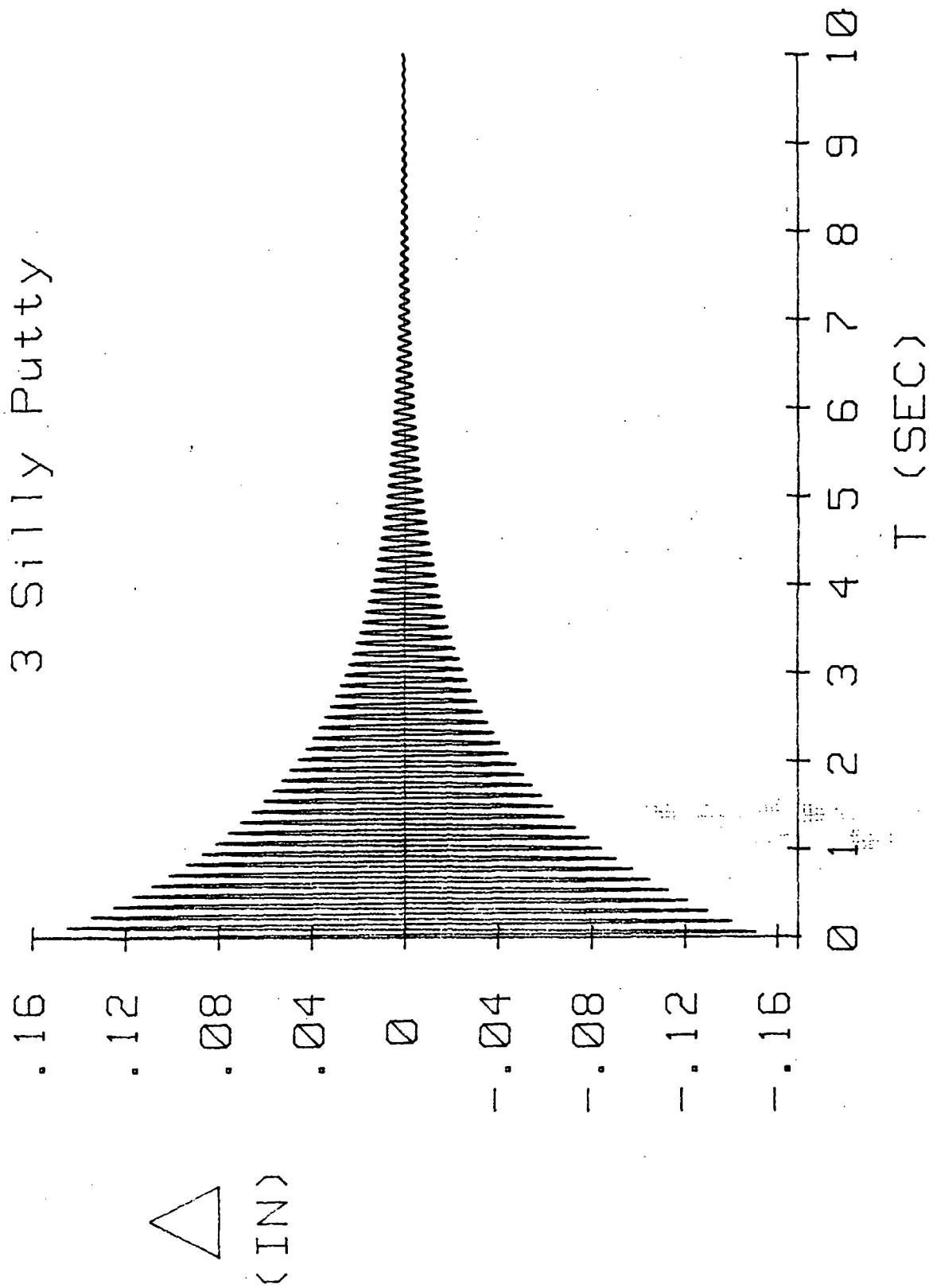


Figure 25. Average  $\Delta$ -t plot for member with 3 silly putty in chamber dampers.

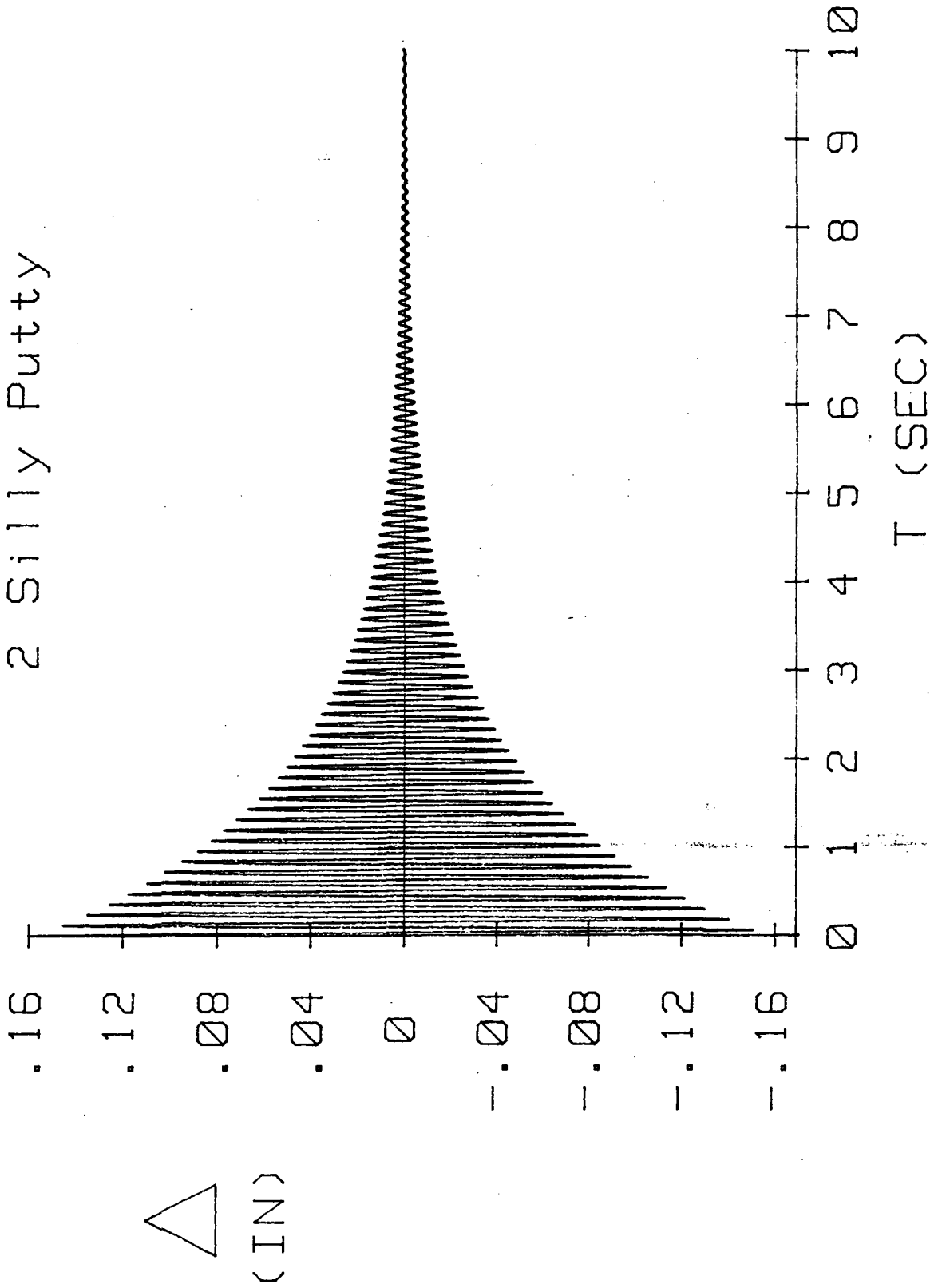


Figure 26. Average  $\Delta$ -t plot for member with 2 silly putty in chamber dampers.

MOST EFF

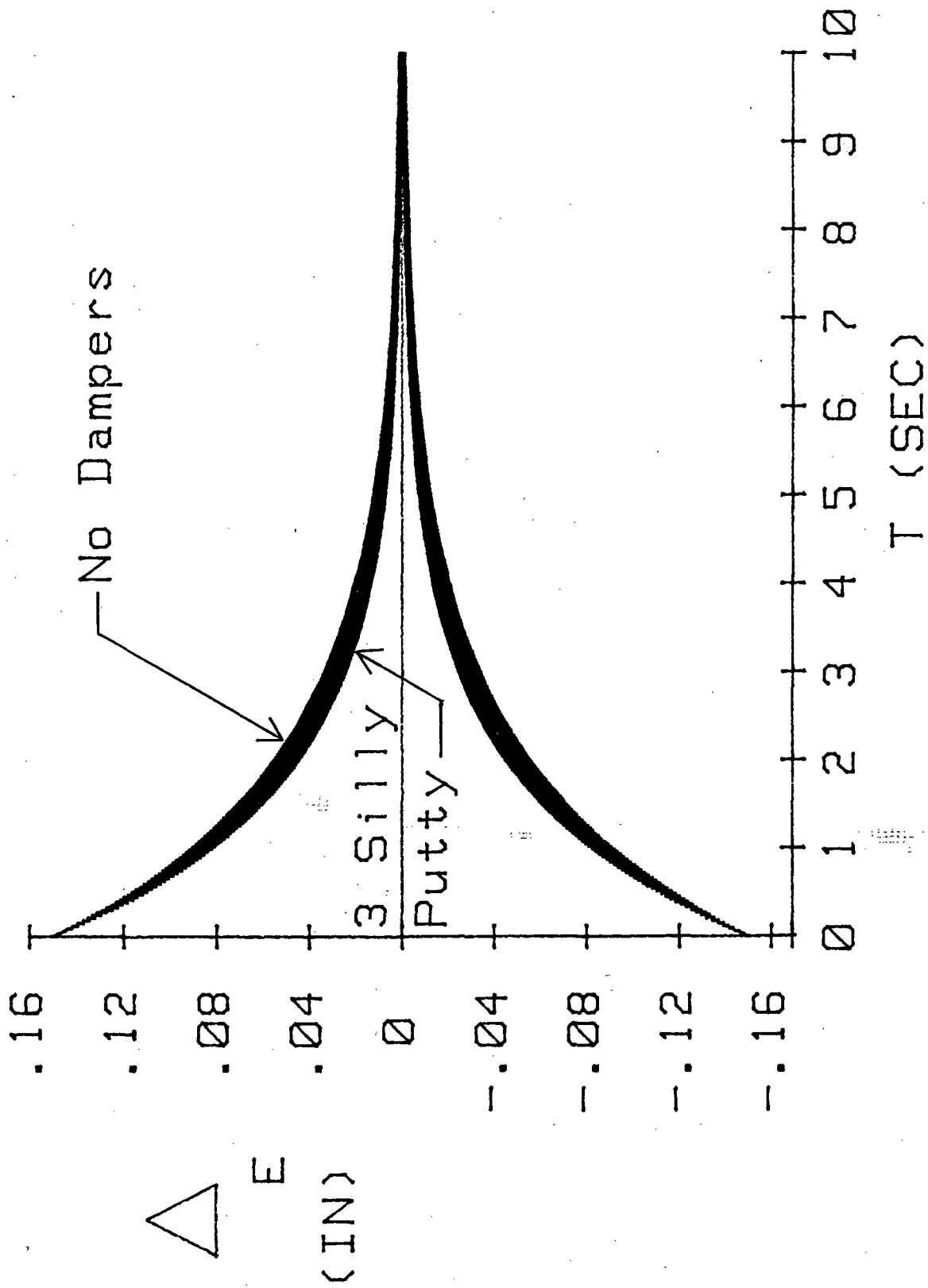


Figure 27. Effect of 3 silly putty in chamber dampers on  $\Delta$ -t.

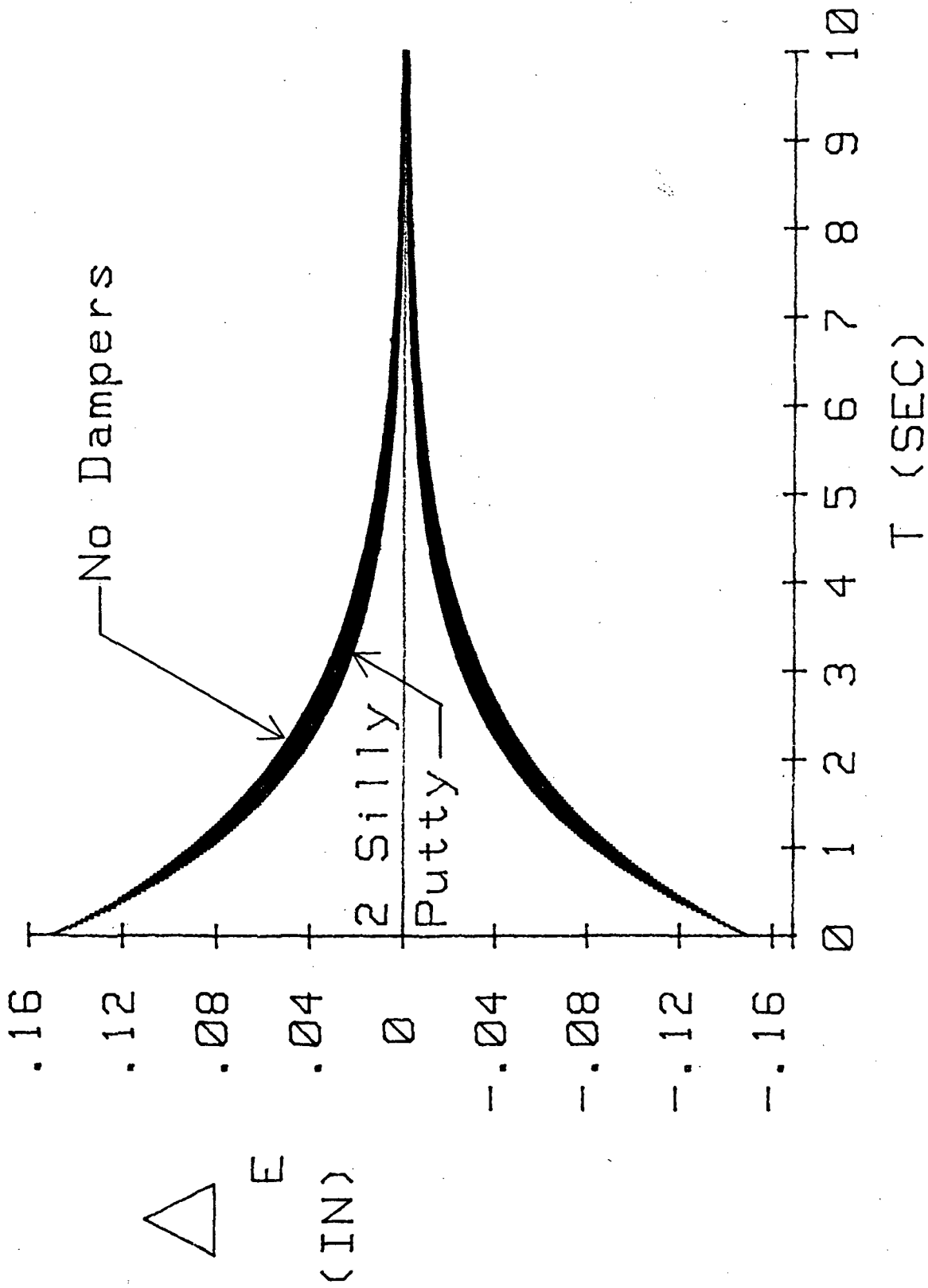


Figure 28. Effect of 2 silly putty in chamber dampers on  $\Delta$ -t envelope.

ORIGINAL PAGE IS  
OF POOR QUALITY

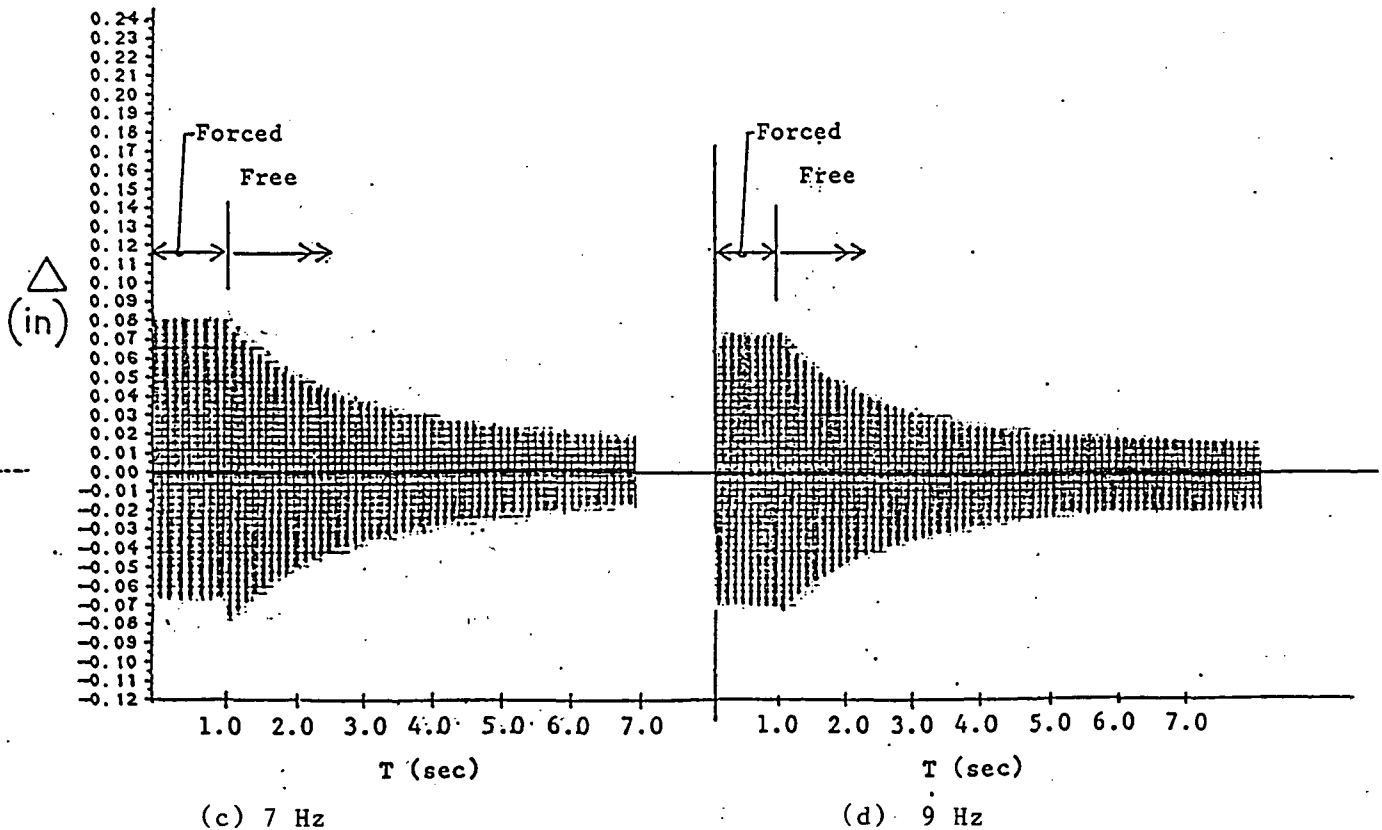
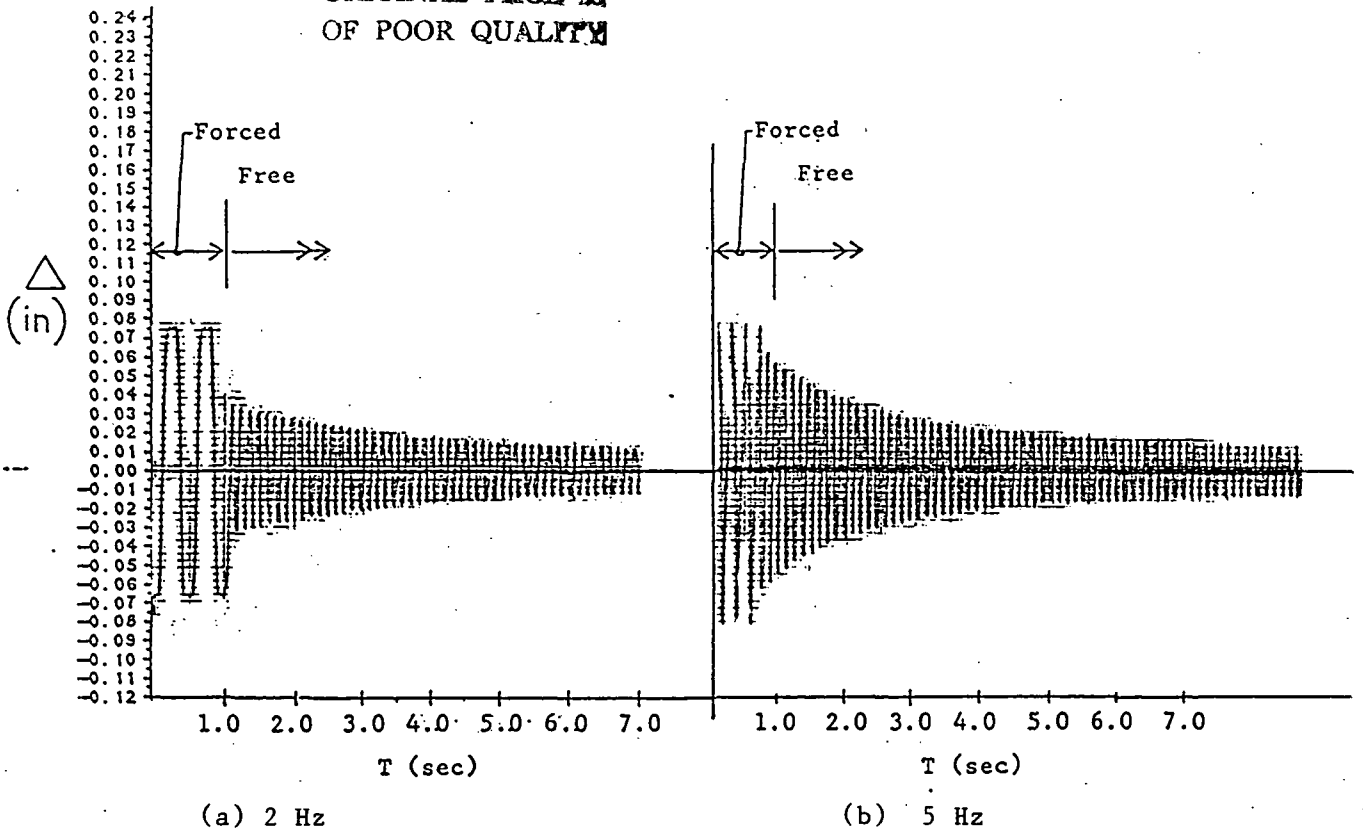


Figure 29. Experimental  $\Delta$ - $t$  plots for member "constrained" forced then free vibration with no dampers and frequencies of 2, 5, 7 and 9 Hz.

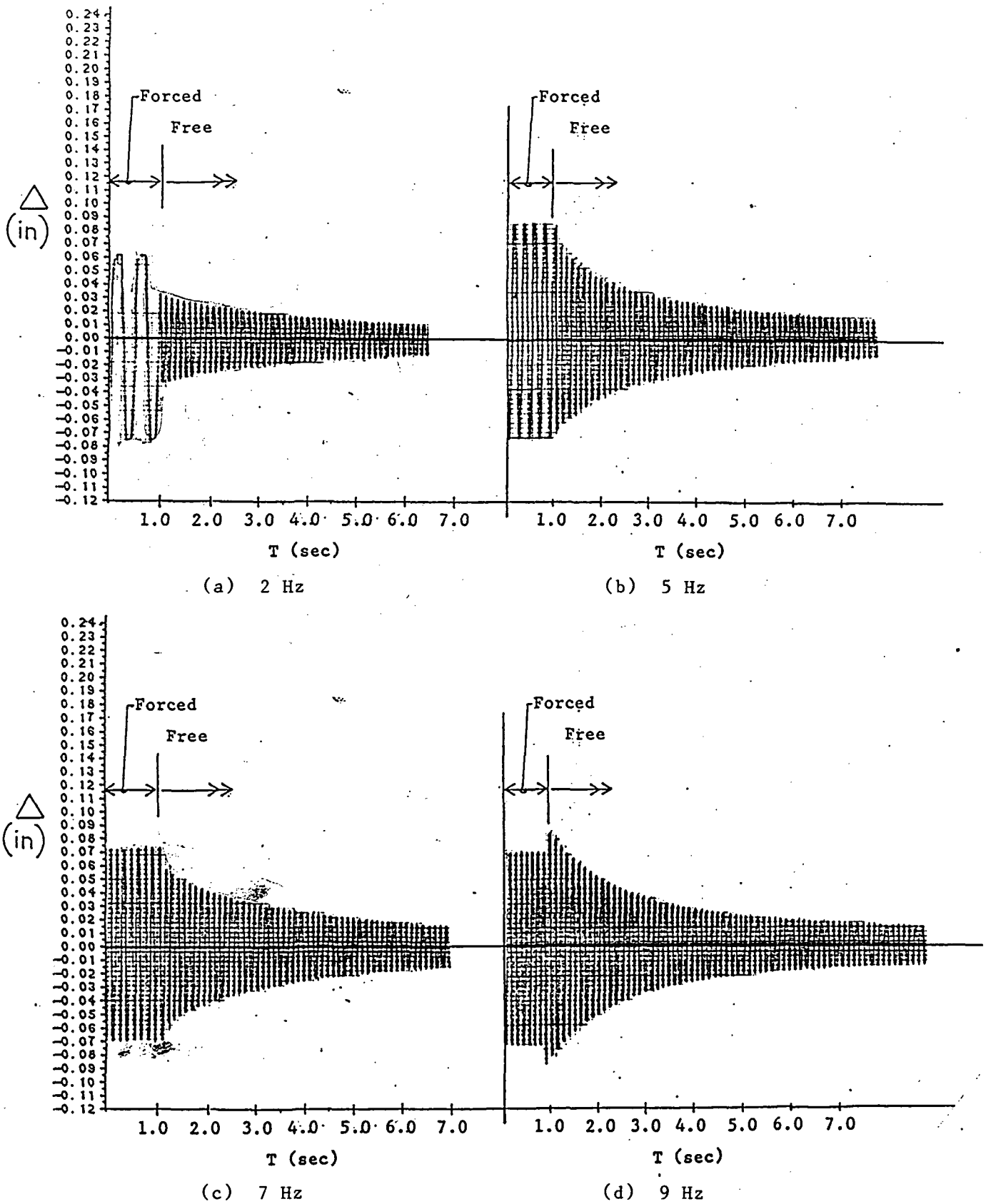


Figure 30. Experimental  $\Delta$ -t plot for member "constrained" forced then free vibration with 2 silly putty in chamber damper and forcing function frequencies of 2, 5, 7 and 9 Hz.

ORIGINAL PAGE IS  
OF POOR QUALITY

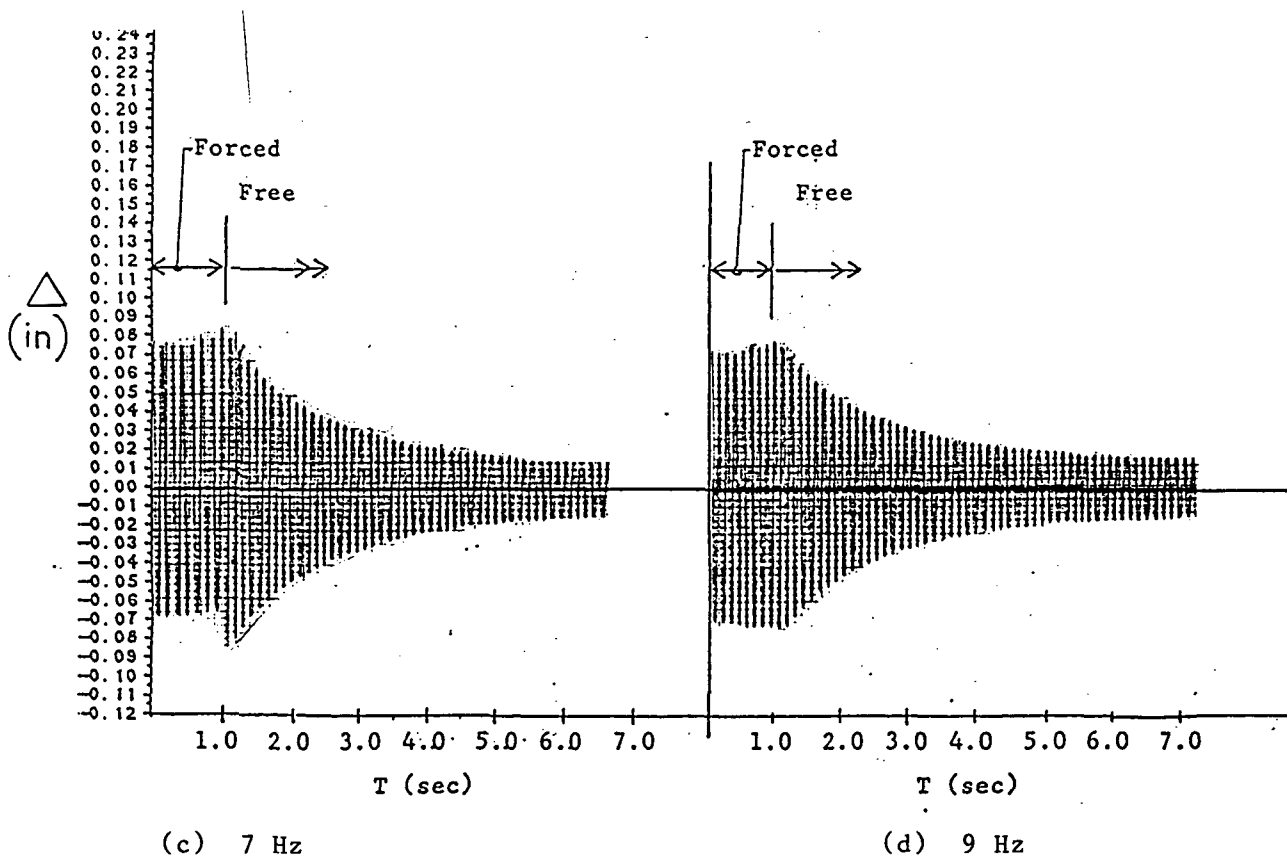
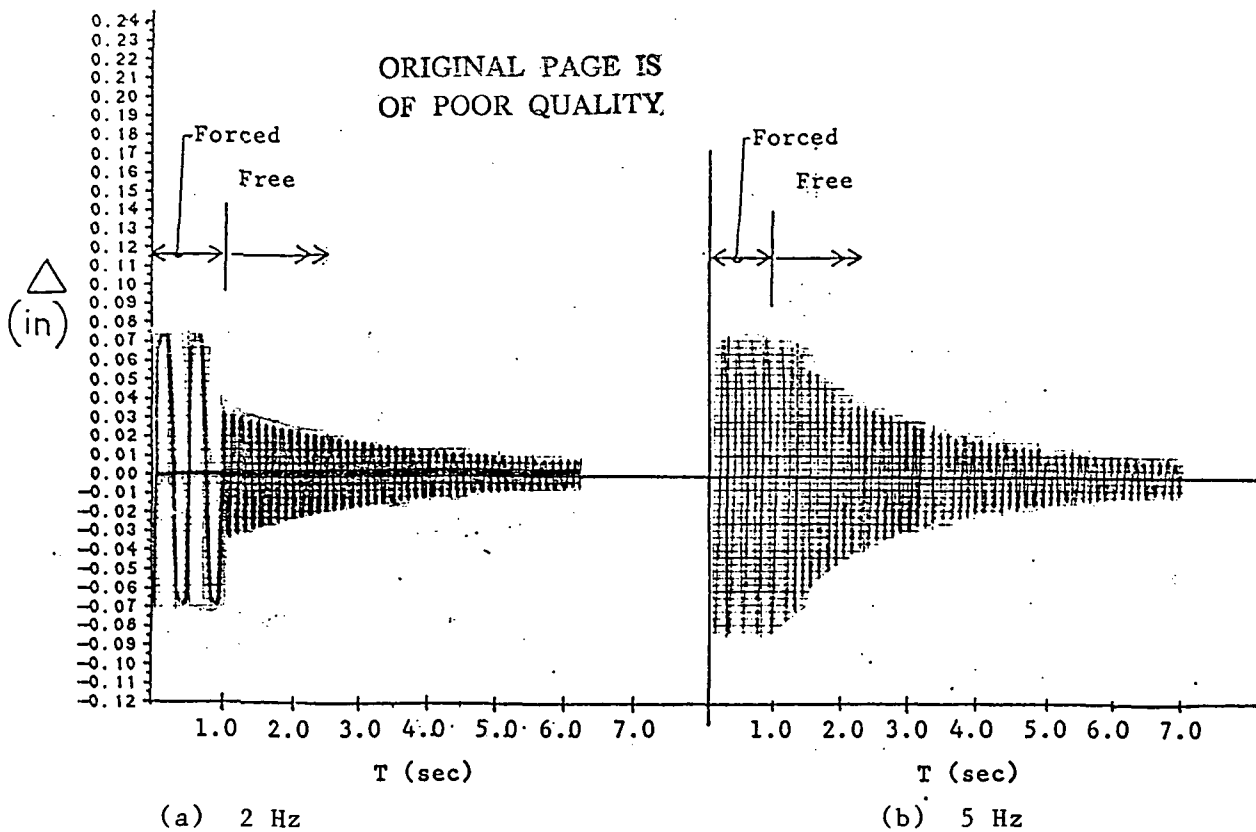
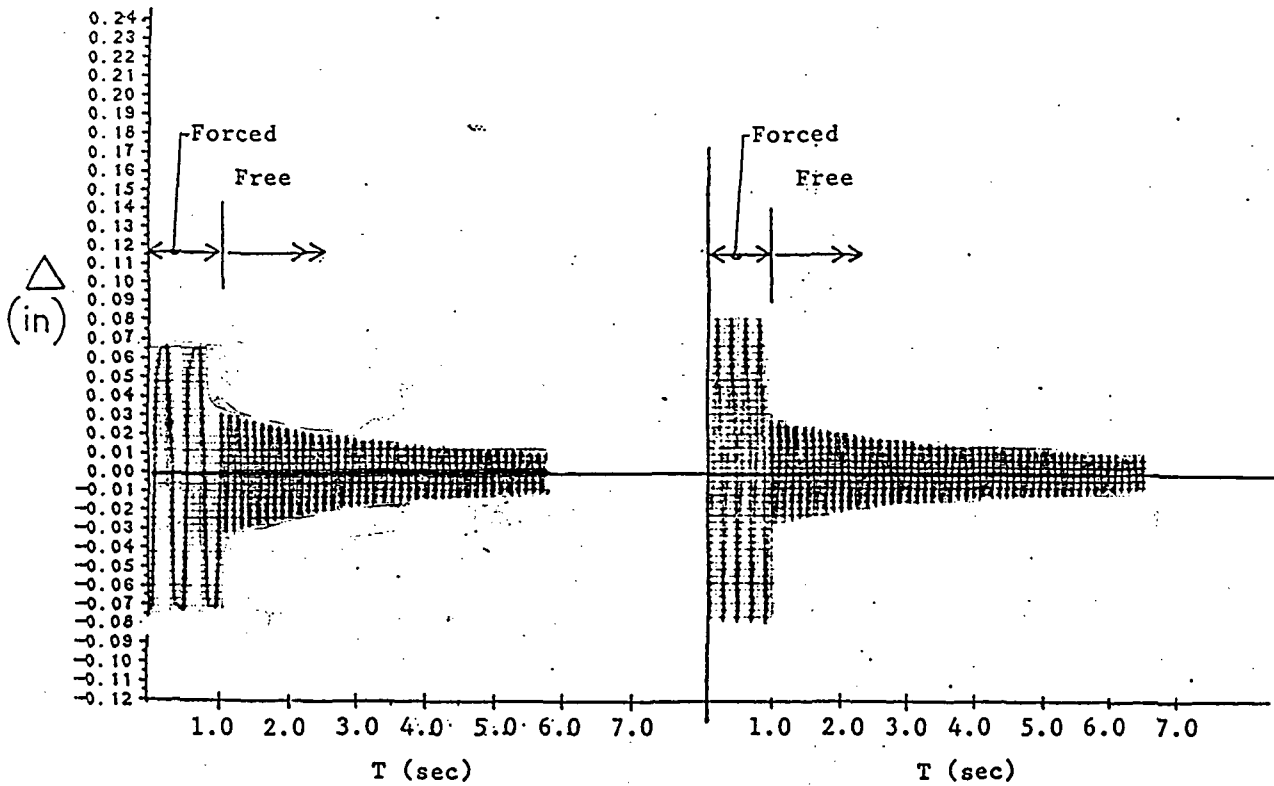


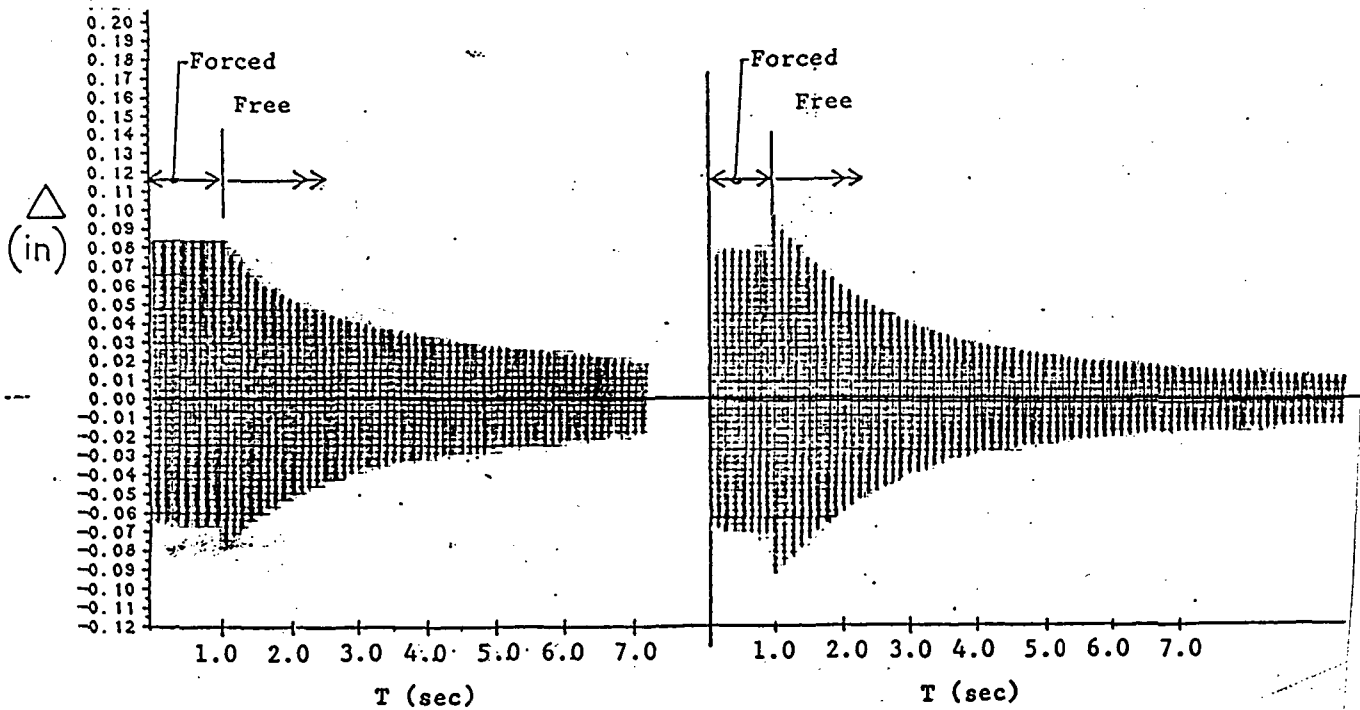
Figure 31. Experimental  $\Delta$ -t plot for member "constrained" forced then free vibration with 1 silly putty in chamber damper and forcing function frequencies of 2, 5, 7 and 9 Hz.





(a) 2 Hz

(b) 5 Hz



(c) 7 Hz

(d) 9 Hz

Figure 32. Experimental  $\Delta$ -t plots for member "constrained" forced then free vibration with 3 silly putty in chamber dampers and forcing function frequencies of 2, 5, 7, and 9 Hz.

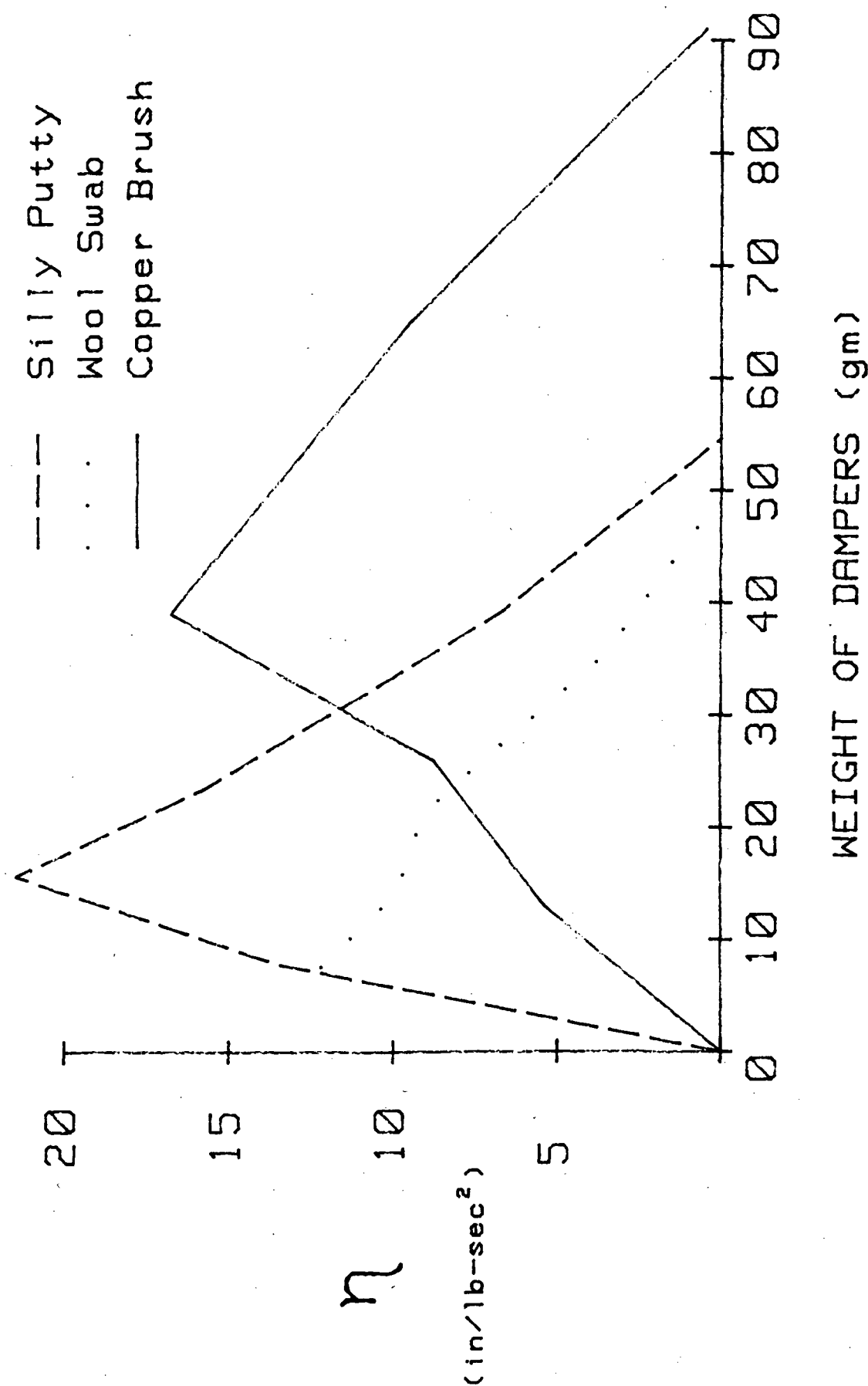


Figure 33. Damping efficiency index versus weight curves for natural vibration tests.

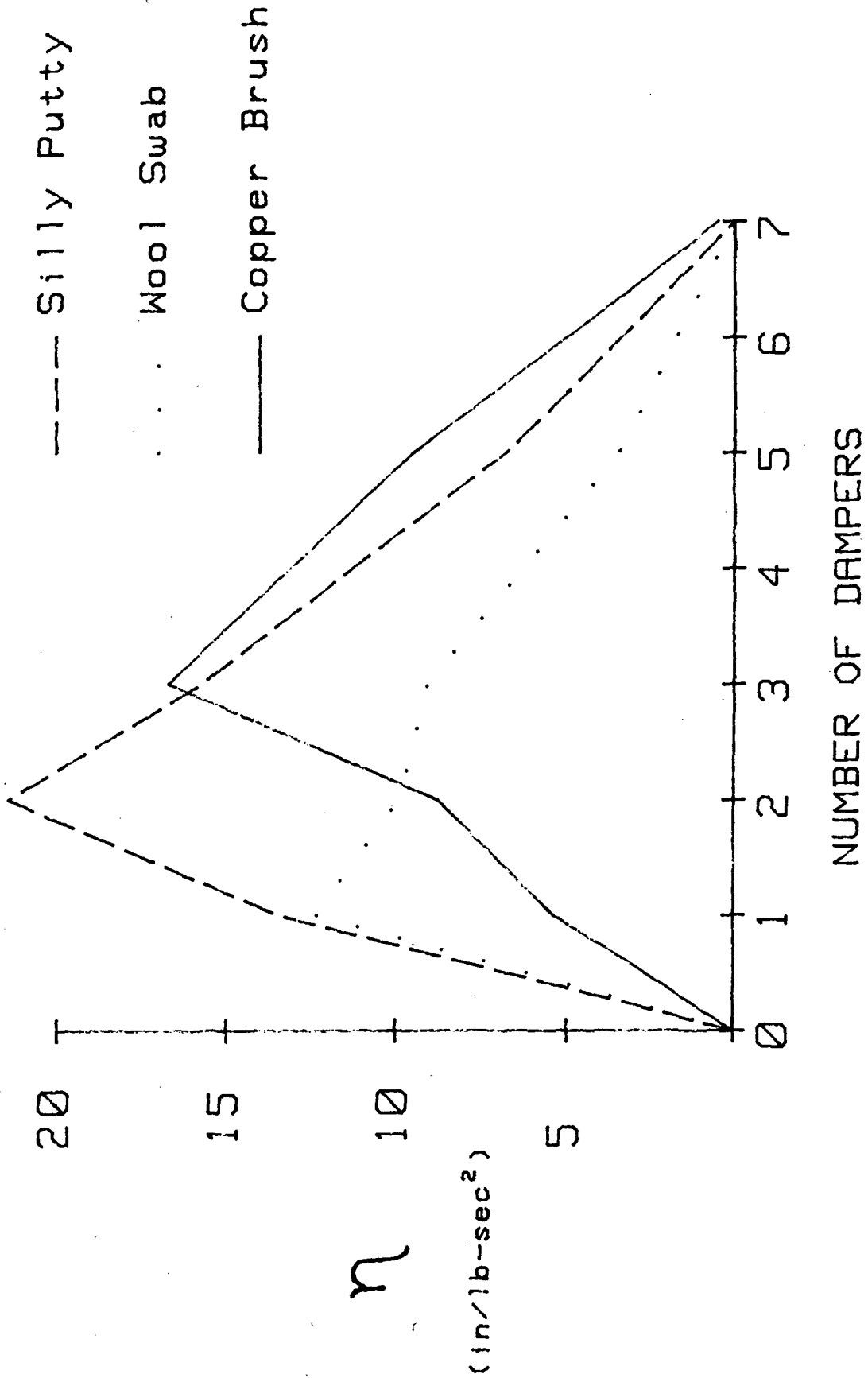


Figure 34. Damping efficiency index versus number of dampers for natural vibration tests.

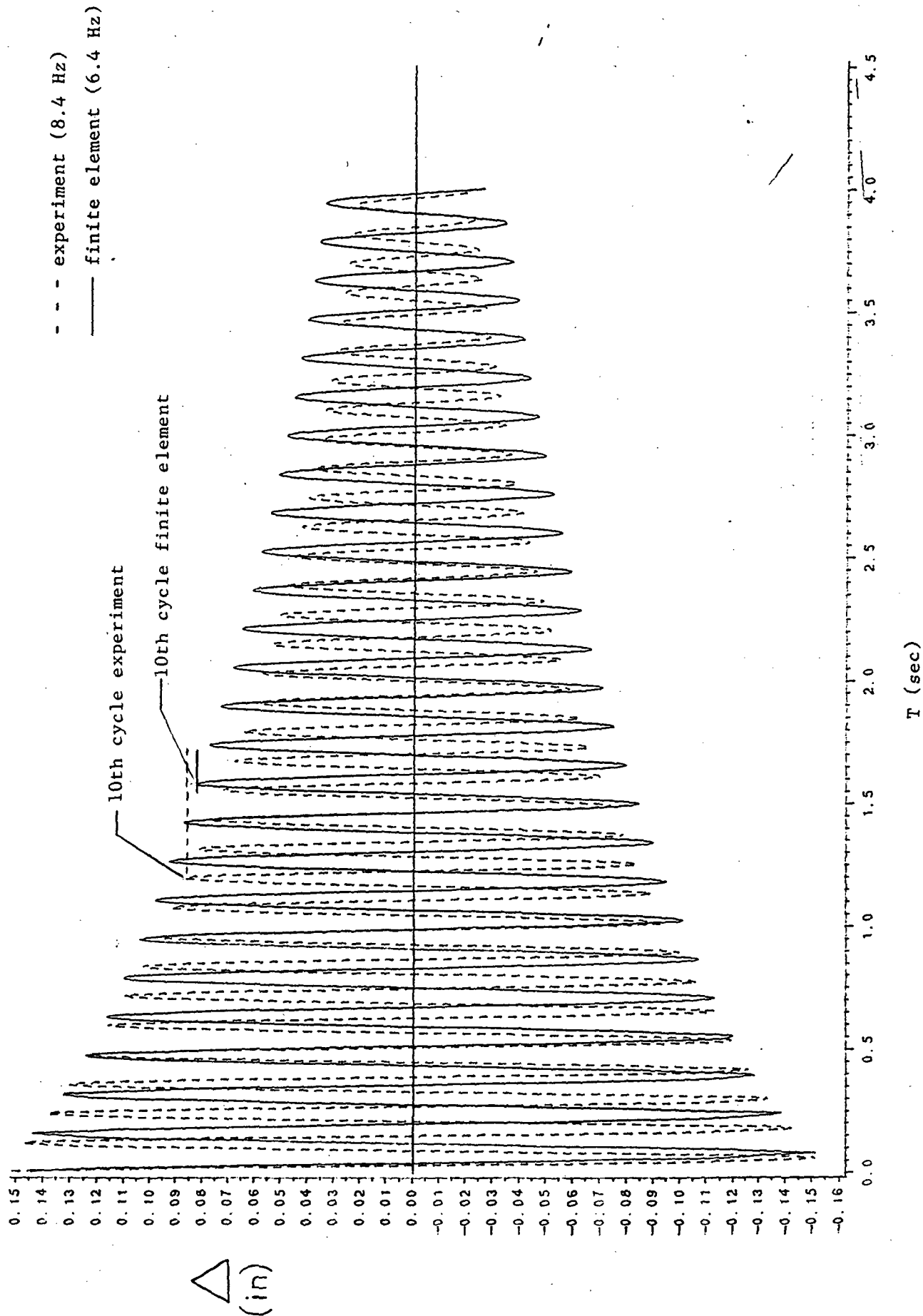


Figure 35. Finite Element versus average experimental  $\Delta$ -t plots for member with no dampers.

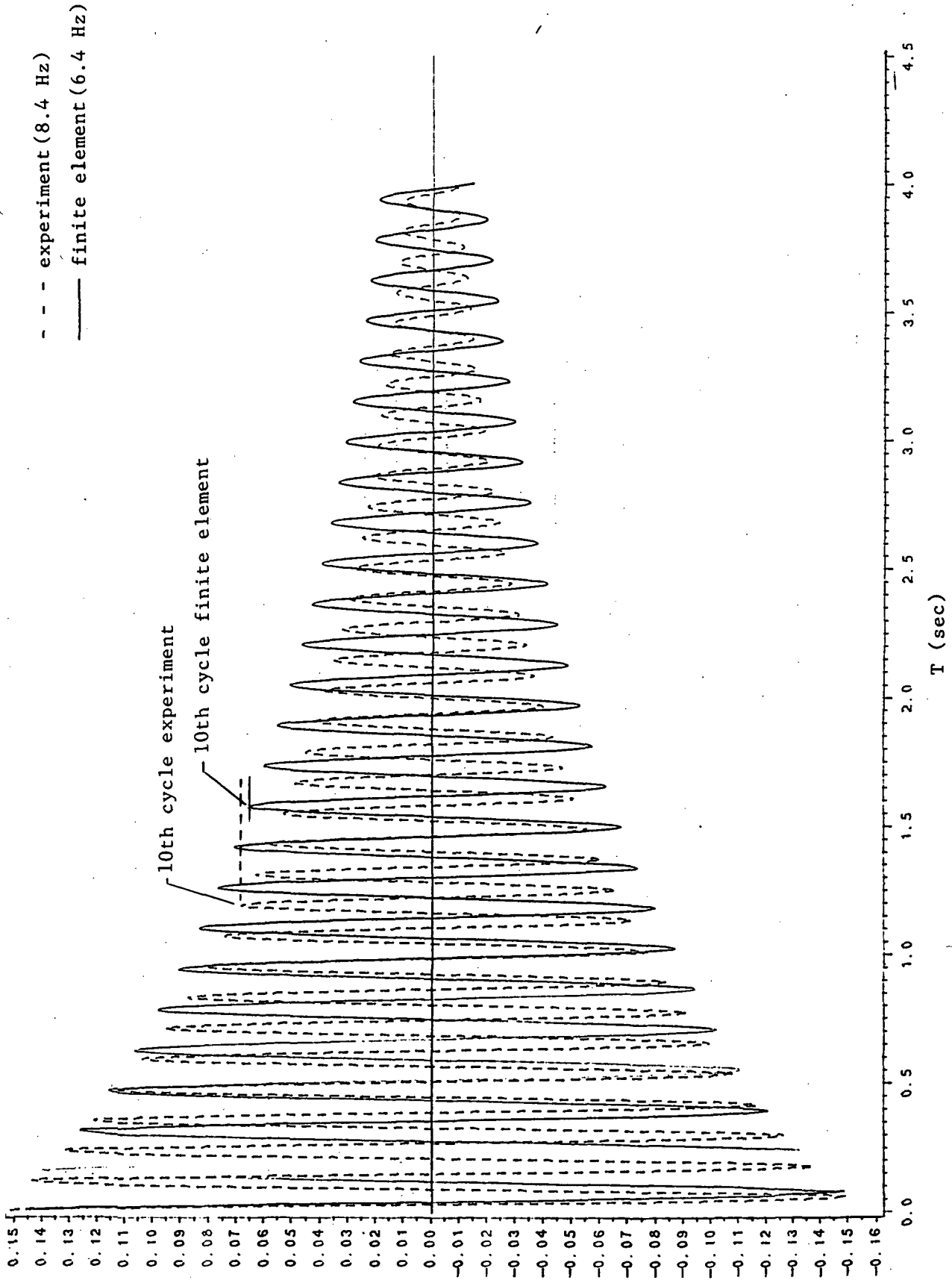


Figure 36. Finite element versus average experimental  $\Delta$ -t plots for member with 3 copper brush dampers.

$\Delta$   
 (in)

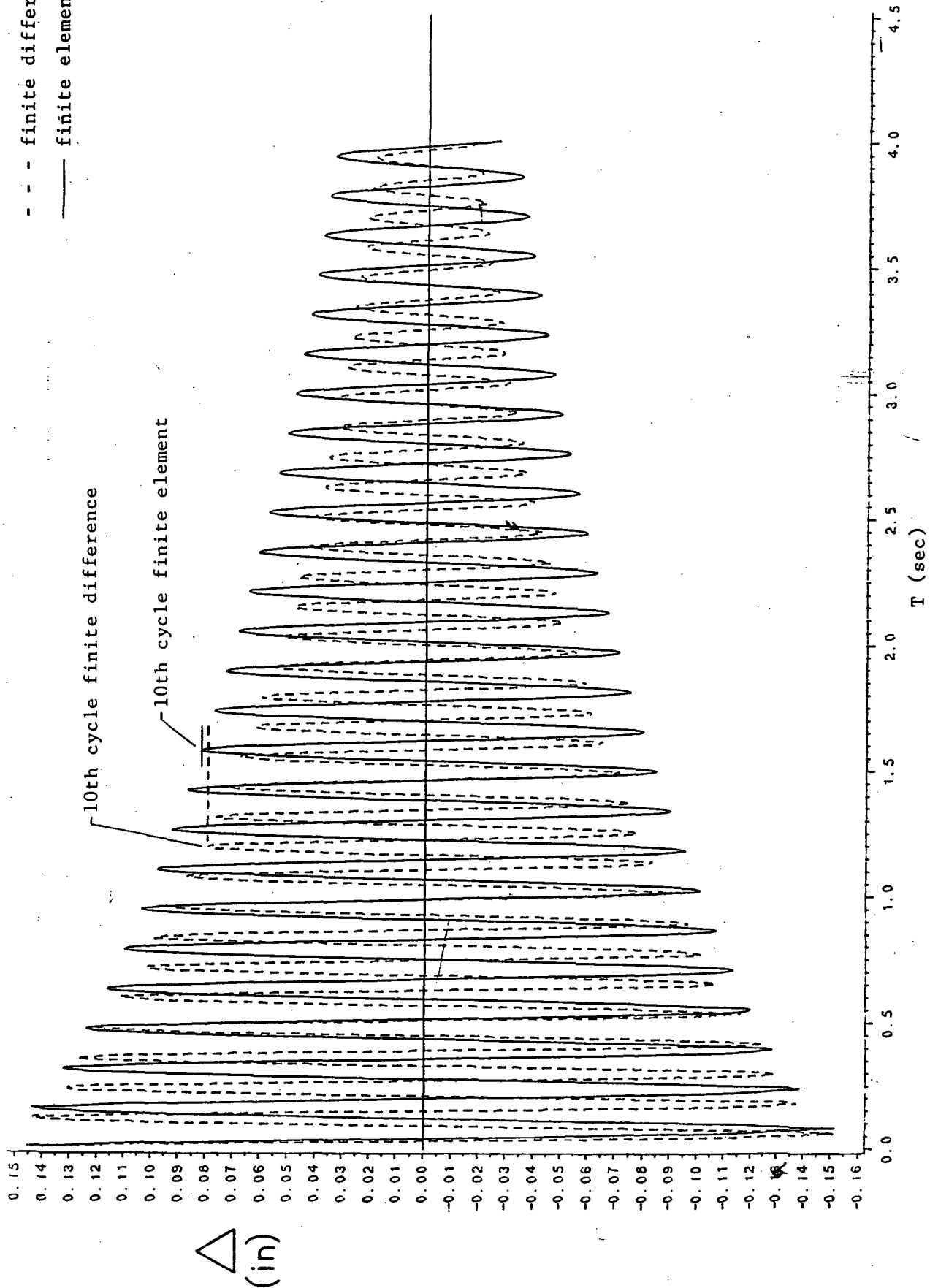


Figure 37. Finite element versus finite difference  $\Delta$ -t plots for member with no dampers.

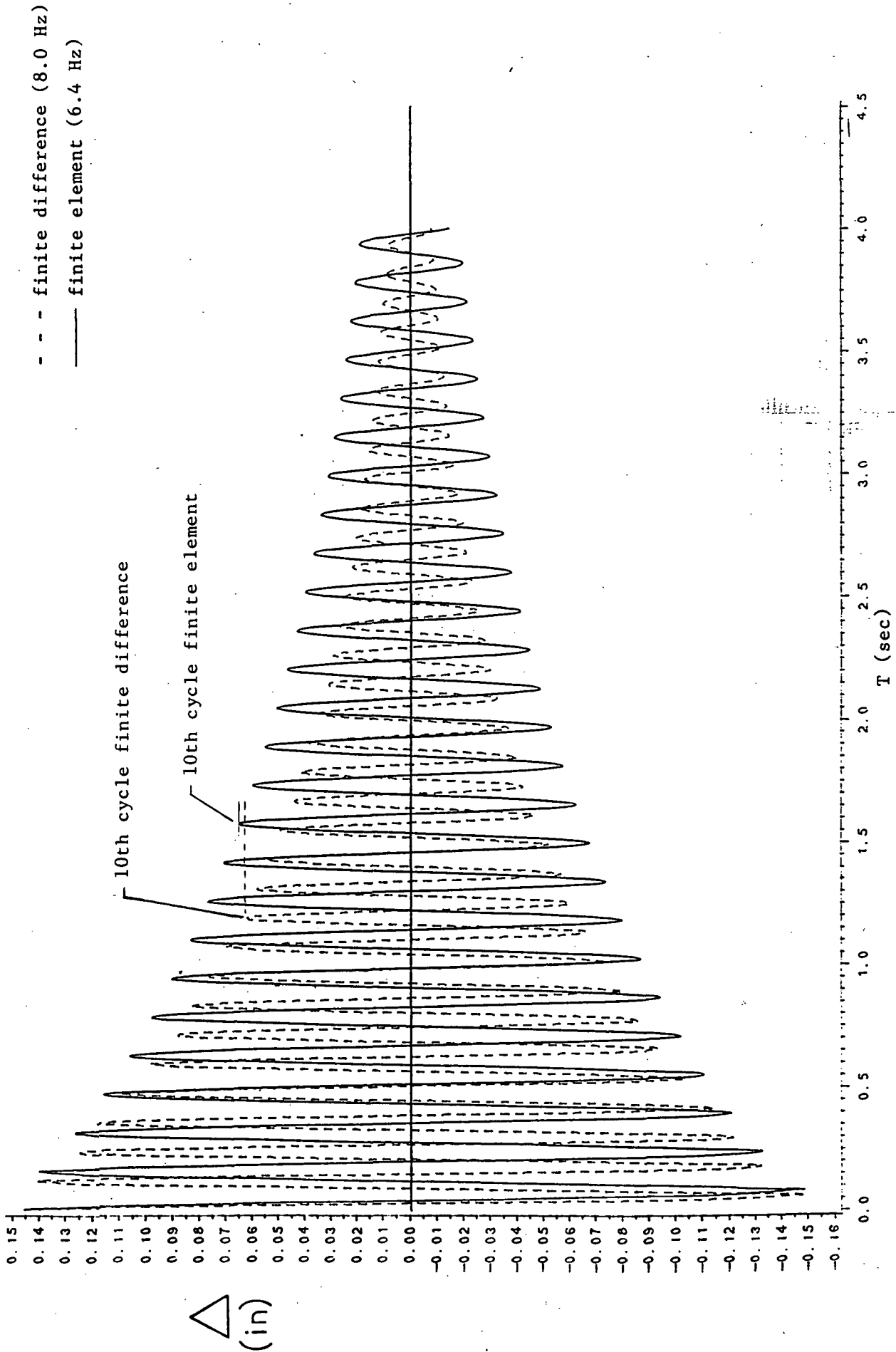


Figure 38. Finite element versus finite difference  $\Delta$ -t plots for member with 3 copper brush dampers.

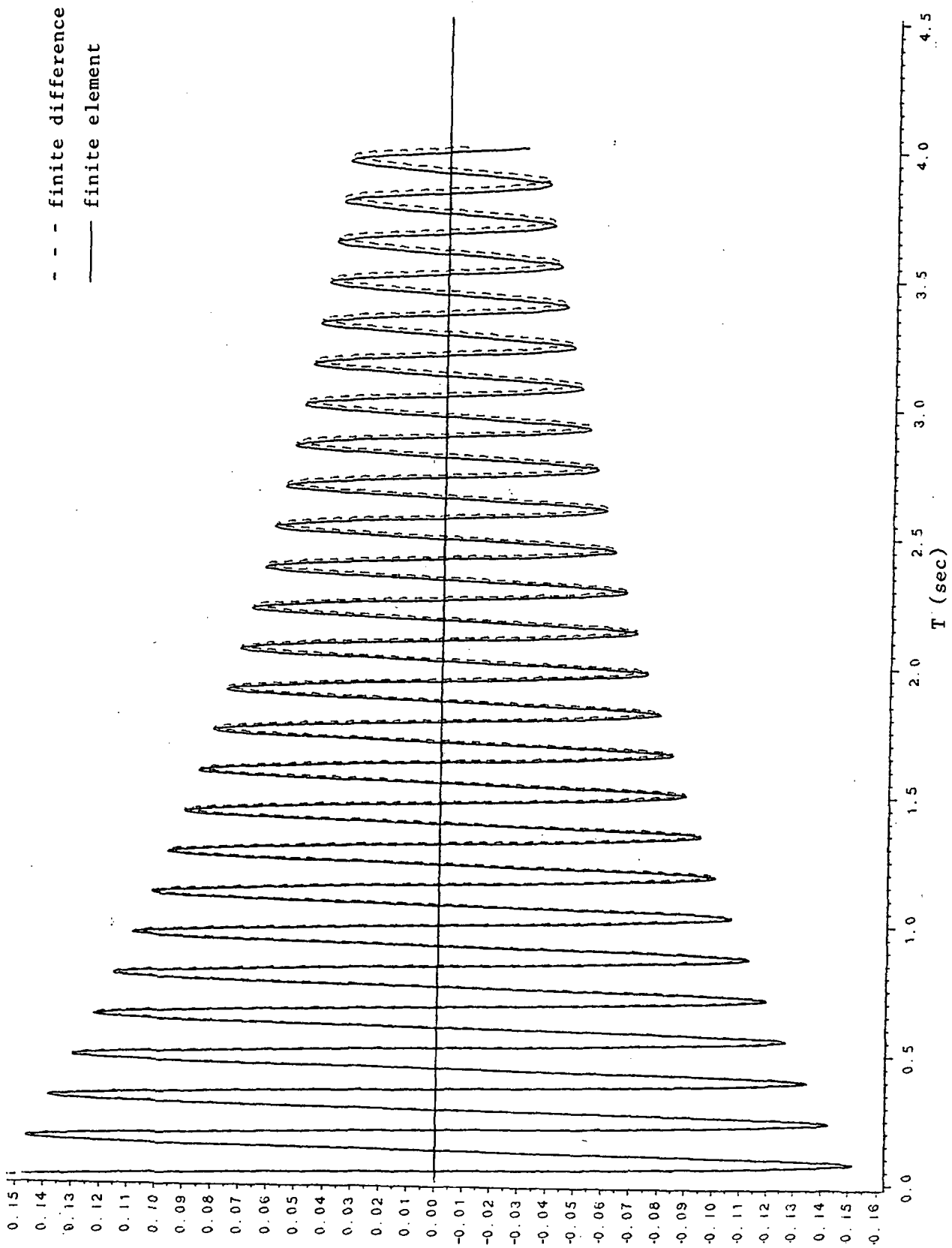


Figure 39. Finite element versus finite difference  $\Delta$ -t plots for simply supported beam with no dampers.



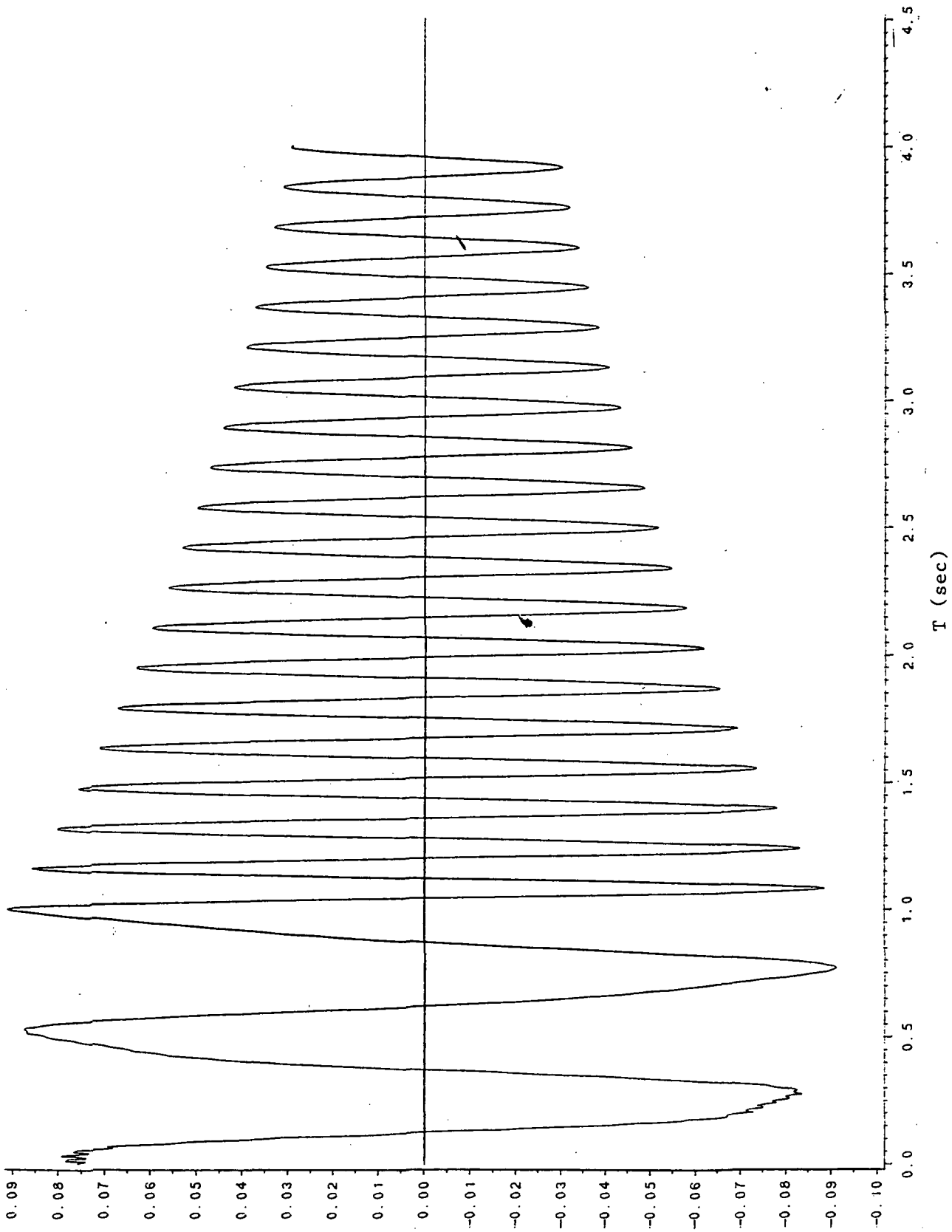


Figure 40. Finite element  $\Delta$ -t plot for member with no dampers and subjected to a 4.0 lb. force at 2 Hz for 1 second.

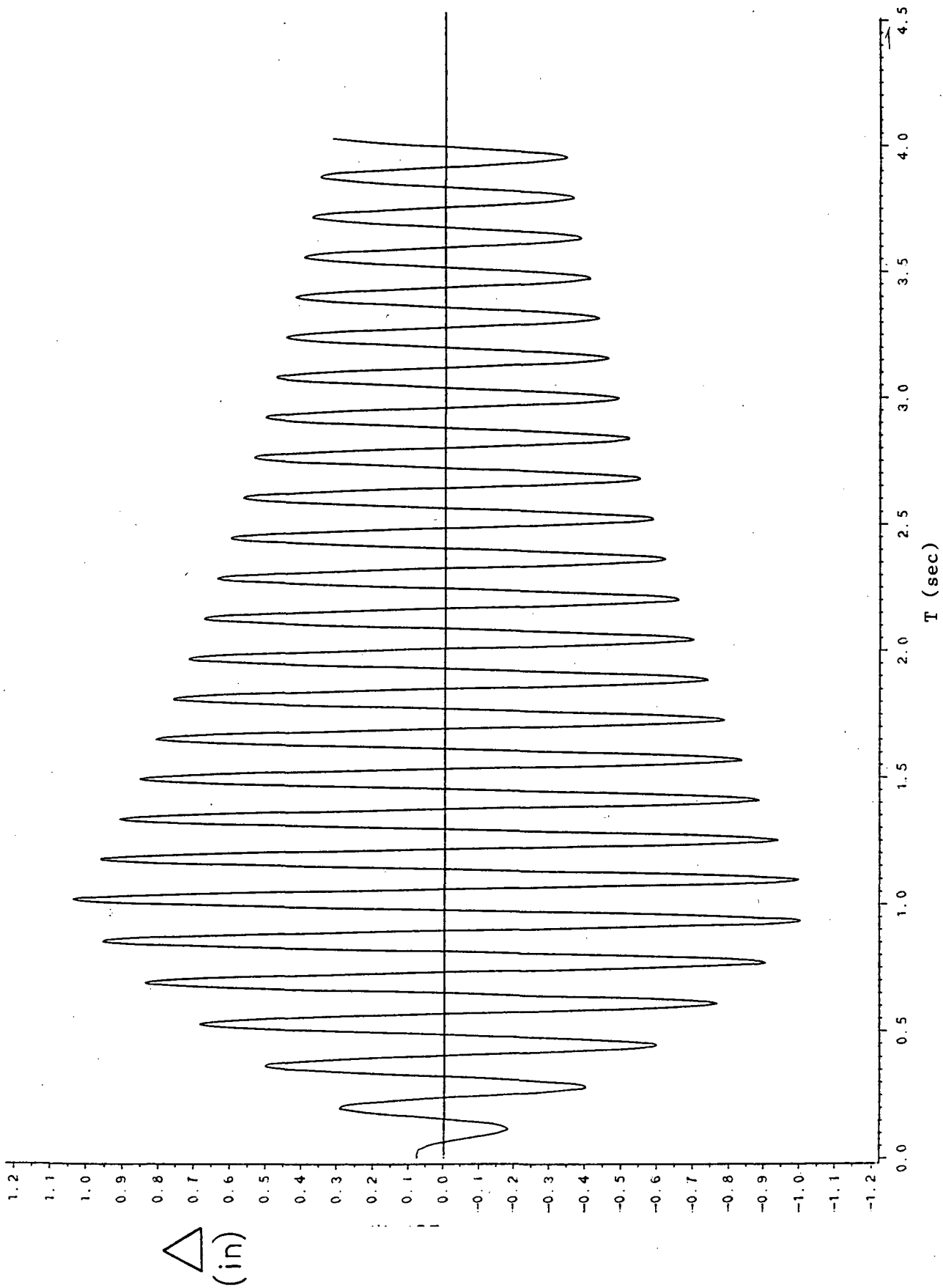
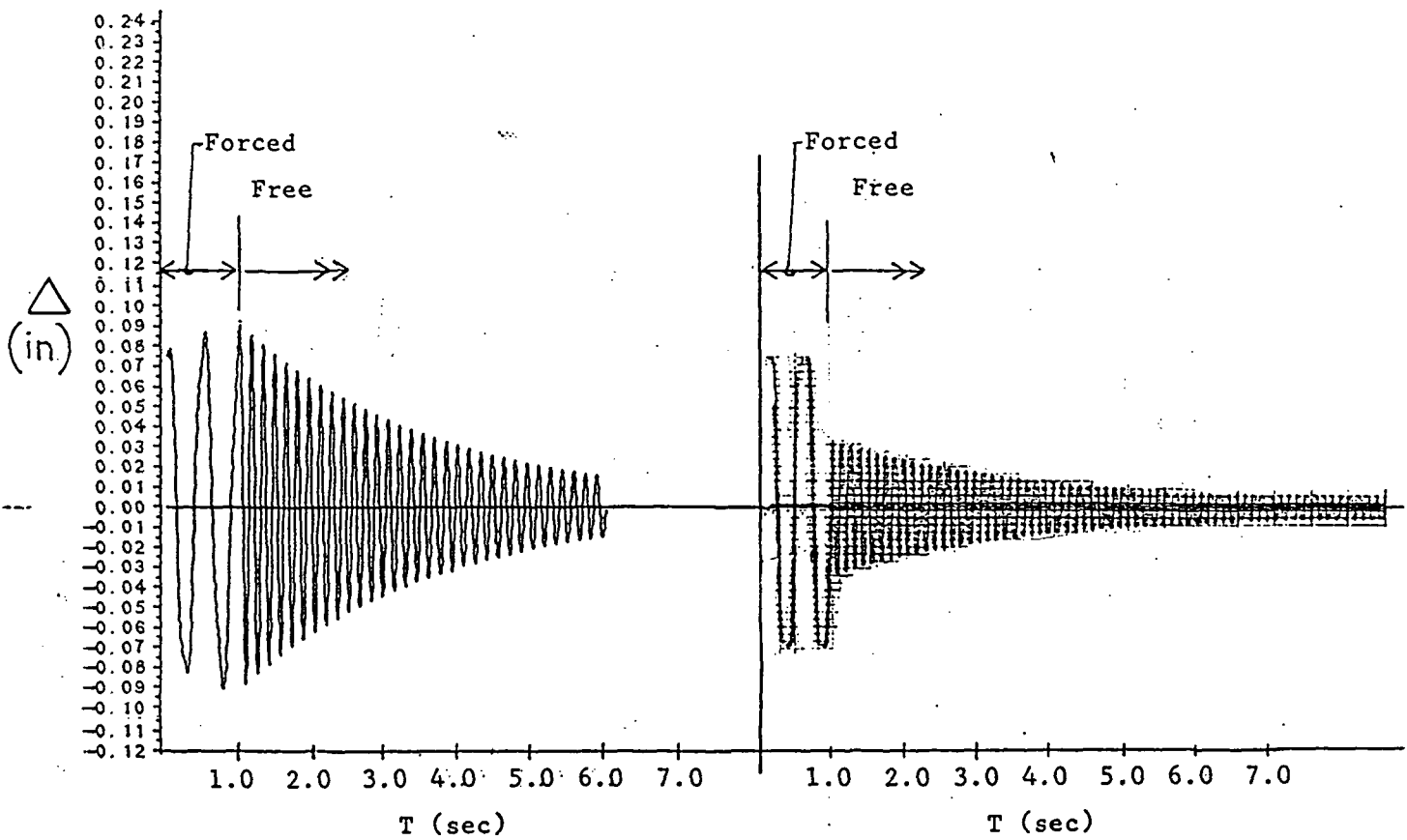


Figure 41. Finite element forced then free  $\Delta$ -t plot for member with no dampers and subjected to a 4.0 lb. force at 6 Hz for 1 second.



Theoretical curve with ideal disengagement.

Experimental curve with mechanical disengagement.

Figure 42. Theoretical and experimental forced then free  $\Delta$ -t plots for a 4.0 lb. force at 2 Hz for 1 second on member with one silly putty in chamber damper.

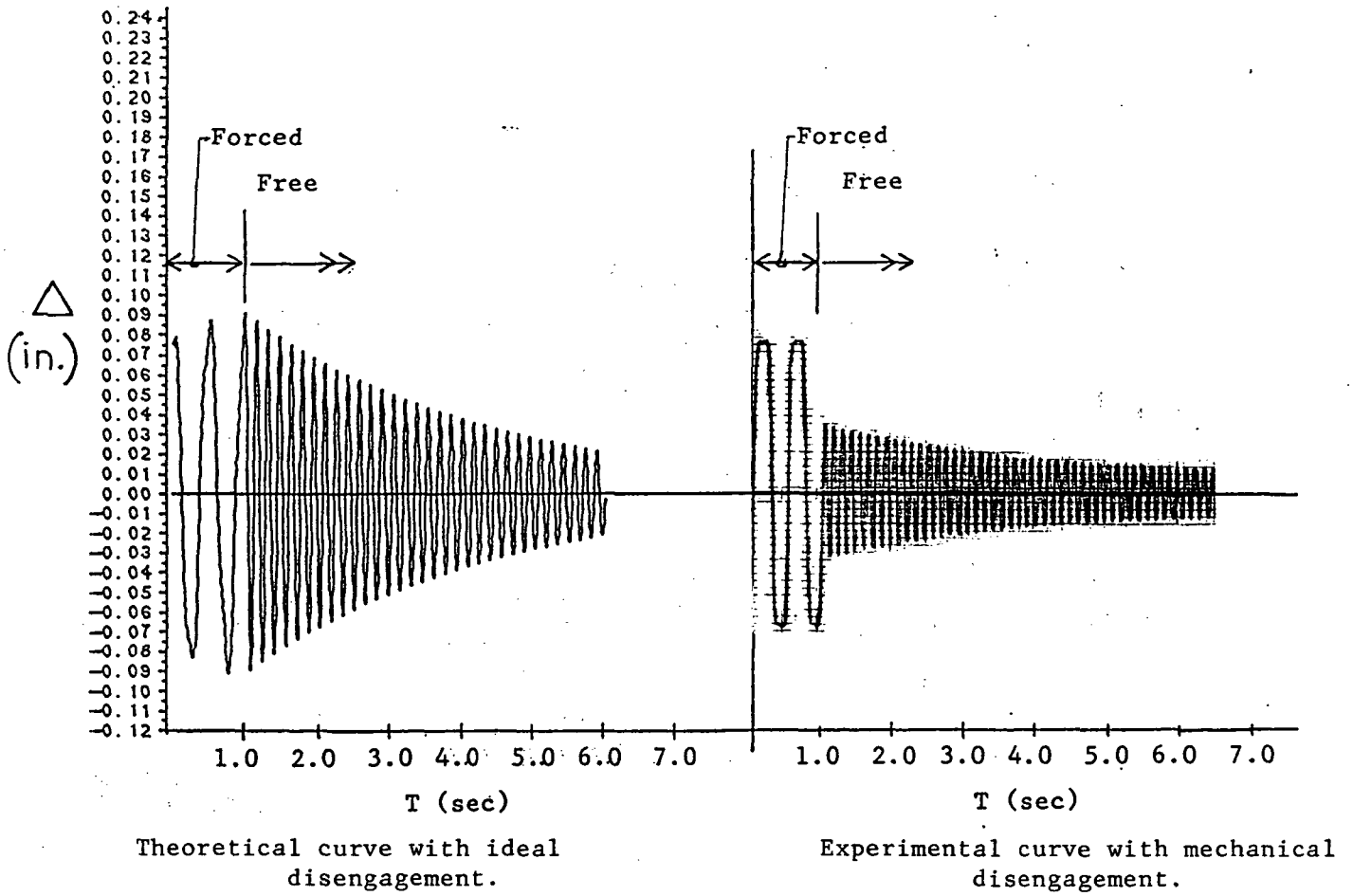


Figure 43. Theoretical and experimental forced then free  $\Delta$ -t plots for a 4.0 lb. force at 2 Hz for 1 second on member with no dampers.

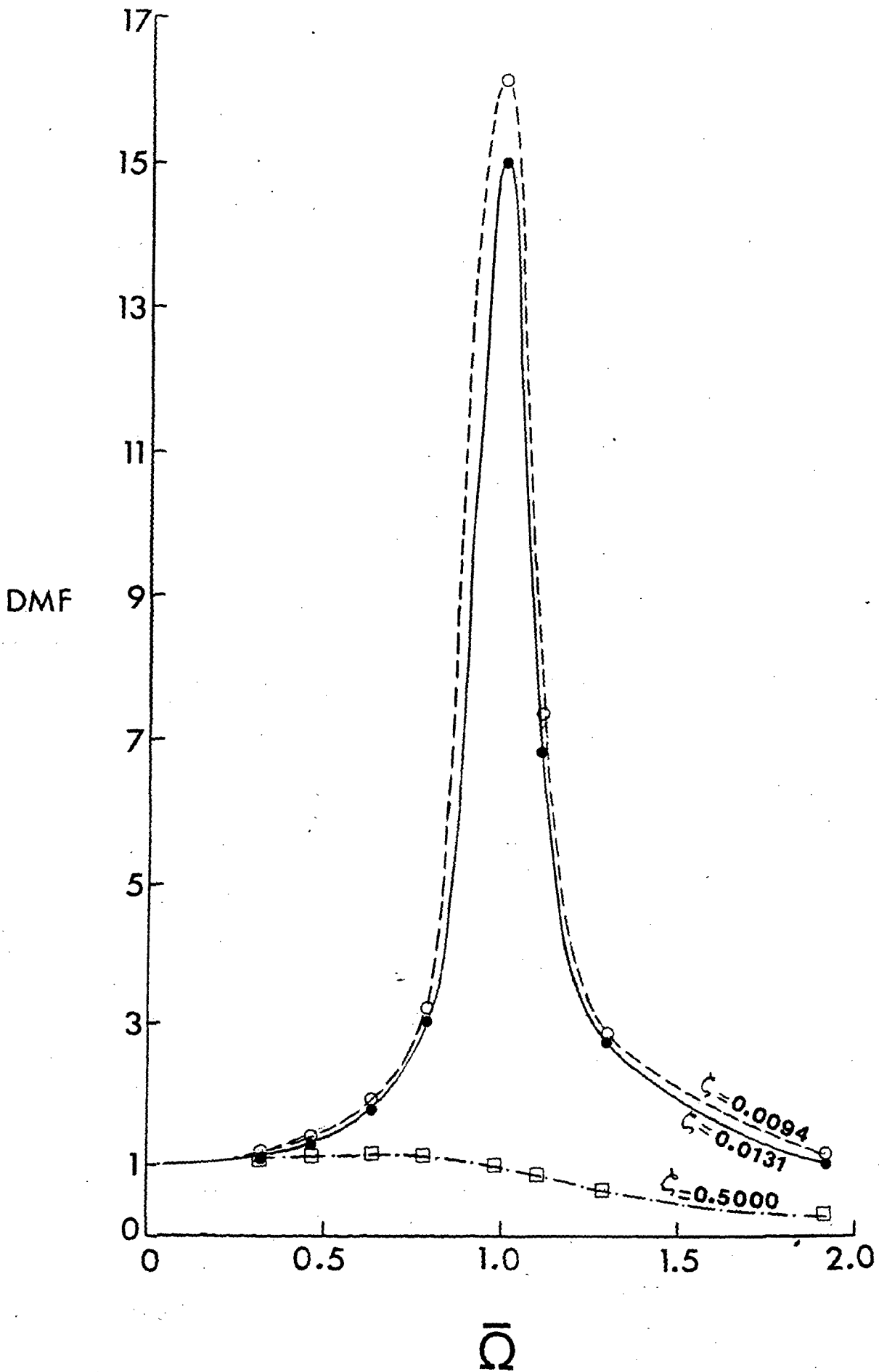


Figure 44. Theoretical dynamic magnification factor versus frequency ratio for damping ratios of 0.0094, 0.0131, and 0.50.

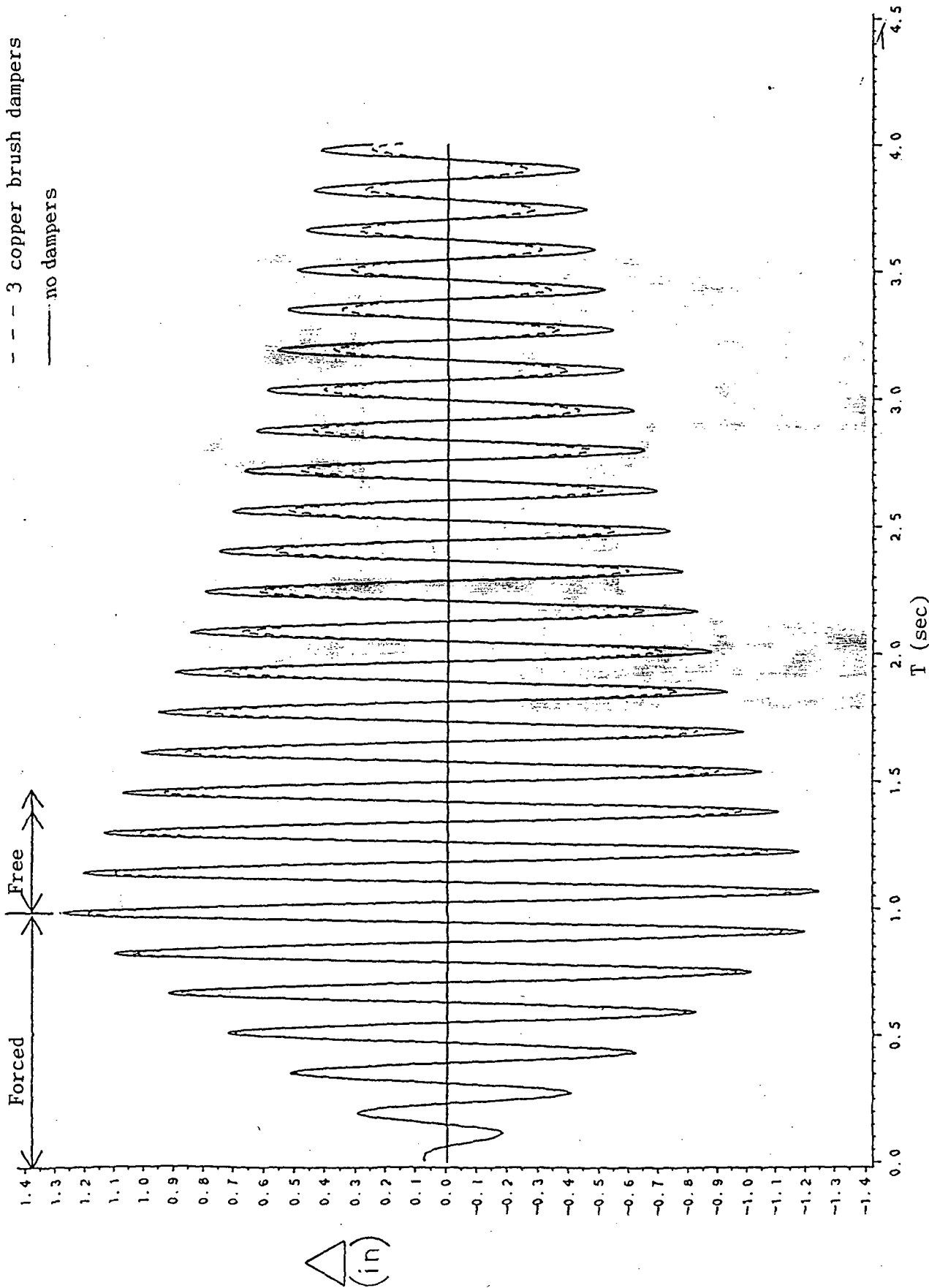


Figure 45. Theoretical  $\Delta$ -t plots for member with no dampers and with 3 copper brush dampers with a forcing function of 6.35 Hz for one second.

## APPENDICES

## APPENDIX A

### EXAMPLE OF FOUR ELEMENT BEAM STIFFNESS MATRIX

In this appendix the procedure used to assemble the beam stiffness matrix using a beam composed of four elements is presented.

The typical element stiffness matrices for Elements b and c as shown in Figure 2 are given as (Reference 6):

$$[K]_{b,c} = \begin{bmatrix} \frac{12EI}{L^3} & \frac{6EI}{L^2} & -\frac{12EI}{L^3} & \frac{6EI}{L^2} \\ & \frac{4EI}{L} & -\frac{6EI}{L^2} & \frac{2EI}{L^2} \\ \text{Symmetric} & & \frac{12EI}{L^3} & -\frac{6EI}{L^2} \\ & & & \frac{4EI}{L} \end{bmatrix} \quad (A.1)$$

Since only planar motion is considered, axial effects are negligible and, therefore, not included in the element stiffness matrix.

Derivation of the stiffness matrix for Element a as shown in Figure 2 is as follows. The flexibility matrix for the element is given by:

$$[F] = [H]^t [F]_{c1} [H] + [F]_m + [F]_{c2} \quad (A.2)$$

in which [H] is the equilibrium matrix given by:

$$[H] = \begin{bmatrix} 1 & 0 & 0 \\ 0 & 1 & L \\ 0 & 0 & 1 \end{bmatrix} \quad (A.3)$$

and  $[F]_{c1}$  represents the flexibility of the connection at end one,  $[F]_m$  is the flexibility of the element itself and  $[F]_{c2}$  is the flexibility of the connection at end two. These are defined as follows:



$$[F]_{c1} = \begin{bmatrix} 0 & 0 \\ 0 & \frac{L}{4EI k} \end{bmatrix} \quad (A.4)$$

$$[F]_m = \begin{bmatrix} \frac{L^3}{3EI} & \frac{L^2}{2EI} \\ \frac{L^2}{2EI} & \frac{L}{EI} \end{bmatrix} \quad (A.5)$$

$$[F]_{c2} = \begin{bmatrix} 0 & 0 \\ 0 & \frac{L}{4EI} \end{bmatrix} \quad (A.6)$$

therefore the flexibility matrix in full can be written as

$$[F] = \begin{bmatrix} \frac{L^3}{EI} \left( \frac{1}{3} + \frac{1}{4k} \right) & \frac{L^2}{EI} \left( \frac{1}{2} + \frac{1}{4k} \right) \\ \frac{L^2}{EI} \left( \frac{1}{2} + \frac{1}{4k} \right) & \frac{L}{EI} \left( 1 + \frac{1}{4k} \right) \end{bmatrix} \quad (A.7)$$

The inverse of [F] is given by:

$$[K_{22}]_a = [F]^{-1} = \begin{bmatrix} \frac{3EI}{L^3} \frac{(4k+1)}{(k+1)} & \frac{-3EI}{L^2} \frac{(2k+1)}{(k+1)} \\ \frac{-3EI}{L^2} \frac{(2k+1)}{(k+1)} & \frac{EI}{L} \frac{(4k+3)}{(k+1)} \end{bmatrix} \quad (A.8)$$

The other stiffness matrices now follow from:

$$[K_{11}]_a = [H] [K_{22}] [H]^t = \begin{bmatrix} \frac{3EI}{L^3} \frac{(4k+1)}{(k+1)} & \frac{3EI}{L^2} \frac{(2k)}{(k+1)} \\ \frac{3EI}{L^2} \frac{(2k)}{(k+1)} & \frac{EI}{L} \frac{(4k)}{(k+1)} \end{bmatrix} \quad (A.9)$$

$$\begin{aligned}
 [K_{12}]_a &= \begin{bmatrix} \frac{-3EI}{L^3} \frac{(4k+1)}{(k+1)} & \frac{3EI}{L^2} \frac{(2k+1)}{(k+1)} \\ \frac{-3EI}{L^2} \frac{(2k)}{(k+1)} & \frac{EI}{L} \frac{(2k)}{(k+1)} \end{bmatrix} \\
 [K_{21}]^t &= -[H] [K_{22}] = \begin{bmatrix} \frac{-3EI}{L^3} \frac{(4k+1)}{(k+1)} & \frac{3EI}{L^2} \frac{(2k+1)}{(k+1)} \\ \frac{-3EI}{L^2} \frac{(2k)}{(k+1)} & \frac{EI}{L} \frac{(2k)}{(k+1)} \end{bmatrix}
 \end{aligned} \tag{A.10}$$

Therefore, the total stiffness matrix for Element a is:

$$[K]_a = \begin{bmatrix} \frac{3EI}{L^3} \frac{(4k+1)}{(k+1)} & \frac{3EI}{L^2} \frac{(2k)}{(k+1)} & \frac{-3EI}{L^3} \frac{(4k+1)}{(k+1)} & \frac{3EI}{L^2} \frac{(2k+1)}{(k+1)} \\ & \frac{EI}{L} \frac{(4k)}{(k+1)} & \frac{-3EI}{L^2} \frac{(2k)}{(k+1)} & \frac{EI}{L} \frac{(2k)}{(k+1)} \\ \text{Symmetric} & & \frac{3EI}{L^3} \frac{(4k+1)}{(k+1)} & \frac{-3EI}{L^2} \frac{(2k+1)}{(k+1)} \\ & & & \frac{EI}{L} \frac{(4k+3)}{(k+1)} \end{bmatrix} \tag{A.11}$$

Similarly, Element d shown in Figure 2:

$$[K_{22}]_d = \begin{bmatrix} \frac{3EI}{L^3} \frac{(4k+1)}{(1+k)} & \frac{-6EI}{L^2} \frac{(k)}{(1+k)} \\ \frac{-6EI}{L^2} \frac{(k)}{(1+k)} & \frac{4EI}{L} \frac{(k)}{(1+k)} \end{bmatrix} \tag{A.12}$$

$$\begin{aligned}
 [K_{11}]_d &= \begin{bmatrix} \frac{3EI}{L^3} \frac{(4k+1)}{(1+k)} & \frac{3EI}{L^2} \frac{(2k+1)}{(1+k)} \\ \frac{3EI}{L^2} \frac{(2k+1)}{(1+k)} & \frac{EI}{L} \frac{(4k+3)}{(1+k)} \end{bmatrix} \\
 [H] [K_{22}]_d [H]^t &= \begin{bmatrix} \frac{3EI}{L^3} \frac{(4k+1)}{(1+k)} & \frac{3EI}{L^2} \frac{(2k+1)}{(1+k)} \\ \frac{3EI}{L^2} \frac{(2k+1)}{(1+k)} & \frac{EI}{L} \frac{(4k+3)}{(1+k)} \end{bmatrix}
 \end{aligned} \tag{A.13}$$

$$[K_{12}]_d = [K_{21}]_d^t = \begin{bmatrix} \frac{3EI}{L^3} \frac{(4k+1)}{(1+k)} & \frac{6EI}{L^2} \frac{k}{(1+k)} \\ \frac{-3EI}{L^2} \frac{(2k+1)}{(1+k)} & \frac{2EI}{L} \frac{(k)}{(k+1)} \end{bmatrix} \quad (A.14)$$

$$[K]_d = \begin{bmatrix} \frac{3EI}{L^3} \frac{(4k+1)}{(1+k)} & \frac{3EI}{L^2} \frac{(2k+1)}{(1+k)} & \frac{-3EI}{L^3} \frac{(4k+1)}{(k+1)} & \frac{6EI}{L^2} \frac{(k)}{(k+1)} \\ & \frac{EI}{L} \frac{(4k+3)}{(1+k)} & \frac{-3EI}{L^2} \frac{(2k+1)}{(1+k)} & \frac{2EI}{L} \frac{(k)}{(1+k)} \\ & \text{Symmetric} & \frac{3EI}{L^3} \frac{(4+1)}{(1+k)} & \frac{-6EI}{L^2} \frac{(k)}{(1+k)} \\ & & & \frac{4EI}{L} \frac{(k)}{(1+k)} \end{bmatrix} \quad (A.15)$$

Using the above element matrices, the following global matrix is assembled:

$$[K] = \begin{bmatrix} [K_{11}]_a & [K_{22}]_a & [0] & [0] & [0] \\ [K_{21}]_a & [K_{22}]_a + [K_{11}]_b & [K_{12}]_b & [0] & [0] \\ [0] & [K_{21}]_b & [K_{22}]_b + [K_{11}]_c & [K_{12}]_c & [0] \\ [0] & [0] & [K_{21}]_c & [K_{22}]_c + [K_{11}]_d & [K_{12}]_d \\ [0] & [0] & [0] & [K_{21}]_d & [K_{22}]_d \end{bmatrix} \quad (A.16)$$

This is an  $n \times n$  matrix where  $n = 2N + 2$ , and  $N =$  the number of elements.

The first two boundary conditions are enforced by putting 1.0 in the diagonal corresponding to the translational degrees of freedom at the supports and setting all other entries in that row and column equal to zero. The last two boundary conditions are accounted for in the derivation of the individual stiffness matrices.

Note that an adjustment to the stiffness matrix must be made when the

stiffness of the rotational restraint at each end approaches zero. For this case the diagonal term corresponding to the rotational stiffness at the support should be set equal to unity.

APPENDIX B  
COMPUTER PROGRAMS

As a part of this study, two computer programs were developed to solve the dynamic equilibrium matrix equation given in Chapter 2. A brief description of these programs along with their listings and sample outputs are given in this appendix.

B.1 NEWMARK

This program is based on the analysis described in Section 2.2. A description of the required input data is given at the beginning of the program listing. Data is input by means of the data statements in lines 48 to 53 of the program listing. The output consists of the time in seconds and corresponding midspan deflection in inches.

B.2 CENDIF

Program CENDIF is based on the analysis described in Section 2.3. Data input and output are the same on NEWMARK.

```

IMPLICIT REAL*8 (A-H,O-Z)
DOUBLE PRECISION L,K1,K2,K(70,70),M(70,70),C(70,70),U(70),UDT(70),
&RT(70),C1(70,70),C2(70,70),C9(70,70),C4(70),KEL(4,4),F(70),C5(70),
&DUM(70),UT(70),MINV(70,70),C8(70,70),UDTP(70),UDDT(70),UDDTP(70),
&TP(70),UTN(70),C3(70),C6(70),FREQ(5),KINV(70,70),X(70,70),A(70,70),
&B(70,70),D(70),EIGV(70),DAMRAT(70),ANS(70,70),RES(70,70),XT(70,70)
IFPR=0
C***** INPUT DATA *****
C**
C** IFPR = PRINT REQUEST VARIABLE FOR JACOBI
C** 0 = DO NOT PRINT INTERMEDIATE VALUES
C** 1 = PRINT INTERMEDIATE VALUES
C**
C** L = LENGTH (IN)
C**
C** NUMEL = NUMBER OF ELEMENTS (MUST BE AN EVEN NUMBER)
C**
C** TS = TIME STEP; DELTA 'T' (SEC)
C**
C** ROW = MASS PER UNIT LENGTH (KIP*SEC**2/IN**2)
C**
C** E = MODULUS OF ELASTICITY (KSI)
C**
C** XI = MOMENT OF INERTIA (IN**4)
C**
C** AR = AREA (IN**2)
C**
C** K1 = ROTATIONAL STIFFNESS AT END 1 (K*IN/RAD)
C**
C** K2 = ROTATIONAL STIFFNESS AT END 2 (K*IN/RAD)
C**
C** ZETA = DAMPING RATIO
C**
C** TT = TOTAL TIME FOR PROGRAM EXECUTION (SEC)
C**
C** PO = MAGNITUDE OF THE FORCING FUNCTION (KIPS)
C**
C** OMEGA = FREQUENCY OF THE FORCING FUNCTION (RAD)
C**
C** DELO = PRESCRIBED INITIAL DEFLECTION AT MEMBER MIDSPAN
C** (IN)
C**
C*****
DATA L,NUMEL,TS,ROW/ 177,10,0.000500,202.1454E-09/
DATA E,XI,AR/10000.,0.32500000,0.7363/
DATA K1,K2,TT/53.1100,53.1100,6.00/
DATA PO,OMEGA,ZETA/0.002226367,12.56637062,0.007200/
DATA GAMA,BETA,DELO/0.50,0.25,0.007914/
ICOUNT=0

```

NEW00010  
 NEW00020  
 NEW00030  
 NEW00040  
 NEW00050  
 NEW00060  
 NEW00070  
 NEW00080  
 NEW00090  
 NEW00100  
 NEW00110  
 NEW00120  
 NEW00130  
 NEW00140  
 NEW00150  
 NEW00160  
 NEW00170  
 NEW00180  
 NEW00190  
 NEW00200  
 NEW00210  
 NEW00220  
 NEW00230  
 NEW00240  
 NEW00250  
 NEW00260  
 NEW00270  
 NEW00280  
 NEW00290  
 NEW00300  
 NEW00310  
 NEW00320  
 NEW00330  
 NEW00340  
 NEW00350  
 NEW00360  
 NEW00370  
 NEW00380  
 NEW00390  
 NEW00400  
 NEW00410  
 NEW00420  
 NEW00430  
 NEW00440  
 NEW00450  
 NEW00460  
 NEW00470  
 NEW00480  
 NEW00490  
 NEW00500  
 NEW00510  
 NEW00520  
 NEW00530  
 NEW00540  
 NEW00550

```

TIME=0.0
WRITE (2,1)
H=L/NUMEL
1  FORMAT (/1X,'THIS IS NEWMARKS SOLUTION')
WRITE (2,1059) K1
1059 FORMAT (/1X,'STIFFNESS -- ',D16.9)
WRITE (2,1060) ZETA
1060 FORMAT (/1X,'DAMPING ---- ',D16.9)
WRITE (2,1061) PO
1061 FORMAT (/1X,'FORCE ----- ',D16.9)
WRITE (2,1062) OMEGA
1062 FORMAT (/1X,'FREQUENCY -- ',D16.9)

N=2*NUMEL+2

C  WRITE (2,176)
C  WRITE (2,177)

DO 10 I=1,N
DO 10 J=1,N
10  K(I,J)=0.0

K(1,1)=1000
K(N-1,N-1)=1000

K(2,2)=E*X1*4.*K1/(H*(K1+1.))
K(2,3)=(-1.)*3.*E*X1*2.*K1/((H**2)*(K1+1.))
K(2,4)=E*X1*2.*K1/(H*(K1+1.))
K(3,2)=K(2,3)
K(3,3)=3.*E*X1*(4.*K1+1.)/((H**3)*(K1+1.))
K(3,4)=(-3.)*E*X1*(2.*K1+1.)/((H**2)*(K1+1.))
K(4,2)=K(2,4)
K(4,3)=K(3,4)
K(4,4)=E*X1*(4.*K1+3.)/(H*(K1+1.))

K(N-3,N-3)=3.*E*X1*(4.*K2+1.)/((H**3)*(K2+1.))
K(N-3,N-2)=(3.)*E*X1*(2.*K2+1.)/((H**2)*(K2+1.))
K(N-3,N)=6.*E*X1*K2/((H**2)*(K2+1.))
K(N-2,N-3)=K(N-3,N-2)
K(N-2,N-2)=E*X1*(4.*K2+3.)/(H*(K2+1.))
K(N-2,N)=2.*E*X1*K2/(H*(K2+1.))
K(N,N-3)=K(N-3,N)
K(N,N-2)=K(N-2,N)
K(N,N)=E*X1*4.*K2/(H*(K2+1.))

KEL(1,1) = 12.*E*X1/(H**3)
KEL(1,2) = 6.*E*X1/(H**2)
KEL(1,3) = (-1.)*KEL(1,1)
KEL(1,4) = KEL(1,2)

```

```

NEW00560
NEW00570
NEW00580
NEW00590
NEW00600
NEW00610
NEW00620
NEW00630
NEW00640
NEW00650
NEW00660
NEW00670
NEW00680
NEW00690
NEW00700
NEW00710
NEW00720
NEW00730
NEW00740
NEW00750
NEW00760
NEW00770
NEW00780
NEW00790
NEW00800
NEW00810
NEW00820
NEW00830
NEW00840
NEW00850
NEW00860
NEW00870
NEW00880
NEW00890
NEW00900
NEW00910
NEW00920
NEW00930
NEW00940
NEW00950
NEW00960
NEW00970
NEW00980
NEW00990
NEW01000
NEW01010
NEW01020
NEW01030
NEW01040
NEW01050
NEW01060
NEW01070
NEW01080
NEW01090
NEW01100

```

```

KEL (2,2) = 4.*E*X1/(H)
KEL (2,3) = (-1.)*KEL (1,2)
KEL (2,4) = KEL (2,2)/2.
KEL (3,3) = KEL (1,1)
KEL (3,4) = KEL (2,3)
KEL (4,4) = KEL (2,2)

IF (K (2,2) .LE.0.00001) K (2,2)=1.0
IF (K (N,N) .LE.0.00001) K (N,N)=1.0
DO 30 I=1,4
DO 30 J=1,4
30 IF (J.GT.1) KEL (J,1)=KEL (1,J)

DO 50 JK =2,NUMEL-1
I1=JK*2-2
JJ=I1
DO 45 I=1,4
DO 40 J=1,4

K (I1+1,JJ+J) = K (I1+1,JJ)+KEL (1,J)

40 CONTINUE
45 CONTINUE
50 CONTINUE

66 DO 75 I=1,N
DO 70 J=1,N
M (I,J)=0.0
C (I,J)=0.0
70 CONTINUE
75 CONTINUE

M (1,1)=39.
M (2,2)=H**2
M (N-1,N-1)=39.
M (N,N)=H**2

DO 80 I=3,N-3,2
J=I+1
M (I,I)=78.
M (J,J)=2.*(H**2)
80 CONTINUE

DO 90 I=1,N
M (I,I)=M (I,I)*(ROW*H/78.)
CALL JACOBI (K,M,N,IFPR,X,EIGV)
DO 95 I=1,N
95 DAMRAT (I)=ZETA

CALL DAMP (N,EIGV,X,M,DAMRAT,C)

PRINT*, 'IN START'

DO 300 I=1,N

```

NEW01110  
NEW01120  
NEW01130  
NEW01140  
NEW01150  
NEW01160  
NEW01170  
NEW01180  
NEW01190  
NEW01200  
NEW01210  
NEW01220  
NEW01230  
NEW01240  
NEW01250  
NEW01260  
NEW01270  
NEW01280  
NEW01290  
NEW01300  
NEW01310  
NEW01320  
NEW01330  
NEW01340  
NEW01350  
NEW01360  
NEW01370  
NEW01380  
NEW01390  
NEW01400  
NEW01410  
NEW01420  
NEW01430  
NEW01440  
NEW01450  
NEW01460  
NEW01470  
NEW01480  
NEW01490  
NEW01500  
NEW01510  
NEW01520  
NEW01530  
NEW01540  
NEW01550  
NEW01560  
NEW01570  
NEW01580  
NEW01590  
NEW01600  
NEW01610  
NEW01620  
NEW01630  
NEW01640  
NEW01650



```

300 RT(1)=0.0 NEW01660
    PI=ACOS(-1.0) NEW01670
    RT(N/2)=PO*(DCOS(OMEGA*TIME)) NEW01680
    CALL INVERT(M,MINV,N) NEW01690
    DO 333 I=1,NUMEL+1 NEW01700
    DUM1=K1*L/(4*PI*E*X1) NEW01710
    Z=PI*H*(1-I)/L NEW01720
    UT(2*I)=(DELO/(1.+DUM1*2))*((PI/L*DCOS(Z))+(DUM1*2*PI/L*DSIN(2*Z NEW01730
&)) NEW01740
    UT(2*I-1)=(DELO/(1.+DUM1*2))*(DSIN(Z)+DUM1*(1.-DCOS(2*Z))) NEW01750
333 CONTINUE NEW01760
    DO 302 I=1,N NEW01770
    SUM=0.0 NEW01780
    DO 301 J=1,N NEW01790
301 SUM=SUM+K(I,J)*UT(J)*(-1.) NEW01800
302 DUM(I)=SUM NEW01810
    DO 306 I=1,N NEW01820
    SUM=0.0 NEW01830
    DO 305 J=1,N NEW01840
305 SUM=SUM+MINV(I,J)*DUM(J) NEW01850
306 UDDT(I)=SUM NEW01860
    DO 310 I=1,N NEW01870
    UDT(I)=0.0 NEW01880
310 CONTINUE NEW01890
    PRINT*, 'OUT START' NEW01900
    DO 320 I=1,N NEW01910
    DO 320 J=1,N NEW01920
320 C1(I,J)=K(I,J)+GAMA*C(I,J)/(BETA*TS)+M(I,J)/(BETA*(TS**2)) NEW01930
    CALL INVERT(C1,C2,N) NEW01940
120 DO 122 I=1,N NEW01950
    C3(I)=(GAMA/(BETA*TS))*UT(I)+(GAMA/BETA-1.0)*UDT(I)+TS*((GAMA/(BE NEW01960
&TA*2.))-1.0)*UDDT(I) NEW01970
    C4(I)=UT(I)/(BETA*(TS**2))+UDT(I)/(BETA*TS)+((1./(2.*BETA))-1.0)*UNEW01980
&DDT(I) NEW01990
122 CONTINUE NEW02000
    DO 130 I=1,N NEW02010
    SUM=0.0 NEW02020
    DO 125 J=1,N NEW02030
125 SUM=SUM+C(I,J)*C3(J) NEW02040
130 C5(I)=SUM NEW02050
    DO 410 I=1,N NEW02060
    SUM=0.0 NEW02070
    DO 400 J=1,N NEW02080
400 SUM=SUM+M(I,J)*C4(J) NEW02090
410 C6(I)=SUM NEW02100
    NEW02110
    NEW02120
    NEW02130
    NEW02140
    NEW02150
    NEW02160
    NEW02170
    NEW02180
    NEW02190
    NEW02200

```

```

DO 420 I=1,N
420 F(I)=RT(I)+C5(I)+C6(I)
NEW02210
NEW02220
NEW02230
DO 430 I=1,N
SUM=0.0
NEW02240
NEW02250
DO 425 J=1,N
NEW02260
425 SUM=SUM+C2(I,J)*F(J)
NEW02270
430 UTP(I)=SUM
NEW02280
NEW02290
ICOUNT=ICOUNT+1
NEW02300
TIME=TIME+TS
NEW02310
IF (TIME.GT.1.00) GO TO 199
NEW02320
RT(N/2)=P0*(DCOS(OMEGA*TIME))
NEW02330
GO TO 200
NEW02340
199 RT(N/2)=0.0
NEW02350
200 EXACT=0.0
NEW02360
JEST=1
NEW02370
IF (ICOUNT.EQ.10) GO TO 141
NEW02380
GO TO 143
NEW02390
141 WRITE(2,175) TIME,UTP(N/2),JEST
NEW02400
ICOUNT=0
NEW02410
NEW02420
143 DO 150 I=1,N
NEW02430
UDDTP(I)=(UTP(I)-UT(I)-(TS*UDT(I))-((TS**2)*(0.5-BETA)*UDDT(I)))*
NEW02440
&(1./((TS**2)*BETA))
NEW02450
150 CONTINUE
NEW02460
NEW02470
DO 161 I=1,N
NEW02480
UDTP(I)=UDT(I)+TS*(((1.0-GAMA)*UDDT(I)+(GAMA*UDDTP(I)))
NEW02490
UT(I)=UTP(I)
NEW02500
UDT(I)=UDTP(I)
NEW02510
UDDT(I)=UDDTP(I)
NEW02520
161 CONTINUE
NEW02530
IF (TIME.GT.TT) GO TO 500
NEW02540
NEW02550
GO TO 120
NEW02560
175 FORMAT(F10.8,1X,F10.8,1X,11)
NEW02570
176 FORMAT(/1X,' TIME DEFLECTION AT L/2')
NEW02580
177 FORMAT('-----')
NEW02590
&-----')
NEW02600
500 STOP
NEW02610
END
NEW02620
NEW02630
NEW02640
SUBROUTINE INVERT(AO,A,N)
NEW02650
DOUBLE PRECISION A(70,70),AO(70,70)
NEW02660
NEW02670
DO 1 I=1,N
NEW02680
DO 1 J=1,N
NEW02690
1 A(I,J)=AO(I,J)
NEW02700
NEW02710
NP=N+1
NEW02720
A(1,NP)=1.0
NEW02730
DO 10 I=2,N
NEW02740
10 A(I,NP)=0.0
NEW02750

```

```

DO 40 J=1,N
DO 20 LX=1,N
20 A(NP,LX)=A(1,LX+1)/A(1,1)
DO 30 KX=2,N
DO 30 LX=1,N
30 A(KX-1,LX)=A(KX,LX+1)-A(KX,1)*A(NP,LX)
DO 40 LX=1,N
40 A(N,LX)=A(NP,LX)

RETURN
END
SUBROUTINE JACOBI(K,M,N,IFPR,X,EIGV)
C SUBROUTINE JACOBI
IMPLICIT REAL*8(A-H,O-Z)
DOUBLE PRECISION A(70,70),B(70,70),X(70,70),EIGV(70),D(70),
&K(70,70),M(70,70)
IFPR=0
C COMMON/K,M/
C WRITE(2,1051)
C1051 FORMAT(/1X,' INPUT DATA ')
C READ(1,*)N,IFPR
C WRITE(2,1001)N,IFPR
C DO 1010 I=1,N
C READ(1,*)(A(I,J),J=1,N)
C WRITE(2,1110)(A(I,J),J=1,N)
C1010 CONTINUE
C DO 1020 I=1,N
C READ(1,*)(B(I,J),J=1,N)
C WRITE(2,1110)(B(I,J),J=1,N)
C1020 CONTINUE
C1001 FORMAT(2I10)
C1110 FORMAT(8F10.4)
DO 2 I=1,N
DO 1 J=1,N
A(I,J)=K(I,J)
B(I,J)=M(I,J)
1 CONTINUE
2 CONTINUE
NSMAX=15
C WRITE(2,1980)
1980 FORMAT(/1X,' EIGENVALUES ')
RTOL=1.D-12
IOUT=2
DO 10 I=1,N
IF(A(I,I).GT.0.AND.B(I,I).GT.0.)GO TO 4
WRITE(IOUT,2020)
STOP
4 D(I)=A(I,I)/B(I,I)
10 EIGV(I)=D(I)
DO 30 I=1,N
DO 20 J=1,N
20 X(I,J)=0.
30 X(I,I)=1.0
IF(N.EQ.1)RETURN
NEW02760
NEW02770
NEW02780
NEW02790
NEW02800
NEW02810
NEW02820
NEW02830
NEW02840
NEW02850
NEW02860
NEW02870
NEW02880
NEW02890
NEW02900
NEW02910
NEW02920
NEW02930
NEW02940
NEW02950
NEW02960
NEW02970
NEW02980
NEW02990
NEW03000
NEW03010
NEW03020
NEW03030
NEW03040
NEW03050
NEW03060
NEW03070
NEW03080
NEW03090
NEW03100
NEW03110
NEW03120
NEW03130
NEW03140
NEW03150
NEW03160
NEW03170
NEW03180
NEW03190
NEW03200
NEW03210
NEW03220
NEW03230
NEW03240
NEW03250
NEW03260
NEW03270
NEW03280
NEW03290
NEW03300

```

```

C
C INITIALIZE SWEEP COUNTER AND EIGEN ITERATION
C
      NSWEEP=0
      NR=N-1
40   NSWEEP=NSWEEP+1
      IF (IFPR.EQ.1) WRITE (IOUT,2000) NSWEEP
      PRINT*, ' SWEEP NUMBER... ',NSWEEP
C
C CHECK IF PRESENT OFF DIAGONAL ELEMENT IS TOO LARGE
C
      EPS=(0.01**NSWEEP)**2
      DO 210 J=1,NR
      JJ=J+1
      DO 210 K1=JJ,N
      IF (DABS (A (J,K1)) .LT.1.D-20) GO TO 211
      EPTOLA=(A (J,K1)*A (J,K1)) / (A (J,J)*A (K1,K1))
      GO TO 212
211  EPTOLA=0.0
212  EPTOLB=(B (J,K1)*B (J,K1)) / (B (J,J)*B (K1,K1))
      IF ((EPTOLA.LT.EPS) .AND. (EPTOLB.LT.EPS)) GO TO 210
      AKK=A (K1,K1)*B (J,K1)-B (K1,K1)*A (J,K1)
      AJJ=A (J,J)*B (J,K1)-B (J,J)*A (J,K1)
      AB=A (J,J)*B (K1,K1)-A (K1,K1)*B (J,J)
      CHECK=(AB*AB+4.*AKK*AJJ)/4.
      IF (CHECK) 50,60,60
50   WRITE (IOUT,2020)
      STOP
60   SQCH=DSQRT (CHECK)
      D1=AB/2.+SQCH
      D2=AB/2.-SQCH
      DEN=D1
      IF (DABS (D2) .GT. DABS (D1)) DEN=D2
      IF (DEN) 80,70,80
70   CA=0.
      CG=(-1.)*A (J,K1)/A (K1,K1)
      GO TO 90
80   CA=AKK/DEN
      CG=(-1.)*AJJ/DEN
90   IF (N-2) 100,190,100
100  JP1=J+1
      JM1=J-1
      KP1=K1+1
      KM1=K1-1
      IF (JM1-1) 130,110,110
110  DO 120 I=1,JM1
      AJ=A (I,J)
      BJ=B (I,J)
      AK=A (I,K1)
      BK=B (I,K1)
      A (I,J)=AJ+CG*AK
      B (I,J)=BJ+CG*BK
      A (I,K1)=AK+CA*AJ
120  B (I,K1)=BK+CA*BJ
130  IF (KP1-N) 140,140,160

```

```

140 DO 150 I=KP1,N
    AJ=A(J,I)
    BJ=B(J,I)
    AK=A(K1,I)
    BK=B(K1,I)
    A(J,I)=AJ+CG*AK
    B(J,I)=BJ+CG*BK
    A(K1,I)=AK+CA*AJ
150 B(K1,I)=BK+CA*BJ
160 IF(JP1-KM1) 170,170,190
170 DO 180 I=JP1,KM1
    AJ=A(J,I)
    BJ=B(J,I)
    AK=A(I,K1)
    BK=B(I,K1)
    A(J,I)=AJ+CG*AK
    B(J,I)=BJ+CG*BK
    A(I,K1)=AK+CA*AJ
180 B(I,K1)=BK+CA*BJ
190 AK=A(K1,K1)
    BK=B(K1,K1)
    A(K1,K1)=AK+2.*CA*A(J,K1)+CA*CA*A(J,J)
    B(K1,K1)=BK+2.*CA*B(J,K1)+CA*CA*B(J,J)
    A(J,J)=A(J,J)+2.*CG*A(J,K1)+CG*CG*AK
    B(J,J)=B(J,J)+2.*CG*B(J,K1)+CG*CG*BK
    A(J,K1)=0.
    B(J,K1)=0.
C
C UPDATE EIGENVECTOR MATRIX
C
    DO 200 I=1,N
    XJ=X(I,J)
    XK=X(I,K1)
    X(I,J)=XJ+CG*XK
200 X(I,K1)=XK+CA*XJ
210 CONTINUE
C
C UPDATE EIGENVALUES
C
    DO 220 I=1,N
    IF(A(I,I).GT.0.AND.B(I,I).GT.0) GO TO 220
    WRITE(IOUT,2020)
    STOP
220 EIGV(I)=A(I,I)/B(I,I)
    IF(IFPR.EQ.0) GO TO 230
    WRITE(IOUT,2030)
    WRITE(IOUT,2010) (EIGV(I),I=1,N)
C
C CHECK FOR CONVERGENCE
C
230 DO 240 I=1,N
    TOL=RTOL*D(I)
    DIF=DABS(EIGV(I)-D(I))
    IF(DIF.GT.TOL) GO TO 280
240 CONTINUE

```

NEW03860  
NEW03870  
NEW03880  
NEW03890  
NEW03900  
NEW03910  
NEW03920  
NEW03930  
NEW03940  
NEW03950  
NEW03960  
NEW03970  
NEW03980  
NEW03990  
NEW04000  
NEW04010  
NEW04020  
NEW04030  
NEW04040  
NEW04050  
NEW04060  
NEW04070  
NEW04080  
NEW04090  
NEW04100  
NEW04110  
NEW04120  
NEW04130  
NEW04140  
NEW04150  
NEW04160  
NEW04170  
NEW04180  
NEW04190  
NEW04200  
NEW04210  
NEW04220  
NEW04230  
NEW04240  
NEW04250  
NEW04260  
NEW04270  
NEW04280  
NEW04290  
NEW04300  
NEW04310  
NEW04320  
NEW04330  
NEW04340  
NEW04350  
NEW04360  
NEW04370  
NEW04380  
NEW04390  
NEW04400

```

C
C CHECK ALL OFF DIAG ELEMENTS TO SEE IF ANOTHER SWEEP IS REQ'D
C
      EPS=RTOL**2
      DO 250 J=1,NR
      JJ=J+1
      DO 250 K1=JJ,N
      IF (DABS (A (J,K1)) .LT.1.D-30) GO TO 251
      EPSA=(A (J,K1)*A (J,K1)) / (A (J,J)*A (K1,K1))
      GO TO 252
251  EPSA=0.0
252  EPSB=(B (J,K1)*B (J,K1)) / (B (J,J)*B (K1,K1))
      IF ((EPSA.LT.EPS) .AND. (EPSB.LT.EPS)) GO TO 250
      GO TO 280
250  CONTINUE
C
C FILL OUT BOTTOM TRIANGLE OF RESULTANT MATRICES & SCALE EIGENVECTORS
C
255  DO 260 I=1,N
      DO 260 J=1,N
      A (J,I)=A (I,J)
260  B (J,I)=B (I,J)
      DO 270 J=1,N
      BB=DSQRT (B (J,J))
      DO 270 K1=1,N
270  X (K1,J)=X (K1,J) /BB
C      WRITE (IOUT,310)
C      DO 300 I=1,N
C300  WRITE (IOUT,2010) (X (I,J),J=1,N)
310  FORMAT (/1X,' THE EIGENVECTORS ARE ')

      RETURN
C
C UPDATE THE 'D' MATRIX AND START NEW SWEEP IF ALLOWED
C
280  DO 290 I=1,N
290  D (I)=EIGV (I)
      IF (NSWEEP.LT.NSMAX) GO TO 40
      GO TO 255
2000  FORMAT (/1X,' SWEEP NUMBER IN JACOBI = ',I4)
2010  FORMAT (/1X,6E20.12)
2020  FORMAT (/1X,' ***** ERROR SOLUTION STOP / MATRICES NOT POSITIVE
&DEFINITE')
2030  FORMAT (/1X,' CURRENT EIGENVALUES IN JACOBI ARE ')
      END

      SUBROUTINE DAMP (N,EIGV,X,M,DAMRAT,C)
      IMPLICIT REAL*8 (A-H,O-Z)
      DOUBLE PRECISION X (70,70), T (70,70), M (70,70), C (70,70), EIGV (70), DAMRNEW04920
&AT (70)
      NEW04410
      NEW04420
      NEW04430
      NEW04440
      NEW04450
      NEW04460
      NEW04470
      NEW04480
      NEW04490
      NEW04500
      NEW04510
      NEW04520
      NEW04530
      NEW04540
      NEW04550
      NEW04560
      NEW04570
      NEW04580
      NEW04590
      NEW04600
      NEW04610
      NEW04620
      NEW04630
      NEW04640
      NEW04650
      NEW04660
      NEW04670
      NEW04680
      NEW04690
      NEW04700
      NEW04710
      NEW04720
      NEW04730
      NEW04740
      NEW04750
      NEW04760
      NEW04770
      NEW04780
      NEW04790
      NEW04800
      NEW04810
      NEW04820
      NEW04830
      NEW04840
      NEW04850
      NEW04860
      NEW04870
      NEW04880
      NEW04890
      NEW04900
      NEW04910
      NEW04920
      NEW04930
      NEW04940
      NEW04950
      DO 10 I=1,N

```

	EIGV(I)=DSQRT(EIGV(I))	NEW04960
	DO 10 J=1,N	NEW04970
10	C(I,J)=0.0	NEW04980
		NEW04990
	DO 20 I=1,N	NEW05000
	DA=2.*DAMRAT(I)*EIGV(I)	NEW05010
	DO 20 I=1,N	NEW05020
	DO 20 J=1,N	NEW05030
20	C(I,J)=C(I,J)+X(I,I)*X(J,I)*DA	NEW05040
		NEW05050
	DO 30 I=1,N	NEW05060
	DO 30 J=1,N	NEW05070
	T(I,J)=0.0	NEW05080
	DO 30 K1=1,N	NEW05090
30	T(I,J)=T(I,J)+M(I,K1)*C(K1,J)	NEW05100
		NEW05110
	DO 40 I=1,N	NEW05120
	DO 40 J=1,N	NEW05130
	C(I,J)=0.0	NEW05140
	DO 40 K1=1,N	NEW05150
40	C(I,J)=C(I,J)+T(I,K1)*M(K1,J)	NEW05160
		NEW05170
C	DO 50 I=1,N	NEW05180
C50	WRITE(2,120)(C(I,J),J=1,N)	NEW05190
120	FORMAT(6D14.4)	NEW05200
	RETURN	NEW05210
		NEW05220
	END	NEW05230

THIS IS NEWMARKS SOLUTION

STIFFNESS -- 0.531100006D+02

DAMPING ---- 0.130999982D-01

FORCE ----- 0.400000066D-02

FREQUENCY -- 0.251300049D+02

TIME	DEFLECTION AT L/2
0.00500000	0.07560742 1
0.01000000	0.07411487 1
0.01500000	0.07822479 1
0.02000000	0.07755833 1
0.02500000	0.07321689 1
0.03000000	0.07439081 1
0.03500001	0.07596175 1
0.04000001	0.07030083 1
0.04500001	0.06480695 1
0.05000001	0.06403831 1
0.05500001	0.05838368 1
0.06000001	0.04628549 1
0.06500001	0.03770042 1
0.07000001	0.03044851 1
0.07500001	0.01549482 1
0.08000001	-0.00155219 1
0.08500001	-0.01381828 1
0.09000001	-0.02866951 1
0.09500002	-0.04917751 1
0.10000002	-0.06667677 1
0.10500002	-0.08058453 1
0.11000002	-0.09807491 1
0.11500002	-0.11601054 1
0.12000002	-0.12788046 1
0.12500002	-0.13797468 1
0.13000002	-0.14964225 1
0.13500002	-0.15657816 1
0.14000002	-0.15730855 1
0.14500002	-0.15770900 1
0.15000002	-0.15621028 1
0.15500003	-0.14753221 1
0.16000003	-0.13531903 1
0.16500003	-0.12327482 1
0.17000003	-0.10672159 1
0.17500003	-0.08461688 1
0.18000003	-0.06275240 1
0.18500003	-0.04085973 1
0.19000003	-0.01462197 1
0.19500003	0.01269540 1
0.20000003	0.03673648 1
0.20500003	0.06085743 1
0.21000003	0.08652612 1



```

      IMPLICIT REAL*8 (A-H,O-Z)
C      THIS PROGRAM SOLVES FOR THE DEFLECTIONS OF A BEAM
C      SUBJECT TO A FORCING FUNCTION AT THE MIDPOINT
C      USING CENTRAL DIFFERENCE METHOD

      DOUBLE PRECISION L,K1,K2,K(70,70),M(70,70),C(70,70),U(70),UTN(70),
&RT(70),C1(70,70),C2(70,70),C3(70,70),C4(70),KEL(4,4),B(70),C5(70),
&DUM(70),UT(70),MINV(70,70),C6(70,70),X(70,70),EIGV(70),DAMRAT(70),
&UDDT(70)
      IFPR=0
C***** SET CONSTANT DATA *****
C**
C** L = LENGTH (IN)
C**
C** NUMEL = NUMBER OF ELEMENTS (MUST BE AN EVEN NUMBER)
C**
C** TS = TIME STEP; DELTA 'T' (SEC)
C**
C** ROW = MASS PER UNIT LENGTH (KIP*SEC**2/IN**2)
C**
C** E = MODULUS OF ELASTICITY (KSI)
C**
C** XI = MOMENT OF INERTIA (IN**4)
C**
C** AR = AREA (IN**2)
C**
C** K1 = ROTATIONAL STIFFNESS AT END 1 (K*IN/RAD)
C**
C** K2 = ROTATIONAL STIFFNESS AT END 2 (K*IN/RAD)
C**
C** ZETA = DAMPING RATIO
C**
C** TT = TOTAL TIME FOR PROGRAM EXECUTION (SEC)
C**
C** PO = MAGNITUDE OF THE FORCING FUNCTION (KIPS)
C**
C** OMEGA = FREQUENCY OF THE FORCING FUNCTION (HZ)
C**
C*****
      DATA L,NUMEL,TS,ROW/177.,12,0.00010,181.9527D-09/
      DATA E,XI,AR/10000.,.325,.7363/
      DATA K1,K2,TT/00.000,00.000,4.00/
      DATA PO,OMEGA,ZETA/0.00,0.000000000,0.0000/
      ICOUNT=0

```

CEN00010  
 CEN00020  
 CEN00030  
 CEN00040  
 CEN00050  
 CEN00060  
 CEN00070  
 CEN00080  
 CEN00090  
 CEN00100  
 CEN00110  
 CEN00120  
 CEN00130  
 CEN00140  
 CEN00150  
 CEN00160  
 CEN00170  
 CEN00180  
 CEN00190  
 CEN00200  
 CEN00210  
 CEN00220  
 CEN00230  
 CEN00240  
 CEN00250  
 CEN00260  
 CEN00270  
 CEN00280  
 CEN00290  
 CEN00300  
 CEN00310  
 CEN00320  
 CEN00330  
 CEN00340  
 CEN00350  
 CEN00360  
 CEN00370  
 CEN00380  
 CEN00390  
 CEN00400  
 CEN00410  
 CEN00420  
 CEN00430  
 CEN00440  
 CEN00450  
 CEN00460  
 CEN00470  
 CEN00480  
 CEN00490  
 CEN00500  
 CEN00510  
 CEN00520  
 CEN00530  
 CEN00540  
 CEN00550

```

TIME=0.0
H=L/NUMEL
N=2*NUMEL-2
DO 10 I=1,N
DO 10 J=1,N
10 K(I,J)=0.0
K(1,1)=3.*E*X1*(4.*K1+1.)/(H**3)*(K1+1.)
K(1,2)=(-1.)*3.*E*X1*(2.*K1+1.)/(H**2)*(K1+1.)
K(2,1)=K(1,2)
K(2,2)=E*X1*(4.*K1+3.)/(H*(K1+1.))
K(N-1,N-1)=3.*E*X1*(4.*K2+1.)/(H**3)*(K2+1.)
K(N-1,N)=3.*E*X1*(2.*K2+1.)/(H**2)*(K2+1.)
K(N,N-1)=K(N-1,N)
K(N,N)=E*X1*(4.*K2+3.)/(H*(K2+1.))
KEL(1,1) = 12.*E*X1/(H**3)
KEL(1,2) = 6.*E*X1/(H**2)
KEL(1,3) = (-1.)*KEL(1,1)
KEL(1,4) = KEL(1,2)
KEL(2,2) = 4.*E*X1/(H)
KEL(2,3) = (-1.)*KEL(1,2)
KEL(2,4) = KEL(2,2)/2.
KEL(3,3) = KEL(1,1)
KEL(3,4) = KEL(2,3)
KEL(4,4) = KEL(2,2)
DO 30 I=1,4
DO 30 J=1,4
30 IF(J.GT.1)KEL(J,I)=KEL(I,J)
DO 50 JK =1,NUMEL-2
I1=JK*2-2
JJ=I1
DO 45 I=1,4
DO 40 J=1,4
K(I1+I,JJ+J) = K(I1+I,JJ+J)+KEL(I,J)
40 CONTINUE
45 CONTINUE
50 CONTINUE
C*****
C THIS IS A TEST OF THE STIFFNESS MATRIX FOR THE STATIC LOAD CASE
C DO 61 I=1,N
C61 RT(I)=0.0
C RT(N/2)=.10
C CALL INVERT(K,C6,N)

```

CEN00560  
CEN00570  
CEN00580  
CEN00590  
CEN00600  
CEN00610  
CEN00620  
CEN00630  
CEN00640  
CEN00650  
CEN00660  
CEN00670  
CEN00680  
CEN00690  
CEN00700  
CEN00710  
CEN00720  
CEN00730  
CEN00740  
CEN00750  
CEN00760  
CEN00770  
CEN00780  
CEN00790  
CEN00800  
CEN00810  
CEN00820  
CEN00830  
CEN00840  
CEN00850  
CEN00860  
CEN00870  
CEN00880  
CEN00890  
CEN00900  
CEN00910  
CEN00920  
CEN00930  
CEN00940  
CEN00950  
CEN00960  
CEN00970  
CEN00980  
CEN00990  
CEN01000  
CEN01010  
CEN01020  
CEN01030  
CEN01040  
CEN01050  
CEN01060  
CEN01070  
CEN01080  
CEN01090  
CEN01100

```

C      DO 63 I=1,N                                CENO1110
C      SUM=0.0                                     CENO1120
C      DO 62 J=1,N                                CENO1130
C62    SUM=SUM+C6(I,J)*RT(J)                     CENO1140
C63    U(I)=SUM                                    CENO1150
C      DO 65 I=1,N                                CENO1160
C      PRINT*, 'DEFLECTION AT NODE ',I,' IS ',U(I) CENO1170
C65    WRITE(2,64) I,U(I)                         CENO1180
C64    FORMAT(/IX, 'STATIC SOLUTION... U(',I2,') = ',D23.16) CENO1190
C      GO TO 500                                    CENO1200
C                                                  CENO1210
C*****                                           CENO1220
66    DO 75 I=1,N                                CENO1230
        DO 70 J=1,N                                CENO1240
        M(I,J)=0.0                                 CENO1250
        C(I,J)=0.0                                 CENO1260
70    CONTINUE                                     CENO1270
75    CONTINUE                                     CENO1280
                                                CENO1290
                                                CENO1300
                                                CENO1310
        DO 80 I=1,N-1,2                            CENO1320
        J=I+1                                       CENO1330
        M(I,I)=78.                                  CENO1340
        M(J,J)=2.*(H**2)                            CENO1350
80    CONTINUE                                     CENO1360
                                                CENO1370
                                                CENO1380
        DO 90 I=1,N                                CENO1390
90    M(I,I)=M(I,I)*(ROW*H/78.)                    CENO1400
C      DO 100 I=1,N                                CENO1410
        IFPR=0                                       CENO1420
        CALL JACOBI(K,M,N,IFPR,X,EIGV)              CENO1430
                                                CENO1440
        DO 100 I=1,N                                CENO1450
100    DAMRAT(I)=ZETA                               CENO1460
                                                CENO1470
        CALL DAMP(N,EIGV,X,M,DAMRAT,C)              CENO1480
                                                CENO1490
                                                CENO1500
                                                CENO1510
C100   C(I,I)=ZETA                                 CENO1520
                                                CENO1530
C***** PRINT STIFFNESS, MASS, AND DAMPING MATRICES ***** CENO1540
C                                                  CENO1550
C      WRITE(2,220) N/2                             CENO1560
C      DO 210 I=1,N                                 CENO1570
C210   WRITE(2,215) (K(I,J),J=1,N/2)              CENO1580
C      WRITE(2,221) N/2                             CENO1590
C      DO 211 I=1,N                                 CENO1600
C211   WRITE(2,215) (K(I,J),J=N/2+1,N)            CENO1610
C      WRITE(2,222) N/2                             CENO1620
C      DO 212 I=1,N                                 CENO1630
C212   WRITE(2,215) (M(I,J),J=1,N/2)              CENO1640
C      WRITE(2,223) N/2                             CENO1650

```

```

C      DO 213 I=1,N                                CEN01660
C213  WRITE (2,215) (M(I,J),J=N/2+1,N)            CEN01670
C      WRITE (2,224) N/2                            CEN01680
C      DO 214 I=1,N                                CEN01690
C214  WRITE (2,215) (C(I,J),J=1,N/2)             CEN01700
C      WRITE (2,225) N/2                            CEN01710
C      DO 216 I=1,N                                CEN01720
C216  WRITE (2,215) (C(I,J),J=N/2+1,N)          CEN01730
                                           CEN01740
215  FORMAT (/1X,5D14.7)                          CEN01750
                                           CEN01760
220  FORMAT (/1X,'THESE ARE THE FIRST ',13,' COLUMNS OF K ') CEN01770
221  FORMAT (/1X,'THESE ARE THE LAST ',13,' COLUMNS OF K ') CEN01780
222  FORMAT (/1X,'THESE ARE THE FIRST ',13,' COLUMNS OF M ') CEN01790
223  FORMAT (/1X,'THESE ARE THE LAST ',13,' COLUMNS OF M ') CEN01800
224  FORMAT (/1X,'THESE ARE THE FIRST ',13,' COLUMNS OF C ') CEN01810
225  FORMAT (/1X,'THESE ARE THE LAST ',13,' COLUMNS OF C ') CEN01820
                                           CEN01830
                                           CEN01840
      PRINT*, 'IN START'                          CEN01850
                                           CEN01860
      DO 300 I=1,N                                CEN01870
300  RT(I)=0.0                                    CEN01880
                                           CEN01890
C      RT(N/2)=PO*(DSIN(OMEGA*TIME))              CEN01900
                                           CEN01910
      CALL INVERT(M,MINV,N)                       CEN01920
                                           CEN01930
                                           CEN01940
      PI=ACOS(-1.0)                               CEN01950
      DO 333 I=1,NUMEL                             CEN01960
      Z=PI*H*I/L                                   CEN01970
      UT(2*I)=(.1563/(1.+DUM1*2))*((PI/L*DCOS(Z))+(DUM1*2*PI/L*DSIN(2*Z)
&)) CEN01980
      UT(2*I-1)=(.1563/(1.+DUM1*2))* (DSIN(Z)+DUM1*(1.-DCOS(2*Z))) CEN01990
333  CONTINUE                                     CEN02000
C      DO 334 I=1,N                                CEN02010
C334  PRINT*, 'UT(',I,',') = ',UT(I)             CEN02020
                                           CEN02030
                                           CEN02040
                                           CEN02050
                                           CEN02060
      DO 302 I=1,N                                CEN02070
      SUM=0.0                                       CEN02080
      DO 301 J=1,N                                  CEN02090
301  SUM=SUM+K(I,J)*UT(J)*(-1.0)                 CEN02100
302  DUM(I)=SUM                                    CEN02110
                                           CEN02120
      DO 306 I=1,N                                CEN02130
      SUM=0.0                                       CEN02140
      DO 305 J=1,N                                  CEN02150
305  SUM=SUM+MINV(I,J)*DUM(J)                   CEN02160
306  UDDT(I)=SUM                                  CEN02170
                                           CEN02180
      DO 303 I=1,N                                CEN02190
303  UTN(I)=UT(I)+UDDT(I)*(TS**2)/2.           CEN02200

```

		CEN02210
		CEN02220
C	DO 302 I=1,N	CEN02230
C	SUM=0.0	CEN02240
C	DO 301 J=1,N	CEN02250
C301	SUM=SUM+MINV(I,J)*RT(J)	CEN02260
C302	UTN(I)=SUM	CEN02270
		CEN02280
C	DO 303 I=1,N	CEN02290
C303	UTN(I)=UTN(I)*(TS**2)/(2.0)	CEN02300
		CEN02310
	DO 310 I=1,N	CEN02320
	U(I)=0.0	CEN02330
C	UT(I)=0.0	CEN02340
310	CONTINUE	CEN02350
		CEN02360
	PRINT*, 'OUT START'	CEN02370
		CEN02380
	DO 320 I=1,N	CEN02390
	DO 315 J=1,N	CEN02400
	C1(I,J) = M(I,J)/(TS**2) + C(I,J)/(2.0*TS)	CEN02410
	C2(I,J) = K(I,J) - (2.*M(I,J)/(TS**2))	CEN02420
	C3(I,J) = (M(I,J)/(TS**2)) - (C(I,J)/(2.*TS))	CEN02430
315	CONTINUE	CEN02440
320	CONTINUE	CEN02450
		CEN02460
	CALL INVERT(C1,C6,N)	CEN02470
		CEN02480
C	DO 122 I=1,N	CEN02490
C122	WRITE(2,123) I,C6(I,I)	CEN02500
123	FORMAT(/1X,'THIS IS C6(',12,') ',D23.16)	CEN02510
C	WRITE(2,176)	CEN02520
C	WRITE(2,177)	CEN02530
130	DO 440 I=1,N	CEN02540
	SUM=0.0	CEN02550
	DO 410 J=1,N	CEN02560
C	WRITE(2,131) TIME,C2(I,J),UT(I)	CEN02570
410	SUM=SUM+C2(I,J)*UT(J)	CEN02580
440	C4(I)=SUM	CEN02590
131	FORMAT(/1X,'TIME ',F5.3,' C2 ',D18.10,' UT ',D18.10)	CEN02600
	DO 442 I=1,N	CEN02610
	SUM=0.0	CEN02620
	DO 411 J=1,N	CEN02630
411	SUM=SUM+C3(I,J)*UTN(J)	CEN02640
442	C5(I)=SUM	CEN02650
		CEN02660
	RT(N/2)=PO*(DSIN(OMEGA*TIME))	CEN02670
		CEN02680
	DO 140 I=1,N	CEN02690
140	B(I)=RT(I)-C4(I)-C5(I)	CEN02700
		CEN02710
C	DO 142 I=1,N	CEN02720
C142	WRITE(2,149) I,B(I)	CEN02730
149	FORMAT(/1X,'THIS IS B(',12,') = ',D23.16)	CEN02740
		CEN02750

```

C      WRITE (2,176)                                CENO2760
C      WRITE (2,177)                                CENO2770
      DO 542 I=1,N                                  CENO2780
      SUM=0.0                                        CENO2790
      DO 511 J=1,N                                  CENO2800
511    SUM=SUM+C6(I,J)*B(J)                         CENO2810
542    U(I)=SUM                                     CENO2820
                                                CENO2830
      ICOUNT=ICOUNT+1                               CENO2840
      TIME=TIME+TS                                  CENO2850
                                                CENO2860
C      SUM=0.0                                       CENO2870
C      DO 199 I=1,7,2                                CENO2880
C      X=1                                           CENO2890
C      D1=((E*X1/(ROW*(L**4)))**0.5)*(X**2)*(9.869604404) CENO2900
C      D2=((DSIN((X)*3.14592654/2.0))**2)           CENO2910
C      D3=1.0-(DCOS(D1*TIME))                      CENO2920
C199    SUM=SUM+D2*D3/(D1**2)                      CENO2930
C199    SUM=SUM+D3/(D1**2)                         CENO2940
C      EXACT=(2.*PO/(ROW*L))*SUM                   CENO2950
                                                CENO2960
C      D1=2.*PO*(DSIN(OMEGA*TIME))*(L**3)/((3.14592654**4)*E*X1) CENO2970
C      SUM=0.0                                       CENO2980
C      DO 199 I=1,NUMEL-1,2                          CENO2990
C      X=1                                           CENO3000
C199    SUM=SUM+(1./((X**4)-0.25))                 CENO3010
C      EXACT=SUM*D1                                  CENO3020
                                                CENO3030
      LINE=3                                         CENO3040
      IF(ICOUNT.EQ.50)GO TO 141                     CENO3050
      GO TO 143                                       CENO3060
141    WRITE (2,175) TIME,U(N/2),LINE               CENO3070
C      DIF=(U(N/2)-EXACT)/EXACT                     CENO3080
C      IF(DABS(DIF).LE.O.15)WRITE (2,177)          CENO3090
      ICOUNT=0                                       CENO3100
                                                CENO3110
143    DO 150 I=1,N                                  CENO3120
      UTN(I)=UT(I)                                   CENO3130
150    UT(I)=U(I)                                    CENO3140
                                                CENO3150
      IF(TIME.GT.TT)GO TO 500                       CENO3160
                                                CENO3170
      GO TO 130                                       CENO3180
175    FORMAT (F10.8,1X,F10.8,1X,11)                CENO3190
176    FORMAT (/1X,' TIME DEFLECTION AT L/2',15X,'EXACT') CENO3200
177    FORMAT ('-----')                          CENO3210
&-----')                                         CENO3220
500    STOP                                          CENO3230
      END                                            CENO3240
                                                CENO3250
                                                CENO3260
      SUBROUTINE INVERT(AO,A,N)                      CENO3270
      DOUBLE PRECISION A(70,70),AO(70,70)          CENO3280
                                                CENO3290
      DO 1 I=1,N                                     CENO3300

```

```

      DO 1 J=1,N
1      A (1,J)=AO (1,J)

      NP=N+1
      A (1,NP)=1.0
      DO 10 I=2,N
10     A (1,NP)=0.0

      DO 40 J=1,N
      DO 20 LX=1,N
20     A (NP,LX)=A (1,LX+1) /A (1,1)
      DO 30 KX=2,N
      DO 30 LX=1,N
30     A (KX-1,LX)=A (KX,LX+1) -A (KX,1) *A (NP,LX)
      DO 40 LX=1,N
40     A (N,LX)=A (NP,LX)

      RETURN
      END

      SUBROUTINE JACOBI (K,M,N,IFPR,X,EIGV)
C      SUBROUTINE JACOBI
      IMPLICIT REAL*8 (A-H,O-Z)
      DOUBLE PRECISION A (70,70) ,B (70,70) ,X (70,70) ,EIGV (70) ,D (70) ,
&K (70,70) ,M (70,70)
      IFPR=0
C      COMMON/K,M/
C      WRITE (2,1051)
C1051 FORMAT (/1X,' INPUT DATA ')
C      READ (1,*) N,IFPR
C      WRITE (2,1001) N,IFPR
C      DO 1010 I=1,N
C      READ (1,*) (A (I,J) ,J=1,N)
C      WRITE (2,1110) (A (I,J) ,J=1,N)
C1010 CONTINUE
C      DO 1020 I=1,N
C      READ (1,*) (B (I,J) ,J=1,N)
C      WRITE (2,1110) (B (I,J) ,J=1,N)
C1020 CONTINUE
C1001 FORMAT (2I10)
C1110 FORMAT (8F10.4)
      DO 2 I=1,N
      DO 1 J=1,N
      A (I,J)=K (I,J)
      B (I,J)=M (I,J)
1      CONTINUE
2      CONTINUE
      NSMAX=15
C      WRITE (2,1980)
1980 FORMAT (/1X,' EIGENVALUES ')
      RTOL=1.D-12
      IOUT=2
      DO 10 I=1,N
C      PRINT*, 'FLAG ',I,' A = ',A (I,1) , ' B = ',B (I,1)
      IF (A (I,1) .GT.0. AND.B (I,1) .GT.0.) GO TO 4

```

CEN03310  
 CEN03320  
 CEN03330  
 CEN03340  
 CEN03350  
 CEN03360  
 CEN03370  
 CEN03380  
 CEN03390  
 CEN03400  
 CEN03410  
 CEN03420  
 CEN03430  
 CEN03440  
 CEN03450  
 CEN03460  
 CEN03470  
 CEN03480  
 CEN03490  
 CEN03500  
 CEN03510  
 CEN03520  
 CEN03530  
 CEN03540  
 CEN03550  
 CEN03560  
 CEN03570  
 CEN03580  
 CEN03590  
 CEN03600  
 CEN03610  
 CEN03620  
 CEN03630  
 CEN03640  
 CEN03650  
 CEN03660  
 CEN03670  
 CEN03680  
 CEN03690  
 CEN03700  
 CEN03710  
 CEN03720  
 CEN03730  
 CEN03740  
 CEN03750  
 CEN03760  
 CEN03770  
 CEN03780  
 CEN03790  
 CEN03800  
 CEN03810  
 CEN03820  
 CEN03830  
 CEN03840  
 CEN03850

	WRITE (IOUT,2020)	CEN03860
	STOP	CEN03870
4	D(I)=A(I,I)/B(I,I)	CEN03880
10	EIGV(I)=D(I)	CEN03890
	DO 30 I=1,N	CEN03900
	DO 20 J=1,N	CEN03910
20	X(I,J)=0.	CEN03920
30	X(I,I)=1.0	CEN03930
	IF(N.EQ.1)RETURN	CEN03940
C		CEN03950
C	INITIALIZE SWEEP COUNTER AND EIGEN ITERATION	CEN03960
C		CEN03970
	NSWEEP=0	CEN03980
	NR=N-1	CEN03990
40	NSWEEP=NSWEEP+1	CEN04000
	IF(IFPR.EQ.1)WRITE(IOUT,2000)NSWEEP	CEN04010
	PRINT*,' SWEEP NUMBER... ',NSWEEP	CEN04020
C		CEN04030
C	CHECK IF PRESENT OFF DIAGONAL ELEMENT IS TOO LARGE	CEN04040
C		CEN04050
	EPS=(0.01**NSWEEP)**2	CEN04060
	DO 210 J=1,NR	CEN04070
	JJ=J+1	CEN04080
	DO 210 K1=JJ,N	CEN04090
	IF(DABS(A(J,K1)).LT.1.D-20)GO TO 211	CEN04100
	EPTOLA=(A(J,K1)*A(J,K1))/(A(J,J)*A(K1,K1))	CEN04110
	GO TO 212	CEN04120
211	EPTOLA=0.0	CEN04130
212	EPTOLB=(B(J,K1)*B(J,K1))/(B(J,J)*B(K1,K1))	CEN04140
	IF((EPTOLA.LT.EPS).AND.(EPTOLB.LT.EPS))GO TO 210	CEN04150
	AKK=A(K1,K1)*B(J,K1)-B(K1,K1)*A(J,K1)	CEN04160
	AJJ=A(J,J)*B(J,K1)-B(J,J)*A(J,K1)	CEN04170
	AB=A(J,J)*B(K1,K1)-A(K1,K1)*B(J,J)	CEN04180
	CHECK=(AB*AB+4.*AKK*AJJ)/4.	CEN04190
C	PRINT*,'THIS IS CHECK... ',CHECK	CEN04200
	IF(CHECK)50,60,60	CEN04210
50	WRITE(IOUT,2020)	CEN04220
	STOP	CEN04230
60	SQCH=DSQRT(CHECK)	CEN04240
	D1=AB/2.+SQCH	CEN04250
	D2=AB/2.-SQCH	CEN04260
	DEN=D1	CEN04270
	IF(DABS(D2).GT.DABS(D1))DEN=D2	CEN04280
	IF(DEN)80,70,80	CEN04290
70	CA=0.	CEN04300
	CG=(-1.)*A(J,K1)/A(K1,K1)	CEN04310
	GO TO 90	CEN04320
80	CA=AKK/DEN	CEN04330
	CG=-1.*AJJ/DEN	CEN04340
90	IF(N-2)100,190,100	CEN04350
100	JP1=J+1	CEN04360
	JM1=J-1	CEN04370
	KP1=K1+1	CEN04380
	KM1=K1-1	CEN04390
	IF(JM1-1)130,110,110	CEN04400



```

110 DO 120 I=1,JM1
    AJ=A(I,J)
    BJ=B(I,J)
    AK=A(I,K1)
    BK=B(I,K1)
    A(I,J)=AJ+CG*AK
    B(I,J)=BJ+CG*BK
    A(I,K1)=AK+CA*AJ
120 B(I,K1)=BK+CA*BJ
130 IF(KP1-N) 140,140,160
140 DO 150 I=KP1,N
    AJ=A(J,I)
    BJ=B(J,I)
    AK=A(K1,I)
    BK=B(K1,I)
    A(J,I)=AJ+CG*AK
    B(J,I)=BJ+CG*BK
    A(K1,I)=AK+CA*AJ
150 B(K1,I)=BK+CA*BJ
160 IF(JP1-KM1) 170,170,190
170 DO 180 I=JP1,KM1
    AJ=A(J,I)
    BJ=B(J,I)
    AK=A(I,K1)
    BK=B(I,K1)
    A(J,I)=AJ+CG*AK
    B(J,I)=BJ+CG*BK
    A(I,K1)=AK+CA*AJ
180 B(I,K1)=BK+CA*BJ
190 AK=A(K1,K1)
    BK=B(K1,K1)
    A(K1,K1)=AK+2.*CA*A(J,K1)+CA*CA*A(J,J)
    B(K1,K1)=BK+2.*CA*B(J,K1)+CA*CA*B(J,J)
    A(J,J)=A(J,J)+2.*CG*A(J,K1)+CG*CG*AK
    B(J,J)=B(J,J)+2.*CG*B(J,K1)+CG*CG*BK
    A(J,K1)=0.
    B(J,K1)=0.
C
C UPDATE EIGENVECTOR MATRIX
C
    DO 200 I=1,N
    XJ=X(I,J)
    XK=X(I,K1)
    X(I,J)=XJ+CG*XK
200 X(I,K1)=XK+CA*XJ
210 CONTINUE
C
C UPDATE EIGENVALUES
C
    DO 220 I=1,N
    IF(A(I,I).GT.0.AND.B(I,I).GT.0) GO TO 220
    WRITE(10OUT,2020)
    STOP
220 EIGV(I)=A(I,I)/B(I,I)
    IF(IFPR.EQ.0) GO TO 230

```

CEN04410  
CEN04420  
CEN04430  
CEN04440  
CEN04450  
CEN04460  
CEN04470  
CEN04480  
CEN04490  
CEN04500  
CEN04510  
CEN04520  
CEN04530  
CEN04540  
CEN04550  
CEN04560  
CEN04570  
CEN04580  
CEN04590  
CEN04600  
CEN04610  
CEN04620  
CEN04630  
CEN04640  
CEN04650  
CEN04660  
CEN04670  
CEN04680  
CEN04690  
CEN04700  
CEN04710  
CEN04720  
CEN04730  
CEN04740  
CEN04750  
CEN04760  
CEN04770  
CEN04780  
CEN04790  
CEN04800  
CEN04810  
CEN04820  
CEN04830  
CEN04840  
CEN04850  
CEN04860  
CEN04870  
CEN04880  
CEN04890  
CEN04900  
CEN04910  
CEN04920  
CEN04930  
CEN04940  
CEN04950

```

      WRITE (10OUT,2030)
      WRITE (10OUT,2010) (EIGV(I),I=1,N)
C
C CHECK FOR CONVERGENCE
C
230 DO 240 I=1,N
      TOL=RTOL*D(I)
      DIF=DABS(EIGV(I)-D(I))
      IF(DIF.GT.TOL)GO TO 280
240 CONTINUE
C
C CHECK ALL OFF DIAG ELEMENTS TO SEE IF ANOTHER SWEEP IS REQ'D
C PRINT*, ' RTOL ',RTOL
      EPS=RTOL**2
      DO 250 J=1,NR
        JJ=J+1
        DO 250 K1=JJ,N
          IF(DABS(A(J,K1)).LT.1.D-30)GO TO 251
          EPSA=(A(J,K1)*A(J,K1))/(A(J,J)*A(K1,K1))
          GO TO 252
251 EPSA=0.0
C PRINT*, ' EPSA ',EPSA, ' EPS ',EPS
252 EPSB=(B(J,K1)*B(J,K1))/(B(J,J)*B(K1,K1))
C PRINT*, ' EPSB ',EPSB, ' EPS ',EPS
      IF((EPSA.LT.EPS).AND.(EPSB.LT.EPS))GO TO 250
      GO TO 280
250 CONTINUE
C
C FILL OUT BOTTOM TRIANGLE OF RESULTANT MATRICES & SCALE EIGENVECTORS
C
255 DO 260 I=1,N
      DO 260 J=1,N
        A(J,I)=A(I,J)
260 B(J,I)=B(I,J)
      DO 270 J=1,N
        BB=DSQRT(B(J,J))
        DO 270 K1=1,N
          X(K1,J)=X(K1,J)/BB
C WRITE(10OUT,310)
C DO 300 I=1,N
C300 WRITE(10OUT,2010) (X(I,J),J=1,N)
310 FORMAT(/1X, ' THE EIGENVECTORS ARE ')

      RETURN
C
C UPDATE THE 'D' MATRIX AND START NEW SWEEP IF ALLOWED
C
280 DO 290 I=1,N
290 D(I)=EIGV(I)
      IF(NSWEEP.LT.NSMAX)GO TO 40
      GO TO 255
2000 FORMAT(/1X, ' SWEEP NUMBER IN JACOBI = ',I4)

```

CEN04960  
 CEN04970  
 CEN04980  
 CEN04990  
 CEN05000  
 CEN05010  
 CEN05020  
 CEN05030  
 CEN05040  
 CEN05050  
 CEN05060  
 CEN05070  
 CEN05080  
 CEN05090  
 CEN05100  
 CEN05110  
 CEN05120  
 CEN05130  
 CEN05140  
 CEN05150  
 CEN05160  
 CEN05170  
 CEN05180  
 CEN05190  
 CEN05200  
 CEN05210  
 CEN05220  
 CEN05230  
 CEN05240  
 CEN05250  
 CEN05260  
 CEN05270  
 CEN05280  
 CEN05290  
 CEN05300  
 CEN05310  
 CEN05320  
 CEN05330  
 CEN05340  
 CEN05350  
 CEN05360  
 CEN05370  
 CEN05380  
 CEN05390  
 CEN05400  
 CEN05410  
 CEN05420  
 CEN05430  
 CEN05440  
 CEN05450  
 CEN05460  
 CEN05470  
 CEN05480  
 CEN05490  
 CEN05500

```

2010 FORMAT (/1X,6E20.12)
2020 FORMAT (/1X,' **** ERROR SOLUTION STOP / MATRICES NOT POSITIVE
&DEFINITE')
2030 FORMAT (/1X,' CURRENT EIGENVALUES IN JACOBI ARE ')
      END

      SUBROUTINE DAMP(N,EIGV,X,M,DAMRAT,C)
      IMPLICIT REAL*8(A-H,O-Z)
      DOUBLE PRECISION X(70,70),T(70,70),M(70,70),C(70,70),EIGV(70),DAMR
&AT(70)

      DO 10 I=1,N
      EIGV(I)=DSQRT(EIGV(I))
      DO 10 J=1,N
10    C(I,J)=0.0

      DO 20 I=1,N
      DA=2.*DAMRAT(I)*EIGV(I)
      DO 20 I=1,N
      DO 20 J=1,N
20    C(I,J)=C(I,J)+X(I,I)*X(J,I)*DA

      DO 30 I=1,N
      DO 30 J=1,N
      T(I,J)=0.0
      DO 30 K1=1,N
30    T(I,J)=T(I,J)+M(I,K1)*C(K1,J)

      DO 40 I=1,N
      DO 40 J=1,N
      C(I,J)=0.0
      DO 40 K1=1,N
40    C(I,J)=C(I,J)+T(I,K1)*M(K1,J)

C    DO 50 I=1,N
C50   WRITE(2,120)(C(I,J),J=1,N)
      120  FORMAT(6D14.4)
      RETURN

      END

```

CEN05510  
CEN05520  
CEN05530  
CEN05540  
CEN05550  
CEN05560  
CEN05570  
CEN05580  
CEN05590  
CEN05600  
CEN05610  
CEN05620  
CEN05630  
CEN05640  
CEN05650  
CEN05660  
CEN05670  
CEN05680  
CEN05690  
CEN05700  
CEN05710  
CEN05720  
CEN05730  
CEN05740  
CEN05750  
CEN05760  
CEN05770  
CEN05780  
CEN05790  
CEN05800  
CEN05810  
CEN05820  
CEN05830  
CEN05840  
CEN05850  
CEN05860  
CEN05870  
CEN05880  
CEN05890  
CEN05900

THIS IS CENTRAL DIFFERENCE SOLUTION

STIFFNESS -- 0.531100006D+02

DAMPING ---- 0.130999982D-01

FORCE ----- 0.400000066D-02

FREQUENCY -- 0.251300049D+02

TIME	DEFLECTION AT L/2
0.00500000	0.07560742 1
0.01000000	0.07411487 1
0.01500000	0.07822479 1
0.02000000	0.07755833 1
0.02500000	0.07321689 1
0.03000000	0.07439081 1
0.03500001	0.07596175 1
0.04000001	0.07030083 1
0.04500001	0.06480695 1
0.05000001	0.06403831 1
0.05500001	0.05838368 1
0.06000001	0.04628549 1
0.06500001	0.03770042 1
0.07000001	0.03044851 1
0.07500001	0.01549482 1
0.08000001	-0.00155219 1
0.08500001	-0.01381828 1
0.09000001	-0.02866951 1
0.09500002	-0.04917751 1
0.10000002	-0.06667677 1
0.10500002	-0.08058453 1
0.11000002	-0.09807491 1
0.11500002	-0.11601054 1
0.12000002	-0.12788046 1
0.12500002	-0.13797468 1
0.13000002	-0.14964225 1
0.13500002	-0.15657816 1
0.14000002	-0.15730855 1
0.14500002	-0.15770900 1
0.15000002	-0.15621028 1
0.15500003	-0.14753221 1
0.16000003	-0.13531903 1
0.16500003	-0.12327482 1
0.17000003	-0.10672159 1
0.17500003	-0.08461688 1
0.18000003	-0.06275240 1
0.18500003	-0.04085973 1
0.19000003	-0.01462197 1
0.19500003	0.01269540 1
0.20000003	0.03673648 1
0.20500003	0.06085743 1
0.21000003	0.08652612 1